Chemical Penetration Enhancers and In Situ-Forming Reservoirs for Trans-Tympanic Drug Delivery: Progress Toward Improved Treatment of Otitis Media

by
Emmanuel J. Simons
A.B. Neuroscience and Music, Harvard College, 2004

SUBMITTED TO THE HARVARD-MIT DIVISION OF HEALTH SCIENCES AND TECHNOLOGY IN PARTIAL FULFILLMENT OF THE REQUIREMENTS FOR THE DEGREE OF

DOCTOR OF PHILOSOPHY IN BIOMEDICAL ENGINEERING
AT THE
MASSACHUSETTS INSTITUTE OF TECHNOLOGY

JUNE 2008

Signature of Author: _____
Harvard-MIT Division of Health Sciences and Technology
May 20, 2008

Certified by: _____
Robert Langer, Sc.D.
Institute Professor
Harvard-MIT Division of Health Sciences and Technology
Thesis Supervisor

Accepted by: _____
Martha L. Gray, Ph.D.
Edward Hood Taplin Professor of Medical and Electrical Engineering
Co-Director, Harvard-MIT Division of Health Sciences and Technology

Η Ιθακη σ εδωσε τ ωραιο ταξειδι...

Chemical Penetration Enhancers and *In Situ*-Forming Reservoirs for Trans-Tympanic Drug Delivery: Progress Toward Improved Treatment of Otitis Media

by

Emmanuel J. Simons

Submitted to the Harvard-MIT Division of Health Sciences and Technology
on May 20, 2008 in Partial Fulfillment of the Requirements for the
Degree of Doctor of Philosophy in Biomedical Engineering

Abstract

Otitis media (OM) is the most common specifically-treated childhood disease in the United States. The widespread use of systemic antibiotics against a disease of such high incidence is believed to be a driving force behind the observed increase in adaptive resistance among pathogenic bacteria in the nasopharynx. Local, sustained delivery of antimicrobial agents to the site of infection allows for higher drug concentrations and optimized release profiles than are permitted by systemic administration. Higher antimicrobial concentrations sustained for longer periods of time also allow for a faster and more complete eradication of OM bacteria (e.g., H. influenzae, S. pneumoniae), and minimize antibiotic exposure to other bacteria and natural flora in the nasopharynx and upper respiratory tract. We have developed in situ-forming hydrogels to serve as sustained release reservoirs for noninvasive trans-tympanic treatment of OM. A hydrogel that includes potentially synergistic chemical penetration enhancer (CPE) combinations and an antimicrobial sufficiently increases antimicrobial flux such that therapeutic levels can traverse the tympanic membrane (TM) within 12 hours, in vitro. We compare excised chinchilla TMs treated with ciprofloxacin (fluoroquinolone antibiotic) alone and with different combinations of sodium lauryl sulfate, limonene, and bupivacaine, with respect to resultant changes in TM electrical resistance and trans-TM ciprofloxacin flux. We also investigate the interactions of CPEs and local anesthetics with respect to both permeability enhancement and changes in nerve block potency and efficacy. Finally, we evaluate our hydrogel formulations in an in vivo chinchilla model of OM, and demonstrate early success in their ability to safely and effectively eradicate middle ear bacteria.

Acknowledgements

I am indebted to many for the education I have received. Any meaningful work requires a collaborative effort, and I am grateful for the support provided by my family, friends, and colleagues. The love and encouragement of my wife, Caroline, and of my brother, Billy, my parents, and my Γιαγια and Παππου have inspired my best work, but also kept this work in proper perspective.

My time here has been the most exciting, most enjoyable of my life, and for this I must express sincere thanks to my advisor, Robert Langer. His mentorship has shaped my view of science and its impact on the lives of others, and his friendship has been invaluable in my development as a scientist and as a human being. I must also thank my thesis committee members, Dr. Daniel Kohane, Dr. John Rosowski, and Dr. William Sewell, for their time and their help in bringing this work together. Dr. Kohane's devoted mentorship and guidance throughout my graduate studies helped keep my work on track, but also reminded me of the importance of family and friendship outside the laboratory. To Dr. Rosowski I express my gratitude for his patience, generosity, and invaluable assistance in bringing the many pieces of this thesis together.

I would also like to thank my friends in the Langer Lab and HST lounge who kept me smiling, kept me humble, and provided a daily reminder that generosity and kindness are not inconsistent with great achievement. Finally, I thank the HST Speech and Hearing Bioscience and Technology Program, and the NIH NIDCD for their funding and support.

Thank you all for the education. I am very fortunate to have had a wonderful graduate experience, and I am grateful to those who made it possible.

Table of Contents

List of Tables

List of Figures

1 Introduction and Background

1.1 Otitis Media

Otitis media (OM) is the most common reason for antibiotic prescriptions among children [1]. Over 20 million physician visits per year in the United States are attributed to otitis media (OM), making it the most common specifically treated childhood disease [3, 4]. Acute OM (AOM) has a prevalence of 90% within the first 5 years of life [5, 6], and 90-95% of all U.S. children have at least one documented middle ear effusion by age 2 [7, 8]. Recurrence of disease is also striking, with one third of all children in the U.S. having 6 or more episodes of AOM by age 7 [9]. Moreover, epidemiological studies suggest that the prevalence of recurrent OM among children, particularly infants, is on the rise [10]. Around the globe, the incidence of OM in children of other industrialized nations is similar to that in the U.S. In less developed countries, however, OM remains a significant cause of childhood mortality due to late-presenting intracranial complications.

OM is by definition an inflammation of the middle ear, regardless of etiology or pathogenesis. Different forms of OM are most often differentiated by the presence of fluid (effusion) and by the duration or persistence of inflammation. Effusions, if present, can be of any consistency, from water-like (serous) to viscid and mucous-like (mucoid), to pus-like (purulent); duration is classified as acute, subacute, or chronic. OM with effusion (OME) indicates inflammation with middle ear fluid (MEF), but in the absence of any indications of acute infection. Acute OM (AOM), with or without effusion, is characterized by rapid onset of the signs and symptoms associated with acute infection in the middle ear (e.g., otalgia, fever) [2].

The etiology of OM often involves a complex combination of host and environmental factors (Figure 1.1), in addition to pathogenic bacteria and/or viruses and their interactions with nasopharyngeal flora. In addition to bacterial and viral OM, nonpathogenic OM is believed to occasionally result from cranial abnormalities or eustachian tube (ET) dysfunction, which in turn lead to atelectasis (high negative pressure) of the middle ear-TM and an associated immune response [11, 12]. The fact that current clinical diagnostic procedures are incapable of determining pathogenic versus non-pathogenic etiology has led to much controversy over the treatment of middle ear effusions, especially in the current climate of rising antimicrobial resistance. Though physician guidelines call for a period of "watchful waiting" before prescribing antibiotics for OME without other signs or symptoms of infection [1], clear cases of AOM, which present with signs and symptoms of acute infection, are treated immediately with systemic antibiotics because of the danger of severe complications that result from the disease's natural course.

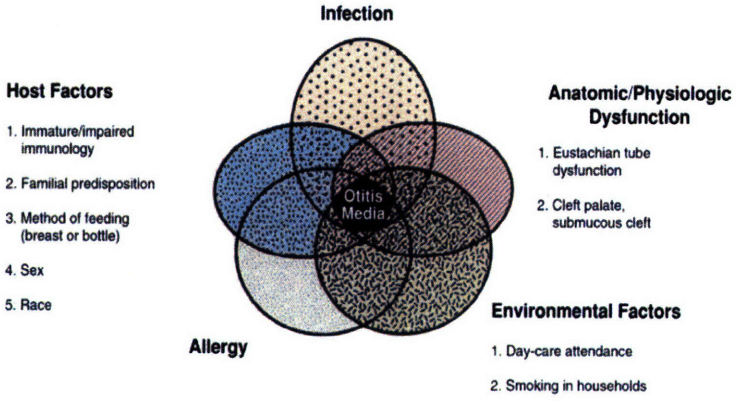

Figure 1.1. Susceptibility to otitis media (OM) is influenced by a broad range of host and environmental factors that contribute to a complex, multifactorial etiology and pathogenesis. Reproduced from [2] .

The intratemporal and intracranial complications and sequelae of AOM are varied and many. The intratemporal (extracranial) complications include hearling loss, vestibular dysfunction, acute tympanic membrane (TM) perforation, mastoiditis, petrositis, labyrinthitis, facial paralysis, and otitis externa; sequelae include middle ear atelectasis, adhesive OM, cholesteatoma, cholesterol granuloma, tympanosclerosis, and ossicular discontinuity and fixation [13].

Intracranial complications of OM can be more severe and, in many cases, fatal [14]. Meningitis, extradural abscess, subdural empyema, focal otitic encephalitis, brain abscess, dural sinus thrombosis, and otitic hydrocephalus can result from intratemporal complications (e.g., mastoiditis), and are responsible for 28,000 deaths annually [15-17].

1.1.1 Epidemiological Trends and Antimicrobial Resistance

Physical evidence of middle ear disease dates back to the 20th century BC in a prehistoric Iranian population [18], and acute disease is apparent in Egyptian mummies over 2,600 years old [19] (see [20] for review of evidence of OM collected by physical anthropologists). From humans' earliest days, up until the introduction of antimicrobial agents in the first half of the 20th century AD, cases of OM that did not resolve spontaneously were treated by myringotomy (perforation of the TM), but commonly resulted in mastoiditis and severe, often fatal, intracranial complications. It was not until the introduction of sulfonamides in 1935 that the incidence of suppurative complications decreased and OM became the relatively benign disease it is known as today. However, nearly a century of widespread antimicrobial use has led to a rapid emergence of bacterial strains that are multidrug resistant. In this context, OM has re-emerged as a major public health concern, particularly because of its heavy dependence on systemic antimicrobials and its role in fueling adaptive antibiotic resistance.

Since the turn of the 21st century, three major factors have been expected to alter the epidemiology of AOM by decreasing incidence of the disease. The introduction of the seven-valent pneumococcal conjugate vaccine (PCV 7) in 2000, the "watchful waiting" management guidelines of the American Academy or Pediatrics (AAP) and American Academy of Family Physicians (AAFP) in 2004, and a national education campaign targeted at parents and

physicians to avoid excessive use of antimicrobial agents were believed to reduce the volume of antimicrobial agents used in infants and children, and thereby reduce the selective pressure that drives multidrug resistance. Though the effects of these efforts remain to be seen over the next decade, most recent evidence suggests that resistance continues to climb in the presence of decreased antibiotic use. One might argue that the anticipated deceleration of resistance is yet to come, and that a certain time lag is expected before the correlation is observed; however, recent studies indicate that the incidence of pneumococcal OM has already decreased substantially, only to be met by an increased incidence of *H. influenzae* and *M. catarrhalis* etiologies [2, 21].

The continued increase in OM incidence and prevalence [22-25] and the remaining dependence on antimicrobial agents to prevent its severe sequelae and intracranial complications highlight the importance of developing treatment strategies that can minimize factors that influence resistance development. Localized delivery to the area of infection and sustained release technology are two strategies that can minimize excessive antibiotic exposure and improve patient compliance problems that contribute to acceleration of resistance generation.

1.1.2 Bacteriology

Microbiologic etiology of OM is traditionally determined by appropriate cultures of middle ear effusions obtained by needle aspiration. This method has consistently demonstrated the importance of *Streptococcus pneumoniae*, *Haemophilus influenzae*, and, to a smaller extent, *Moraxella catarrhalis* in AOM.

Nasopharyngeal colonization of *H. influenzae* is common among children. Within the first 2 years of life, 44% of children are colonized at least once, with a 2-month median duration of infection [26]. Prior to 1940, these bacteria were rarely, if ever, observed in AOM isolates. For reasons that are not understood, *H. influenzae* emerged as a leading cause of AOM in the 1940s,

and since the introduction of the pneumococcal conjugate vaccine (see below), are now believed to exceed pneumococcus as the most frequent bacteriologic etiology of AOM [27, 28].

Pneumococcal OM etiology was first described in 1888, and by the beginning of the antimicrobial era, in the 1930s, much of its pathogenicity was understood (see [29] for review). Of the 90 antigenically distinct serotypes of *S. pneumoniae*, some initially described as early as 1897, MEF analyses suggest a relative few are responsible for most cases of AOM: types 19F, 23, 14, 6B, and 3 have been identified as the most common, in order of decreasing frequency (see Table 1.1). It should be noted that though the specific serotypes and their relative distribution may differ according to geography or economic development, 6 to 8 types are typically responsible for 75% of pnuemococcal isolates [30]. The emergence of several polysaccharide vaccines with broad serotype coverage has led to effective reduction of pneumococcal middle ear infections, but not the incidence or prevalence of AOM, due to the subsequent increase in *H. influenzae* and *M. catarrhalis* etiologies.

Author	Year of Publication	# Patients	% Pneumo	% H. flu	% GAS	% M. cat	% Staph. aureus
Supfle*	1906	52	33	-	58	-	9
Kummel*	1907	144	28	-	66	-	6
Neumann*	1909	97	19	-	58	-	11
Wirth*	1929	271	40	-	44	-	8
Richardson[31]	1942	665	17.1	2.1	25.4	0.6	20.3
Bjuggern & Tunevall[32]	1952	131	50.0	17.0	21.0	-	4.0
Lahikainen[33]	1953	734	38.4	15.3	24.4	-	1.7
Rudberg[34]	1954	1365	38.6	7.0	19.4	-	4.8
Halsted, et al.[35]	1968	106	36.8	17.9	4.7	1.9	-
Howie, et al.[36]	1970	858	37.7	24.0	2.6	7.8	-
Bluestone, et al.[37]	1992	2807	35	23	3	14	1
Casey & Pichichero[28]	2004						
	1995-1997	195	29.2	22.6	1.5	2.1	-
	1998-2000	204	30.0	26.5	1.5	3.9	-
	2001-2003	152	23.0	35.2	1.3	3.3	-
Block, et al.[27]	2004						
	1992-1998	336	48	41	2	9	-
	2000-2003	83	31	56	2	11	-

Table 1.1. Bacteriology of AOM. *Data reviewed in [33]. Adapted from [2].

1.1.3 Pathophysiology

Despite a multifactorial etiology, a common sequence of events is characteristic of OM's pathogenesis in children. An initial event, most often a viral upper respiratory tract infection, triggers an inflammatory response in the respiratory mucosa of the nose, nasopharynx, and eustachian tube (ET), leading to congestion and obstruction of the ET. This congestion prevents proper opening of the ET and impairs the equalization of middle-ear pressure [38, 39]. This negative pressure encourages fluid infiltration from the mucosa, causing a middle ear effusion. If pathogenic bacteria from the nasopharynx invade the middle ear, which is normally sterile, signs and symptoms of acute infection ensue, leading to AOM. However, inflammation of the middle ear (i.e., OM) appears to be possible without bacterial infection of the middle ear mucosa itself, and can result simply by pathology of the ET and the subsequent stresses of prolonged

negative pressure within the middle ear. This is confirmed by induction of nonpathogenic induction of OME in animal models, and subsequent analysis of the immunologic response of the middle ear mucosa [11, 16, 40-50].

Pathophysiology of the ET is complex, and can involve various aspects of ET protective and/or clearance functions. Direct impairment of the ET pressure regulation function can result from intraluminal, periluminal, or peritubal anatomic abnormalities, or by motor or sensory dysfunction of the levator veli palatini or tensor tympani, respectively. Loss of ET protective function can occur as a result of abnormal patency, tube length, intratympanic or nasopharyngeal gas pressures, or mucociliary function [51-71].

Middle ear effusions commonly persist for 2 or more months after acute symptoms have subsided [2]. These persistent effusions appear to have a common pathogenicity among bacterial, viral, and negative-pressure (ET dysfunction) etiologies; stimulation of cytokine (IL 1, 2, 6), TNF, IFN-γ, and growth factor release is followed by an inflammation pattern consisting of (1) up-regulation of submucosal selectins and integrins that trigger additional inflammatory mediators via interaction with lymphocytes, and (2) stimulation of additional leukotrienes, prostaglandins, thromboxane, prostacyclin that promote fluid leakage from the middle ear mucosa [42-50, 72].

Recent evidence of biofilm involvement in OM has led to hypotheses implicating their importance in the high rates of OM recurrence, the extended persistence of middle ear effusions, and modest efficacies of many antibacterial treatments. Trans-bulla infection of chinchillas with *H. influenzae* results in biofilm formation on the middle ear mucosa within 24 hours, and persists for 21 days in the presence of systemic ampicillin at dosages sufficient for sterilization [73]. These biofilms, comparable to those identified in intravascular catheters infected with coagulase-

negative staphylococci, likely prolong effusions via interference with middle ear mucosa immunology, and remain a source of recurrent infection.

1.1.4 Diagnosis and Treatment

The rise of antibiotic resistant bacteria in OM has increased pressure to accurately diagnose the disease in order to avoid unnecessary treatment [1, 74]. Despite this need, OM diagnosis continues to be determined from medical history and physical examination, neither of which is an accurate predictor of the extent of bacterial involvement or the specific bacterial strains responsible. AOM is determined by evidence of TM inflammation upon otoscopic investigation combined with presence of signs and/or symptoms of acute infection (e.g., otalgia and fever); presence of negative middle ear pressure or effusion is assessed by evidence of TM compliance changes via tympanometry or pneumatic otoscopy.

Infants and children diagnosed with AOM receive a 10-15-day course of an oral antibiotic with efficacy against *S. pneumoniae, H. influenzae*, and *M. catarrhalis*. In addition to their microbiologic efficacy profiles, drugs are selected on the basis of characteristics of the oral preparation and its influence on patient compliance; acceptability of formulation taste and texture, absence of gastrointestinal side-effects, convenience of dosing schedule, and cost are common determining factors used by the physician [2]. The United States Food and Drug Administration (FDA) has approved 19 antimicrobial agents for treatment of AOM (Table 1.2), including ofloxacin otic and ciprofloxacin (with dexamethasone) as topical formulation for children with acute otorrhea and tympanostomy tubes.

Drug	Doses (#/Day)	Days of Tx	Dosage (mg/day)
Penicillins			
Amoxicillin	2-3	10	40-80 mg
Amoxicillin-clavulanate	2	10	40-80 mg (90 mg for Augmentin ES 600
Cephalosporins			
Cefaclor	3	10	40 mg
Cefdinir	1-2	5 or 10	14 mg
Cefixime	1	10	8 mg
Cefpodoxime protexil	2	5	10 mg
Cefprozil	2	10	30 mg
Ceftibuten	1	10	9 mg
Ceftriaxone	1 (IM)	-	50 mg
Cefuroxime axetil	2	10	30 mg
Cephalexin	4	10	25-50 mg
Loracarbef	2	10	30 mg
Macrolides			
Azithromycin	1	1	30 mg
	1	3	10 mg
	1	5	Day 1: 10 mg Days 2-5: 5 mg
Clarithromycin	2	10	15 mg
Erythromycin + sulfisoxazole	4	10	50 mg (E) + 150 mg (S)
Sulfonamides			
Trimethoprim HCL oral solution	2	10	10 mg
Trimethoprim-sulfamethoxazole	2	10	8 mg (T) + 40 mg (S)
Ototopicals (via tympanostomy tubes)			
Ofloxacin otic	2	10	5 drops
Ciprofloxacin	2	7	4 drops

Table 1.2. Antibiotics FDA-approved for treatment of otitis media [2]. IM = intramuscular.

Duration of treatment for oral antibiotics has been established by a combination of convention and of clinical trails, with consensus on a 10-day course, though a 5-day course has been approved for azithromycin, cefpodoxime, and cefdinir [75]. Systemic administration that avoids first-pass metabolism and therefore has higher bioavailability, such as by intra-muscular cefriaxone, typically requires only a single dose to be as effective as a 10-day course of amoxicillin and trimethoprim-sulfamethoxazole [76, 77]. Because children who receive appropriate oral antibiotic therapy experience resolution of acute signs within 72 hours, it is

common that the treatment course is abandoned before it is half complete; this behavior increases likelihood of recurrent infection and likely contributes to accelerated antibiotic resistance.

An accepted treatment regimen for OME is less clear than for AOM, and remains a controversial subject debated among physician and public health researchers. Some consensus has been reached due to an accumulated body of evidence-based information suggesting that OME is best left untreated unless there is an increased risk of complications or severe sequelae. This is based on the fact that OME in most children resolves without treatment after 2 or 3 months [78]. However, it is noteworthy that middle ear effusions cause significant hearing impairment [79, 80], which, when prolonged, may impair cognitive and language function and lead to disturbances in psychosocial adjustment [5]. It should be made clear that the treatment versus no-treatment controversy is not due to the ineffectiveness of antibiotic therapy, but rather exists because the danger of increased antibiotic resistance outweighs the benefit of treatment. If the danger of increased resistance associated with antibiotic treatment were reduced, such as by a sustained-release topical treatment, there would be compelling reason for immediate, widespread use in order to decrease time to resolution and likelihood of complications.

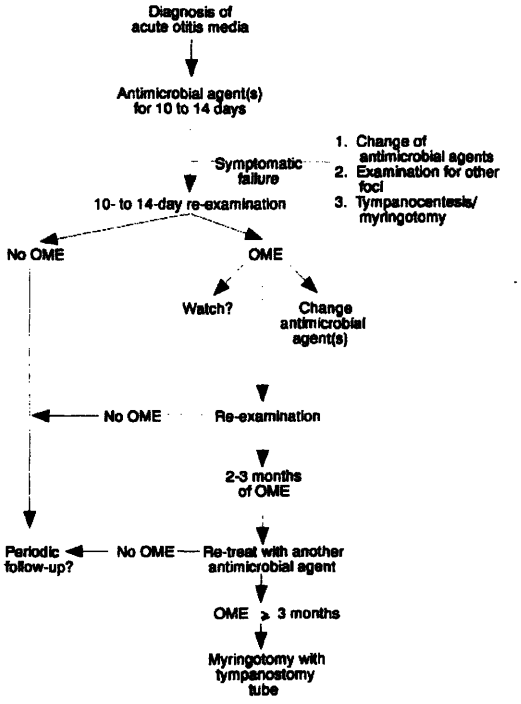

Figure 1.2. Diagnosis of AOM is initially met with a 10-day course of antibiotic, most commonly oral amoxicillin. Continued antibiotic therapy beyond this period is recommended only if signs and symptoms of acute infection persist. Otherwise, asymptomatic effusions are followed for 2-3 months until spontaneous resolution. Antibiotic therapy options are revisited if effusion persists beyond 3 months or the patient is at increased risk of complications. Reproduced from [2].

1.2 Drug Delivery to the Middle Ear

Prior to the antibiotic era, OME, with and without acute infection, was treated locally by perforation of the TM to relieve otalgia associated with negative middle ear pressure and accumulated fluid. The emergence of antibiotics brought the ability to treat middle ear infections noninvasively, as well as to reduce the risk of serious complications. Since then, myringotomy (with tympanostomy tubes) has been used increasingly sparingly, relegated to a last-resort treatment of chronic effusions. Current drug delivery vehicles used in the treatment of middle ear disease consist of tablets, suspension syrups and drops, and injected solutions, all intended for systemic antimicrobial delivery. Not until the mid-1980s did researchers begin considering local application of antibiotic drops in the nonintact TM [81], and it was not for another decade that studies demonstrated efficacy and safety of antibiotic ear drops in children with OM and tympanostomy tubes [82].

Though the low permeability of the TM is well documented, it has been studied entirely in the context of TM anesthesia [83, 84] and gas exchange [85, 86]; to date there are no published studies investigating changes in TM permeability with respect to drug delivery to the middle ear. Local, non-invasive treatment of OM in particular allows for improvements over traditional systemic antibiotic therapies that can result in (i) deceleration of adaptive resistance to commonly used antibiotics, (ii) increased recovery time despite fewer treatment administrations and a decrease in total treatment time, and (iii) increased patient compliance and reduced likelihood of recurrent infection. These advantages not only reduce the research, public health, and economic pressures to develop increasingly efficacious, next-generation antibiotics to treat increasingly resistant strains, but also help minimize the economic and public health resources required for management of recurrent OM due to inadequately treated initial infections.

Furthermore, noninvasive trans-TM drug delivery allows for treatment of OM-associated pain concurrently with treatment of its bacterial etiology. Finally, non-invasive penetration of the TM can facilitate development of methods and devices to improve diagnosis of OM and aid in selecting optimal therapeutic approaches. The following chapters discuss these benefits in further detail, and provide the first evidence of a drug delivery system that provides local, noninvasive treatment of AOM.

1.3 References

1. *Diagnosis and management of acute otitis media.* Pediatrics, 2004. **113**(5): p. 1451-65.
2. Bluestone, C.D. and J.O. Klein, *Otitis Media in Infants and Children.* 2007, Hamilton: BC Decker, Inc.
3. Berman, S., *Management of acute and chronic otitis media in pediatric practice.* Curr Opin Pediatr, 1995. **7**(5): p. 513-22.
4. Freid, V.M., D.M. Makuc, and R.N. Rooks, *Ambulatory health care visits by children: principal diagnosis and place of visit.* Vital Health Stat 13, 1998(137): p. 1-23.
5. Teele, D.W., J.O. Klein, and B. Rosner, *Epidemiology of otitis media during the first seven years of life in children in greater Boston: a prospective, cohort study.* J Infect Dis, 1989. **160**(1): p. 83-94.
6. Teele, D.W., et al., *Recent advances in otitis media. Epidemiology and natural history.* Ann Otol Rhinol Laryngol Suppl, 1989. **139**: p. 11-3.
7. Casselbrant, M.L. and E.M. Mandel, *Genetic susceptibility to otitis media.* Curr Opin Allergy Clin Immunol, 2005. **5**(1): p. 1-4.
8. Casselbrant, M.L. and E.M. Mandel, *The genetics of otitis media.* Curr Allergy Asthma Rep, 2001. **1**(4): p. 353-7.
9. Faden, H., L. Duffy, and M. Boeve, *Otitis media: back to basics.* Pediatr Infect Dis J, 1998. **17**(12): p. 1105-12; quiz 1112-3.
10. Lanphear, B.P., et al., *Increasing prevalence of recurrent otitis media among children in the United States.* Pediatrics, 1997. **99**(3): p. E1.
11. Casselbrant, M.L., et al., *Experimental paralysis of tensor veli palatini muscle.* Acta Otolaryngol, 1988. **106**(3-4): p. 178-85.

12. Ingelstedt, S., Ivarsson, and B. Jonson, *Mechanics of the human middle ear. Pressure regulation in aviation and diving. A non-traumatic method.* Acta Otolaryngol, 1967: p. Suppl 228:1-58.

13. Bluestone, C.D., ed. *Extracranial Complications of Otitis Media.* Decision making in ear, nose and throat disorders, ed. C.M. Alper, E.N. Myers, and D.E. Eibling. 2001, WB Saunders: Philadelphia. 40-42.

14. Penido, N., et al., *Intracranial complications of otitis media: 15 years of experience in 33 patients.* Otolaryngol Head Neck Surg, 2005. **132**: p. 37-42.

15. Bluestone, C.D., et al., eds. *Pediatric otolaryngology.* 4th ed. 2003, WB Saunders: Philadelphia. 765-768.

16. Alper, C.M., E.N. Myers, and D.E. Eibling, eds. *Decision making in ear, nose and throat disorders.* 2001, WB Saunders: Philadelphia.

17. Acuin, J., *Chronic suppurative otitis media.* Clin Evid, 2004(12): p. 710-29.

18. Rathbun, T.A. and R. Mallin, *Middle ear disease in a prehistoric Iranian population.* Bull N Y Acad Med, 1977. **53**(10): p. 901-5.

19. Lynn, G.E. and J.T. Benitez, *Temporal bone preservation in a 2600-year-old Egyptian mummy.* Science, 1974. **183**(121): p. 200-2.

20. Daniel, H.J., 3rd, et al., *Otitis media: a problem for the physical anthropologist.* Year Phys Anthropol, 1988. **31**: p. 143-167.

21. Finkelstein, J. and e. al., in *Pediatric Academic Society Meeting.* 2007: San Francisco, CA.

22. Schappert, S.M., *Office visits for otitis media: United States, 1975-90. Data from vital and health statistics of the Centers for Disease Control*, in *No. 214*. 1992, National Center for Heatlh Statistics: Hyattsville, MD. p. 1-18.

23. Auinger, P., et al., *Trends in otitis media among children in the United States.* Pediatrics, 2003. **112**(3 Pt 1): p. 514-20.

24. Kozak, L.J., et al., *Ambulatory surgery in the United States, 1994. Data from vital and health statistics of the Centers for Disease Control*, in *No. 283*. 1997, National Center for Health Statistics: Hyattsville, MD. p. 1-15.

25. Hoekelman, R.A., *Infectious illness during the first year of life.* Pediatrics, 1977. **59**(1): p. 119-21.

26. Faden, H., *Comparison of the local immune response to nontypable Haemophilus influenzae (nHI) and Moraxella catarrhalis (MC) during otitis media.* Adv Exp Med Biol, 1995. **371B**: p. 733-6.

27. Block, S.L., et al., *Community-wide vaccination with the heptavalent pneumococcal conjugate significantly alters the microbiology of acute otitis media.* Pediatr Infect Dis J, 2004. **23**(9): p. 829-33.

28. Casey, J.R. and M.E. Pichichero, *Changes in frequency and pathogens causing acute otitis media in 1995-2003.* Pediatr Infect Dis J, 2004. **23**(9): p. 824-8.

29. White, B., *The biology of pneumococcus*. 1979, Cambridge: Harvard University Press.

30. Hausdorff, W.P., G. Siber, and P.R. Paradiso, *Geographical differences in invasive pneumococcal disease rates and serotype frequency in young children.* Lancet, 2001. **357**(9260): p. 950-2.

31. Richardson, J.R., *Observation in acute otitis media.* Ann Otol Rhinol Laryngol, 1942. **551**: p. 804-816.

32. Bjuggren, G. and G. Tunevall, *Otitis in childhood: a clinical and serobacteriologic study with special reference to the significance of Haemophilus influenzae in relapses.* Acta Otolaryngol (Stockh), 1952. **42**(311-328).

33. Lahikainen, E.A., *Clinico-bacteriologic studies on acute otitis media: aspiration of tympanum as diagnostic and therapeutic method.* Acta Otolaryngol (Stockh), 1953. **107**: p. 1-82.

34. Rudberg, R.D., *Acute otitis media; comparative therapeutic results of sulphonamide and penicillin administered in various forms.* Acta Otolaryngol Suppl, 1954. **113**: p. 1-79.

35. Halsted, C., et al., *Otitis media. Clinical observations, microbiology, and evaluation of therapy.* Am J Dis Child, 1968. **115**(5): p. 542-51.

36. Howie, V.M., J.H. Ploussard, and R.L. Lester, Jr., *Otitis media: a clinical and bacteriological correlation.* Pediatrics, 1970. **45**(1): p. 29-35.

37. Bluestone, C.D., J.S. Stephenson, and L.M. Martin, *Ten-year review of otitis media pathogens.* Pediatr Infect Dis J, 1992. **11**(8 Suppl): p. S7-11.

38. Doyle, W.J., et al., *Nasal and otologic effects of experimental influenza A virus infection.* Ann Otol Rhinol Laryngol, 1994. **103**(1): p. 59-69.

39. Moody, S.A., C.M. Alper, and W.J. Doyle, *Daily tympanometry in children during the cold season: association of otitis media with upper respiratory tract infections.* Int J Pediatr Otorhinolaryngol, 1998. **45**(2): p. 143-50.

40. Alper, C.M., et al., *Magnetic resonance imaging of the development of otitis media with effusion caused by functional obstruction of the eustachian tube.* Ann Otol Rhinol Laryngol, 1997. **106**(5): p. 422-31.

41. Swarts, J.D., et al., *In vivo observation with magnetic resonance imaging of middle ear effusion in response to experimental underpressures.* Ann Otol Rhinol Laryngol, 1995. **104**(7): p. 522-8.

42. Palacios, S.D., et al., *Growth factors and their receptors in the middle ear mucosa during otitis media.* Laryngoscope, 2002. **112**(3): p. 420-3.

43. Cooter, M.S., et al., *Transforming growth factor-beta expression in otitis media with effusion.* Laryngoscope, 1998. **108**(7): p. 1066-70.

44. Himi, T., et al., *Immunologic characteristics of cytokines in otitis media with effusion.* Ann Otol Rhinol Laryngol Suppl, 1992. **157**: p. 21-5.

45. Juhn, S.K., et al. *Role of cytokines in the pathogenesis of otitis media.* in *Recent advances in otitis media: proceedings of the fifth international symposium.* 1991. Ft. Lauderdale, FL: BC Decker Inc.

46. Ophir, D., et al., *Tumor necrosis factor in middle ear effusions.* Arch Otolaryngol Head Neck Surg, 1988. **114**(11): p. 1256-8.

47. Willett, D.N., et al., *Relationship of endotoxin to tumor necrosis factor-alpha and interleukin-1 beta in children with otitis media with effusion.* Ann Otol Rhinol Laryngol, 1998. **107**(1): p. 28-33.

48. Yan, S.D. and C.C. Huang, *Tumor necrosis factor alpha in middle ear cholesteatoma and its effect on keratinocytes in vitro.* Ann Otol Rhinol Laryngol, 1991. **100**(2): p. 157-61.

49. Yellon, R.F., et al., *Characterization of cytokines present in middle ear effusions.* Laryngoscope, 1991. **101**(2): p. 165-9.

50. Nonomura, N., et al., *Early biochemical events in pneumococcal otitis media: arachidonic acid metabolites in middle ear fluid.* Ann Otol Rhinol Laryngol, 1991. **100**(5 Pt 1): p. 385-8.

51. Bluestone, C.D., E.I. Cantekin, and Q.C. Beery, *Effect of inflammation of the ventilatory function of the eustachian tube.* Laryngoscope, 1977. **87**(4 Pt 1): p. 493-507.

52. Buchman, C.A., et al., *Otologic manifestations of experimental rhinovirus infection.* Laryngoscope, 1994. **104**(10): p. 1295-9.

53. Friedman, R.A., et al., *Immunologic-mediated eustachian tube obstruction: a double-blind crossover study.* J Allergy Clin Immunol, 1983. **71**(5): p. 442-7.

54. McBride, T.P., et al., *Alterations of the eustachian tube, middle ear, and nose in rhinovirus infection.* Arch Otolaryngol Head Neck Surg, 1989. **115**(9): p. 1054-9.

55. Bluestone, C.D., et al., *Eustachian tube ventilatory function in relation to cleft palate.* Ann Otol Rhinol Laryngol, 1975. **84**(3 Pt 1): p. 333-8.

56. Bluestone, C.D., E.I. Cantekin, and Q.C. Beery, *Certain effects of adenoidectomy of Eustachian tube ventilatory function.* Laryngoscope, 1975. **85**(1): p. 113-27.

57. Buchman, C.A. and S.E. Stool, *Functional-anatomic correlation of eustachian tube obstruction related to the adenoid in a patient with otitis media with effusion: a case report.* Ear Nose Throat J, 1994. **73**(11): p. 835-8.

58. Wright, E.D., A.J. Pearl, and J.J. Manoukian, *Laterally hypertrophic adenoids as a contributing factor in otitis media.* Int J Pediatr Otorhinolaryngol, 1998. **45**(3): p. 207-14.

59. Bylander, A. and O. Tjernstrom, *Changes in Eustachian tube function with age in children with normal ears. A longitudinal study.* Acta Otolaryngol, 1983. **96**(5-6): p. 467-77.

60. Bluestone, C.D., J.L. Paradise, and Q.C. Beery, *Physiology of the eustachian tube in the pathogenesis and management of middle ear effusions.* Laryngoscope, 1972. **82**(9): p. 1654-70.

61. Bluestone, C.D., Q.C. Beery, and W.S. Andrus, *Mechanics of the Eustachian tube as it influences susceptibility to and persistence of middle ear effusions in children.* Ann Otol Rhinol Laryngol, 1974. **83**: p. Suppl 11:27-34.

62. Bluestone, C.D., et al., *Function of the Eustachian tube related to surgical management of acquired aural cholesteatoma in children.* Laryngoscope, 1978. **88**(7 Pt 1): p. 1155-64.

63. Stenstrom, C., A. Bylander-Groth, and L. Ingvarsson, *Eustachian tube function in otitis-prone and healthy children.* Int J Pediatr Otorhinolaryngol, 1991. **21**(2): p. 127-38.

64. Aoki, H., I. Sando, and H. Takahashi, *Anatomic relationships between Ostmann's fatty tissue and eustachian tube.* Ann Otol Rhinol Laryngol, 1994. **103**(3): p. 211-4.

65. Proctor, B., *Embryology and anatomy of the eustachian tube.* Arch Otolaryngol, 1967. **86**(5): p. 503-14.

66. Sakakihara, J., et al., *Compliance of the patulous eustachian tube.* Ann Otol Rhinol Laryngol, 1993. **102**(2): p. 110-2.

67. Ishijima, K., et al., *Length of the eustachian tube and its postnatal development: computer-aided three-dimensional reconstruction and measurement study.* Ann Otol Rhinol Laryngol, 2000. **109**(6): p. 542-8.

68. Jorgensen, F. and J. Holmquist, *Toynbee phenomenon and middle ear disease.* Am J Otol, 1984. **5**(4): p. 291-4.

69. Thompson, A.C. and J.A. Crowther, *Effect of nasal packing on eustachian tube function.* J Laryngol Otol, 1991. **105**(7): p. 539-40.

70. Ohashi, Y., et al., *Mucociliary disease of the middle ear during experimental otitis media with effusion induced by bacterial endotoxin.* Ann Otol Rhinol Laryngol, 1989. **98**(6): p. 479-84.

71. Takahashi, H., et al., *Clearance function of eustachian tube and negative middle ear pressure.* Ann Otol Rhinol Laryngol, 1992. **101**(9): p. 759-62.

72. Rhee, C., et al. *Effect of platelet-activating factor on the mucociliary function of the eustachian tube in guinea pigs.* in *Recent advances in otitis media: proceedings of the sixth international symposium.* 1996. Ft. Lauderdale, FL: BC Decker Inc.

73. Ehrlich, G.D., et al., *Mucosal biofilm formation on middle-ear mucosa in the chinchilla model of otitis media.* JAMA, 2002. **287**(13): p. 1710-5.

74. *Otitis media with effusion.* Pediatrics, 2004. **113**(5): p. 1412-29.

75. Paradise, J.L., *Short-course antimicrobial treatment for acute otitis media: not best for infants and young children.* JAMA, 1997. **278**(20): p. 1640-2.

76. Barnett, E.D., et al., *Comparison of ceftriaxone and trimethoprim-sulfamethoxazole for acute otitis media. Greater Boston Otitis Media Study Group.* Pediatrics, 1997. **99**(1): p. 23-8.

77. Green, S.M. and S.G. Rothrock, *Single-dose intramuscular ceftriaxone for acute otitis media in children.* Pediatrics, 1993. **91**(1): p. 23-30.

78. Casselbrant, M.L., et al., *Otitis media with effusion in preschool children.* Laryngoscope, 1985. **95**(4): p. 428-36.

79. Fria, T.J., E.I. Cantekin, and J.A. Eichler, *Hearing acuity of children with otitis media with effusion.* Arch Otolaryngol, 1985. **111**(1): p. 10-6.

80. Ravicz, M.E., J.J. Rosowski, and S.N. Merchant, *Mechanisms of hearing loss resulting from middle-ear fluid.* Hear Res, 2004. **195**(1-2): p. 103-30.

81. Fairbanks, D.N., *Antibiotic ear drop use in the nonintact tympanic membrane.* Pediatr Ann, 1984. **13**(5): p. 411-5.

82. Suzuki, K. and S. Baba, *Antimicrobial ear drop medication therapy.* Acta Otolaryngol Suppl, 1996. **525**: p. 68-72.

83. Bingham, B., M. Hawke, and J. Halik, *The safety and efficacy of Emla cream topical anesthesia for myringotomy and ventilation tube insertion.* J Otolaryngol, 1991. **20**(3): p. 193-5.

84. Hoffman, R.A. and C.L. Li, *Tetracaine topical anesthesia for myringotomy.* Laryngoscope, 2001. **111**(9): p. 1636-8.

85. Doyle, W.J., et al., *Exchange rates of gases across the tympanic membrane in rhesus monkeys.* Acta Otolaryngol, 1998. **118**(4): p. 567-73.

86. Felding, U.N., J.M. Banks, and W.J. Doyle, *Gas diffusion across the tympanic membrane in chinchillas: effect of repeated perforations.* Auris Nasus Larynx, 2004. **31**(4): p. 353-9.

2 Rationale and Approach

Otitis Media is treated almost exclusively by systemic administration of antibiotics, but, for reasons explained here, would be optimally treated locally and noninvasively for bacteriologic, public health, and economic reasons. In order for appropriate delivery to be optimized, however, there must be an understanding of (1) the best candidate antibiotics and their efficacies' dependence on drug concentration and exposure time, (2) the effects of chemical penetration enhancers (CPEs) on the tympanic membrane (TM) and middle ear with respect to permeability and toxicity, and (3) the desired mechanical properties of a delivery carrier that facilitates easy application and minimizes effects on hearing. Each of these is addressed in turn with a brief introduction and background of the design rationale of the strategies incorporated.

2.1 Antibiotic Selection and Benefits of Local Delivery

The antibiotic in a locally-applied, sustained-release treatment for OM must be selected with consideration of several parameters, including those relevant to stratum corneum permeability, those governing solubility and stability, and those determining pharmacodynamics and bioactivity. Amoxicillin, a penicillin derivative, is the most common first-line treatment for OM. However, faced with the pressures of increased antibiotic, in particular beta-lactam, resistance, physicians turn to a number of broad-spectrum cephalosporins, macrolides, and sulfonamides in order to treat persistent or recurrent infections (Table 2.1) [1]. In addition to those approved for OM indications and those commonly used off-label in pediatrics, additional antibiotics are suitable for OM but not used in children because of their systemic side-effects. Quinolones (e.g., ofloxacin and ciprofloxacin) are potent broad-spectrum antibiotics contraindicated for systemic

use in children because of their effects on bone growth plates (see [2] for review), but are approved for topical treatment of otorrhea in children with tympanostomy tubes.

Antibiotic	Class	MW	Log P
Amoxicillin	Penicillin	365.4	0.87 [3]
Azithromycin	Macrolide	748.9	4.02 [4]
Cefuroxime	$Ceph_2$	424.4	-0.16 [5]
Ceftriaxone	$Ceph_3$	554.6	-1.47*
Trimethoprim	Sulfonamide	290.3	0.91 [6]
Ciprofloxacin	Quinolone	331.4	0.28 [7]

Table 2.1. $Ceph_2$ = 2nd-generation cephalosporin; $Ceph_3$ = 3rd-generation cephalosporin; MW = molecular weight; Log P = logarithm of the octanol:water partition coefficient. *Log P value calculated based on molecular structure (KowWin (LogKow) Online Database).

Because stratum corneum permeability is highest to moderately hydrophobic (log P > 0) and low-molecular weight (MW < 400) molecules, certain candidate antibiotics can be eliminated based on their small log P (e.g., cefuroxime) or high MW (e.g., azithromycin). Other antibiotics, such as amoxicillin, are poor candidates because of their low stability in solution. Ciprofloxacin, by contrast, is a small, hydrophobic antibiotic that is highly soluble at low pH (pK_a = 6.16) and has broad-spectrum bactericidal activity.

Depending on the antibiotic and the target bacteria of interest, efficacy is dependent on the antibiotic concentration and/or its duration of contact with the bacteria. Clinicial efficacy of penicillins and cephalosporins correlates with the duration of time the drug concentration exceeds the minimum inhibitory concentration (MIC) for the relevant bacteria. With fluoroquinolones and most macrolides, however, efficacy is correlated with the ratio of the area under the concentration-time curve during a 24-hour period to the MIC ($AUC_{0\text{-}24}$:MIC). Fluoroquinolone efficacy has also been found to correlate with the ratio of the maximum or peak concentration (C_{max}) to the MIC value [8-19]. There is some debate over which parameter,

C_{max}:MIC or AUC_{0-24}, is most important for fluoroquinolone eradication of gram-negative infections, but most clinical studies suggest C_{max}:MIC values are the strongest predictors of clinical efficacy. In general, the C_{max}:MIC is the pharmacodynamic parameter best correlated with successful outcome when it reaches a value of 10 or greater (equivalent to an AUC_{0-24}:MIC of 100 or greater); when less than 10, however, the AUC_{0-24}:MIC is more likely to predict successful outcome.

A simple, local delivery system is capable of addressing both of these efficacy determinants by (1) providing higher concentrations of antibiotics than can be tolerated systemically, and (2) maintaining these high concentrations by sustained release mechanisms in order to maximize the AUC. These advantages have important implications for minimizing antibiotic resistance. In one recent study, patients who achieved ciprofloxacin levels at AUC_{0-24}:MIC equal to 100 or greater had a 9% probability of developing bacterial resistance by day 20 of therapy; but when AUC_{0-24}:MIC ciprofloxacin values were less than 100, the probability of resistance in the same time frame jumped to 82.4% [20].

The recommended treatment for OM is a 10-day course of four-a-day oral antibiotics [1, 21]. Though studies have investigated the effectiveness of 5-day treatment programs, and though some drugs have been approved for only 5-day courses, evidence suggests a lack of vigilance in adhering to the entire 10-day course can lead to recurrent infections and accelerate adaptive resistance generation [20]. Maximization of local antibiotic concentration and AUC, however, should theoretically reduce treatment time, and as a single ear drop can carry enough drug required for complete disease eradication, localized antibiotic delivery allows for minimal treatment applications, thereby eliminating the problem of patient compliance and its effects on antibiotic resistance.

Until the early 1980s, over 99% of *Streptococcus pneumoniae* isolates were fully susceptible to penicillin. By 1990, 40% of clinical isolates in children demonstrated intermediate- to high-level beta-lactam resistance, enough for penicillin- and multidrug- resistant *S. pneumoniae* to be considered a major public health issue (see [22] for a review of *S. pneumoniae* resistance epidemiology). In the past decade, a similar responsive development of beta-lactamase and mutated penicillin binding proteins has become dominant in nontypable *Haemophilus influenzae* [23-27]. This explosion of resistance among respiratory tract pathogens is the hypothesized result of increased antibiotic use and its role as the driving force in subsequent selective pressure on bacterial respiratory flora; the seasonal relationship between antibiotic prescriptions and resistance development, and an observed correlation between country specific antimicrobial prescribing patterns and resistance support this hypothesis [28].

These alarming data concerning antibiotic resistance have led to active campaigns encouraging limited use of antimicrobials. The CDC, for example, has developed a targeted campaign for the judicious use of antimicrobial therapy on children with acute OM, because young children have the highest antibiotic-use rates of any age group [29]. The AAP has similarly pushed guidelines that specify a strategy of "watchful waiting" and selective use of antimicrobial agents in children with OM. In addition, a pneumococcal conjugate vaccine was introduced in 2000 for all children less than 2 years of age. The vaccine is highly immunogenic in children and prevents both invasive disease as well as nasopharyngeal acquisition of vaccine serotypes of *Streptococus pneumoniae*. Together with the CDC and AAP programs, which led to a substantial decrease in antimicrobial prescribing, this vaccine was expected to have a major impact on resistance among *Streptococcus pneumoniae*, as the majority of resistant isolates were vaccine serotypes. However, a recent analysis of resistance in the greater Boston community

[30] demonstrates ongoing progression of resistance in the community, with resistance now emerging among non vaccine serotypes of *S. pneumoniae*. Thus, although immunization was effective in virtually eliminating NP carriage of vaccine serotypes, and though antibiotic prescribing in children has declined 20%, a progressive increase in beta-lactam and multidrug resistance among nonvaccine serotypes has been observed, negating both the introduction of pneumococcal conjugate vaccine and the decline in antibiotic prescribing [25]. As 30% of all antibiotic prescriptions for children continue to be written for treatment of OM [29, 31, 32], there remains opportunity for new technology to further reduce systemic exposure to antimicrobial agents, and thereby decrease the rate of resistance generation.

2.2 Tympanic Membrane Permeability and Chemical Penetration Enhancers

Despite being the thinnest layer of skin, the stratum corneum is the major resistive barrier to transdermal drug delivery (TDD) [33]. The stratum corneum of the TM, though substantially thinner than that covering the rest of the body, remains an imposing barrier to trans-TM diffusion. The vast majority of studies that identify or otherwise address TM permeability problems are done in the context of TM anesthesia for myringotomy procedures [34-38]. These include the earliest studies, which conclude that simple solutions of local anesthetics are unable to penetrate the TM to induce sensory block, to more recent investigations that incorporate advanced formulation chemistry and/or iontophoresis to increase TM permeability for local anesthesia. No studies to date, however, have investigated TM permeability or its modification for the purposes of drug delivery to the middle ear.

Researchers have shown that within the brick-and-mortar corneocyte-lipid matrix of the stratum corneum, hydrophobic permeation occurs primarily through the intercellular lipid lamellar bilayers, described by

$$P = \left(\frac{\varepsilon}{\tau}\right)\frac{K_b D_b}{L},$$

where P is the steady-state permeability, K_b is the permeant vehicle-bilayer partition coefficient, D_b is the bilayer diffusion coefficient of the permeant, and L, ε, and τ are the thickness, porosity, and tortuosity of the stratum corneum, respectively [39-44]. Chemical penetration enhancers (CPEs) have a long history of use in TDD [45] for their ability to increase permeability by disruption of corneocyte and intercellular bilayers. Despite safety concerns over irritation [46], and only moderate effectiveness compared to physical methods of stratum corneum disruption (e.g., iontophoresis, sonophoresis), interest in CPEs and their incorporation in TDD systems continue to increase because of their simplicity, low cost, and ease of use [47]. Many classes of molecules have been employed as CPEs, with varying degrees of permeability enhancing effect [47, 48], including common solvents (e.g., ethanol, dimethyl sulfoxide), fatty acids (e.g., oleic acid, palmitic acid), fatty esters (e.g., isopropyl myristate), surfactants (e.g., sodium lauryl sulfate), amino amides (e.g., tetracaine), and terpenes (e.g., limonene) [45, 48-53].

Different mechanisms of stratum corneum disruption result in a range of different toxicity-efficacy profiles amongst CPE classes. Dimethyl sulfoxide (DMSO), for example, is known to denature intercellular structural proteins and disrupt the ordered structure of lipids in the stratum corneum, which combine to contribute to significant skin irritation [54]. Anionic surfactants (e.g., sodium lauryl sulfate), in contrast, alter stratum corneum barrier function by removing

water-soluble agents that act as plasticizers among lipids. This reversible lipid modification in the absence of stratum corneum protein involvement results in an overall lower inflammation response. Terpenes similarly disrupt the stratum corneum by opening pathways within intercellular bilayers, without altering protein structural integrity [54].

Efficacy and toxicity limitations of individual CPEs can be overcome by synergistic mixtures of two or more CPEs [55-71], and recent work has demonstrated use of high throughput methods for determining binary combinations most likely to demonstrate synergy [72]. Limonene in particular has been identified as a CPE with high enhancement properties and high frequency of synergistic interaction with other CPEs, as have representative anionic surfactants (e.g., sodium octyl sulfate) and amino amides (e.g., tetracaine) [47, 48, 72]. The CPEs in a locally-applied, sustained-release delivery system for OM must be selected with permeation enhancement, irritation potential, and synergistic potential in mind, but must also be compatible with the selected vehicle/reservoir material(s).

2.3 *In Situ* Hydrogels as Sustained-Release Reservoirs

In situ-forming drug delivery systems are important to the effective, controlled release of therapeutic compounds *in vivo*. Such systems have been applied to a vast number of organ systems, intra- and extra-corporally, and can be controlled by polymer or cross-linking sensitivity to pH, light, force, temperature, or solvent exchange.

Thermoresponsive polymer solutions can be utilized as delivery systems that gel *in situ*, thereby providing easily-applied sustained-release reservoirs. Cellulose derivatives, xyloglycan, chitosan, and other polysaccharides, as well as N-isopropylacrylamide and various poloxamers are well known polymers commonly used to this end (see [73] for review). Poloxamers in

particular are attractive for use in biomedical applications because of their thermoreversible gelation properties and their established biocompatibility in many FDA-approved preparations [74].

Poloxamer block copolymers consist of ethylene oxide (EO) and propylene oxide (PO) arranged in a triblock structure of EO_x-PO_y-EO_x. Poloxamer 407 (x = 95-105, y = 54-60) has an average molecular weight of 12,600 (9,840-14,600), and is characterized by a hydrophilic-lipophilic balance (HLB) of 22 at 22°C [75, 76] and a concentration-dependent sol-gel transition temperature ($T_{sol\text{-}gel}$). The mechanism of P407 gelation is believed to be dependent on copolymer molecule aggregation into micelles, as a result of hydrophobic PO block dehydration [77]. If the P407 solution is sufficiently concentrated, these micelles organize into a face-centered cubic structure [78], resulting in gelation (Figure 2.1). These properties, and the high viscosity and slow dissolution of the resultant gels, allow for incorporation of both hydrophilic and hydrophobic compounds [79].

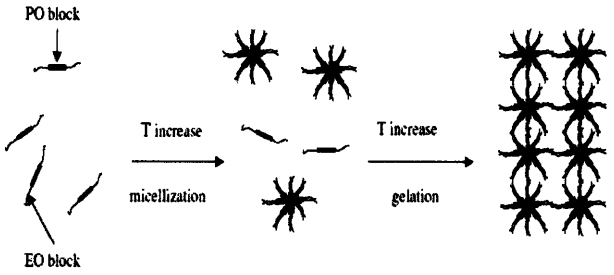

Figure 2.1. P407 copolymer molecules form spherical micelles, with a dehydrated polyPO core and an outer shell of hydrated swollen polyEO chains. The ordered packing of these micelles in the presence of increased temperature results in gelation at sufficiently high P407 concentrations [79].

Chitosan (Ch), β-(1,4)-[2-amino-2-deoxy-β-D-glucan], is a polysaccharide obtained from *N*-deacetylation of chitin, and is comprised of glucosamine and *N*-acetylglucosamine. Because it is an antimicrobial amino-polysaccharide with demonstrated biocompatibility following implantation, injection, topical application and ingestion [80, 81], Ch has attracted attention for its potential use in biomedical applications. Because of its amino groups, Ch is a polycation able to form intermolecular complexes with a broad range of polyanions, including lipids [82, 83],

collagen [84], glycosaminoglycans [85], alginate [86], and charged synthetic polymers (see [87] for review). It is therefore an ideal candidate for polyelectrolyte complex (PEC) formation for an *in situ*-forming delivery system.

Chondroitin sulfate (CS) is an important structural component of connective tissue. It is an anionic polysaccharide of the glycosaminoglycan family, and consists of alternating β(1,4)-D-glucuronic acid and β(1,3)-*N*-acetyl-D-galactosamine polymers. Though its biocompatibility and bioresorbability make it an appealing and broadly applicable delivery reservoir, CS is highly soluble under physiological conditions, and therefore unable to remain a solid-state sustained-release vehicle *in vivo*. Its negative charge, however, makes it eligible for PEC formation with cationic polysaccharides, such as chitosan.

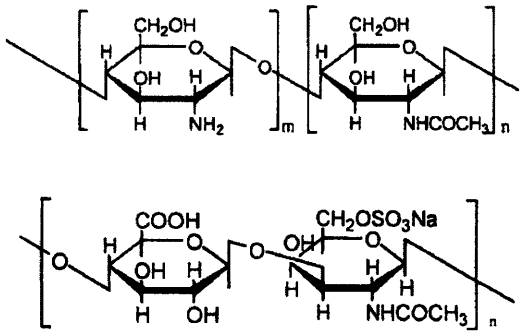

Figure 2.2. Chitosan (top) and chondroitin sulfate (bottom) polysaccharide units.

Ch-CS PEC formation requires a pH within the pK_a of each polymer. As the intrinsic pK_a of Ch is 6.5 with one charge per residue [88], and the dissociation constant pK_a of CS is 3.8 based on glucuronic residue content [89], the stoichiometric balance under which electrostatic interactions occur can be determined by:

$$C_{SO_3H} + \alpha C_{COOH} = \beta C_{NH_2}$$

$$pK_a = pH - 1.25 \log \frac{[COO^-]}{[COOH]} = 3.8$$

$$pK_a = pH - \log \frac{[NH_2]}{[NH_3^+]} = 6.5,$$

where C_{SO_3H}, C_{COOH}, and C_{NH_2} are the molarities of the dissociable groups in CS and Ch. The Henderson-Hasselbalch equations above can be used to evaluate the relative empirical dissociation of COOH and NH_2, α and β, at a given pH (SO_3H is generally considered to be 100% dissociated) [90]. Chen et al. [90] have shown that Ch/CS PEC formation can occur at a range of pHs (2.0 – 6.0) and at many molar ratios (CS/Ch from 0.09/1 to 1.36/1), with varying degrees of complexing. The extent of complex formation dictates the consistency and mechanical properties of the resultant gel, and can vary widely from solid block gels to viscous fluids. The Ch/CS ratio chosen these studies is a 1:1 mixture that provides an optimal degree of complexing for fast transition from a liquid that can be easily injected to an elastic, adhesive gel.

2.4 Specific Aims

The research in this thesis is intended to addresses the following specific aims:

1. Develop a method for measuring the electrical resistance and permeability of the tympanic membrane *in vitro*, and compare the electrical resistance and permeability of human epidermis/stratum corneum (HES) with that of the chinchilla tympanic membrane (TM).
2. Measure the flux of a model antibiotic across the chinchilla TM, *in vitro*, with and without individual and combination chemical penetration enhancers (CPEs)
3. Develop a hydrogel formulation that is easily applied to the external ear canal to contact the lateral surface of the TM, and serve as a biocompatible reservoir for sustained-release antibiotic delivery to the middle ear.
4. Investigate interactions between local anesthetics and CPEs with respect to flux enhancement and nerve block efficacy.

Evaluate the *in vivo* safety, efficacy, and behavioral effects of an antibiotic hydrogel drop in a chinchilla model of otitis media (OM).

The main goal of this work is to demonstrate the feasibility of a local drug delivery approach for treatment of OM. In the following chapters, I present a series of experiments that address the major challenges associated with sustained, trans-TM delivery, and demonstrate successful eradication of OM *in vivo*.

I first developed a technique for quantifying the flux of pharmaceutical agents across the TM with and without CPE of various classes and mechanisms. This technique, described in Chapter 3, includes a measure of the electrical resistance of the TM, and allows for the first

demonstration of resistance-permeability correlation that will help guide future work. Chapter 4 describes an assessment of CPE effects on the duration of local anesthetic-induced nerve block. Because nerve fibers are bound and surrounded by hydrophobic membranes similar in composition to the dermal layer of the TM, the CPE-local anesthetic interactions uncovered in this work are therefore relevant to the choice of enhancers selected for continued use with TMs.

Chapter 5 considers the use of two *in situ*-forming gels as sustained-release reservoirs for CPE-drug mixtures. *In vitro* demonstration of sustained release ciprofloxacin at therapeutic levels is followed by *in vivo* assessment of the gels' effects on hearing thresholds, and of their efficacy with respect to OM clearance. The former experiment is conducted in a normal chinchilla middle ear, and measures changes in auditory thresholds and toxicity following gel administration for 10 days; the latter experiment investigates the efficacy of the gel-CPE-drug mixtures in a chinchilla model of OM.

2.5 References

1. Bluestone, C.D. and J.O. Klein, *Otitis Media in Infants and Children.* 2007, Hamilton: BC Decker, Inc.
2. Stahlmann, R. and H. Lode, *Toxicity of quinolones.* Drugs, 1999. **58 Suppl 2**: p. 37-42.
3. Sangster, M.Y., et al., *Mapping the Flv locus controlling resistance to flaviviruses on mouse chromosome 5.* J Virol, 1994. **68**(1): p. 448-52.
4. McFarland, J.W., et al., *Quantitative structure-activity relationships among macrolide antibacterial agents: in vitro and in vivo potency against Pasteurella multocida.* J Med Chem, 1997. **40**(9): p. 1340-6.
5. Sangster, M.Y., et al., *Genetic studies of flavivirus resistance in inbred strains derived from wild mice: evidence for a new resistance allele at the flavivirus resistance locus (Flv).* J Virol, 1993. **67**(1): p. 340-7.
6. Hansch, C., et al., *The expanding role of quantitative structure-activity relationships (QSAR) in toxicology.* Toxicol Lett, 1995. **79**(1-3): p. 45-53.
7. Takacs-Novak, K., et al., *Relationship between partitioning properties and (calculated) molecular surface. SPR investigation of imidazoquinazolone derivatives.* Acta Pharm Hung, 1992. **62**(1-2): p. 55-64.
8. Craig, W.A. and D. Andes, *Pharmacokinetics and pharmacodynamics of antibiotics in otitis media.* Pediatr Infect Dis J, 1996. **15**(3): p. 255-9.
9. Kays, M.B., K.K. Wood, and D.O. Miles, *In vitro activity and pharmacodynamics of oral beta-lactam antibiotics against Streptococcus pneumoniae from southeast Missouri.* Pharmacotherapy, 1999. **19**(11): p. 1308-14.

10. Lacy, M.K., et al., *The pharmacodynamics of aminoglycosides.* Clin Infect Dis, 1998. **27**(1): p. 23-7.

11. Freeman, C.D., et al., *Once-daily dosing of aminoglycosides: review and recommendations for clinical practice.* J Antimicrob Chemother, 1997. **39**(6): p. 677-86.

12. Urban, A.W. and W.A. Craig, *Daily dosage of aminoglycosides.* Curr Clin Top Infect Dis, 1997. **17**: p. 236-55.

13. Moore, R.D., P.S. Lietman, and C.R. Smith, *Clinical response to aminoglycoside therapy: importance of the ratio of peak concentration to minimal inhibitory concentration.* J Infect Dis, 1987. **155**(1): p. 93-9.

14. Kashuba, A.D., J.S. Bertino, Jr., and A.N. Nafziger, *Dosing of aminoglycosides to rapidly attain pharmacodynamic goals and hasten therapeutic response by using individualized pharmacokinetic monitoring of patients with pneumonia caused by gram-negative organisms.* Antimicrob Agents Chemother, 1998. **42**(7): p. 1842-4.

15. Kashuba, A.D., et al., *Optimizing aminoglycoside therapy for nosocomial pneumonia caused by gram-negative bacteria.* Antimicrob Agents Chemother, 1999. **43**(3): p. 623-9.

16. Lode, H., K. Borner, and P. Koeppe, *Pharmacodynamics of fluoroquinolones.* Clin Infect Dis, 1998. **27**(1): p. 33-9.

17. Turnidge, J., *Pharmacokinetics and pharmacodynamics of fluoroquinolones.* Drugs, 1999. **58 Suppl 2**: p. 29-36.

18. Forrest, A., et al., *Pharmacodynamics of intravenous ciprofloxacin in seriously ill patients.* Antimicrob Agents Chemother, 1993. **37**(5): p. 1073-81.

19. Preston, S.L., et al., *Pharmacodynamics of levofloxacin: a new paradigm for early clinical trials.* JAMA, 1998. **279**(2): p. 125-9.

20. Thomas, J.K., et al., *Pharmacodynamic evaluation of factors associated with the development of bacterial resistance in acutely ill patients during therapy.* Antimicrob Agents Chemother, 1998. **42**(3): p. 521-7.

21. *Diagnosis and management of acute otitis media.* Pediatrics, 2004. **113**(5): p. 1451-65.

22. Forward, K.R., *The epidemiology of penicillin resistance in Streptococcus pneumoniae.* Semin Respir Infect, 1999. **14**(3): p. 243-54.

23. Fireman, B., et al., *Impact of the pneumococcal conjugate vaccine on otitis media.* Pediatr Infect Dis J, 2003. **22**(1): p. 10-6.

24. Eskola, J., et al., *Efficacy of a pneumococcal conjugate vaccine against acute otitis media.* N Engl J Med, 2001. **344**(6): p. 403-9.

25. Prymula, R., et al., *Pneumococcal capsular polysaccharides conjugated to protein D for prevention of acute otitis media caused by both Streptococcus pneumoniae and non-typable Haemophilus influenzae: a randomised double-blind efficacy study.* Lancet, 2006. **367**(9512): p. 740-8.

26. Block, S.L., et al., *Community-wide vaccination with the heptavalent pneumococcal conjugate significantly alters the microbiology of acute otitis media.* Pediatr Infect Dis J, 2004. **23**(9): p. 829-33.

27. Casey, J.R. and M.E. Pichichero, *Changes in frequency and pathogens causing acute otitis media in 1995-2003.* Pediatr Infect Dis J, 2004. **23**(9): p. 824-8.

28. Dagan, R., et al., *Seasonality of Antibiotic-Resistant Streptococcus pneumoniae That Causes Acute Otitis Media: A Clue for an Antibiotic-Restriction Policy?* J Infect Dis, 2008. **197**(8): p. 1094-1102.

29. Nelson, W.L., et al. *Outpatient pediatric antibiotic use in the US: trends and therapy for otitis media, 1977-1986.* in *27th Interscience Conference on Antimicrobial Agents and Chemotherapy*. 1987. Washington: American Society for Microbiology.

30. Finkelstein, J. and e. al., in *Pediatric Academic Society Meeting*. 2007: San Francisco, CA.

31. Nelson, W.L., et al., *Outpatient systemic antiinfective use by children in the United States, 1977 to 1986.* Pediatr Infect Dis J, 1988. 7(7): p. 505-9.

32. Fosarelli, P., M. Wilson, and C. DeAngelis, *Prescription medications in infancy and early childhood.* Am J Dis Child, 1987. **141**(7): p. 772-5.

33. Jarrett, A., ed. *The Physiology and Pathology of the Skin*. 1978, Academic: London.

34. Bingham, B., M. Hawke, and J. Halik, *The safety and efficacy of Emla cream topical anesthesia for myringotomy and ventilation tube insertion.* J Otolaryngol, 1991. **20**(3): p. 193-5.

35. Hasegawa, M., Y. Saito, and I. Watanabe, *Iontophoretic anaesthesia of the tympanic membrane.* Clin Otolaryngol Allied Sci, 1978. **3**(1): p. 63-6.

36. Hoffman, R.A. and C.L. Li, *Tetracaine topical anesthesia for myringotomy.* Laryngoscope, 2001. **111**(9): p. 1636-8.

37. Ochs, I.L., *Topical anesthesia for myringotomy.* Trans Am Acad Ophthalmol Otolaryngol, 1967. **71**(6): p. 918-22.

38. Ochs, I.L., *Topical anesthesia for myringotomy.* Arch Otolaryngol, 1966. **83**(1): p. 57.

39. Michaels, A.S., S.K. Chandraskeran, and J.E. Shaw, *Drug permeation through human skin: theory and in vitro experimental measurement.* Am Inst Chem Eng J, 1975. **21**: p. 985-996.

40. Cussler, E., et al., *Barrier membranes.* J Membr Sci, 1988. **38**: p. 161-174.

41. Lange-Lieckfeldt, R. and G. Lee, *Use of a model lipid matrix to demonstrate the dependence of the stratum corneum's barrier properties on its internal geometry.* J Control Release, 1992. **20**: p. 183-194.

42. Edwards, D.A. and R. Langer, *A linear theory of transdermal transport phenomena.* J Pharm Sci, 1994. **83**(9): p. 1315-34.

43. Johnson, M.E., D. Blankschtein, and R. Langer, *Evaluation of solute permeation through the stratum corneum: lateral bilayer diffusion as the primary transport mechanism.* J Pharm Sci, 1997. **86**(10): p. 1162-72.

44. Kushner, J.t., et al., *First-principles, structure-based transdermal transport model to evaluate lipid partition and diffusion coefficients of hydrophobic permeants solely from stratum corneum permeation experiments.* J Pharm Sci, 2007. **96**(12): p. 3236-51.

45. Sweeney, T.M., A.M. Downes, and A.G. Matoltsy, *The effect of dimethyl sulfoxide on the epidermal water barrier.* J Invest Dermatol, 1966. **46**(3): p. 300-2.

46. Kanikkannan, N., et al., *Structure-activity relationship of chemical penetration enhancers in transdermal drug delivery.* Curr Med Chem, 2000. **7**(6): p. 593-608.

47. Karande, P., A. Jain, and S. Mitragotri, *Relationships between skin's electrical impedance and permeability in the presence of chemical enhancers.* J Control Release, 2006. **110**(2): p. 307-13.

48. Karande, P., et al., *Design principles of chemical penetration enhancers for transdermal drug delivery.* Proc Natl Acad Sci U S A, 2005. **102**(13): p. 4688-93.

49. Sugibayashi, K., et al., *Effect of the absorption enhancer, Azone, on the transport of 5-fluorouracil across hairless rat skin.* J Pharm Pharmacol, 1985. **37**(8): p. 578-80.

50. Francoeur, M.L., G.M. Golden, and R.O. Potts, *Oleic acid: its effects on stratum corneum in relation to (trans)dermal drug delivery.* Pharm Res, 1990. **7**(6): p. 621-7.

51. Tanojo, H., et al., *In vivo human skin permeability enhancement by oleic acid: a laser Doppler velocimetry study.* J Control Release, 1999. **58**(1): p. 97-104.

52. Kikwai, L., et al., *Effect of vehicles on the transdermal delivery of melatonin across porcine skin in vitro.* J Control Release, 2002. **83**(2): p. 307-11.

53. Baroli, B., et al., *Microemulsions for topical delivery of 8-methoxsalen.* J Control Release, 2000. **69**(1): p. 209-18.

54. Walker, R.B. and E.W. Smith, *The role of percutaneous penetration enhancers.* Adv Drug Delivery Rev, 1996. **18**: p. 295-301.

55. El-Kattan, A.F., et al., *Effect of formulation variables on the percutaneous permeation of ketoprofen from gel formulations.* Drug Deliv, 2000. **7**(3): p. 147-53.

56. Mura, P., et al., *Evaluation of transcutol as a clonazepam transdermal permeation enhancer from hydrophilic gel formulations.* Eur J Pharm Sci, 2000. **9**(4): p. 365-72.

57. Huang, Y.B., et al., *Cyclic monoterpene extract from cardamom oil as a skin permeation enhancer for indomethacin: in vitro and in vivo studies.* Biol Pharm Bull, 1999. **22**(6): p. 642-6.

58. Kim, D.D. and Y.W. Chien, *Transdermal delivery of zalcitabine: in vitro skin permeation study.* AIDS, 1995. **9**(12): p. 1331-6.

59. Gorukanti, S.R., L. Li, and K.H. Kim, *Transdermal delivery of antiparkinsonian agent, benztropine. I. Effect of vehicles on skin permeation.* Int J Pharm, 1999. **192**(2): p. 159-72.

60. Gwak, H.S., S.U. Kim, and I.K. Chun, *Effect of vehicles and enhancers on the in vitro permeation of melatonin through hairless mouse skin.* Arch Pharm Res, 2002. **25**(3): p. 392-6.

61. Gwak, H.S., I.S. Oh, and I.K. Chun, *Transdermal delivery of ondansetron hydrochloride: effects of vehicles and penetration enhancers.* Drug Dev Ind Pharm, 2004. **30**(2): p. 187-94.

62. Loftsson, T., G. Somogyi, and N. Bodor, *Effect of choline esters and oleic acid on the penetration of acyclovir, estradiol, hydrocortisone, nitroglycerin, retinoic acid and trifluorothymidine across hairless mouse skin in vitro.* Acta Pharm Nord, 1989. **1**(5): p. 279-86.

63. Thomas, N.S. and R. Panchagnula, *Combination strategies to enhance transdermal permeation of zidovudine (AZT).* Pharmazie, 2003. **58**(12): p. 895-8.

64. Larrucea, E., et al., *Combined effect of oleic acid and propylene glycol on the percutaneous penetration of tenoxicam and its retention in the skin.* Eur J Pharm Biopharm, 2001. **52**(2): p. 113-9.

65. Larrucea, E., et al., *Interaction of tenoxicam with cyclodextrins and its influence on the in vitro percutaneous penetration of the drug.* Drug Dev Ind Pharm, 2001. **27**(3): p. 251-60.

66. Sugibayashi, K., C. Sakanoue, and Y. Morimoto, *Utility of topical formulations of morphine hydrochloride containing azone and N-methyl-2-pyrrolidone.* Sel Cancer Ther, 1989. **5**(3): p. 119-28.

67. Levison, K.K., et al., *Formulation optimization of indomethacin gels containing a combination of three kinds of cyclic monoterpenes as percutaneous penetration enhancers.* J Pharm Sci, 1994. **83**(9): p. 1367-72.

68. Sinico, C., et al., *Liposomes as carriers for dermal delivery of tretinoin: in vitro evaluation of drug permeation and vesicle-skin interaction.* J Control Release, 2005. **103**(1): p. 123-36.

69. Sintov, A.C. and L. Shapiro, *New microemulsion vehicle facilitates percutaneous penetration in vitro and cutaneous drug bioavailability in vivo.* J Control Release, 2004. **95**(2): p. 173-83.

70. Zhao, K. and J. Singh, *In vitro percutaneous absorption enhancement of propranolol hydrochloride through porcine epidermis by terpenes/ethanol.* J Control Release, 1999. **62**(3): p. 359-66.

71. Nicolazzo, J.A., et al., *Synergistic enhancement of testosterone transdermal delivery.* J Control Release, 2005. **103**(3): p. 577-85.

72. Karande, P., A. Jain, and S. Mitragotri, *Insights into synergistic interactions in binary mixtures of chemical permeation enhancers for transdermal drug delivery.* J Control Release, 2006. **115**(1): p. 85-93.

73. Ruel-Gariepy, E. and J.C. Leroux, *In situ-forming hydrogels--review of temperature-sensitive systems.* Eur J Pharm Biopharm, 2004. **58**(2): p. 409-26.

74. Rowe, R., P. Sheskey, and S. Owen, *Pharmaceutical Handbook of Pharmaceutical Excipients*. 5 ed. 2005, Washington: American Pharmaceutical Association.

75. Kabanov, A.V., E.V. Batrakova, and V.Y. Alakhov, *Pluronic block copolymers as novel polymer therapeutics for drug and gene delivery.* J Control Release, 2002. **82**(2-3): p. 189-212.

76. Moghimi, S.M. and A.C. Hunter, *Poloxamers and poloxamines in nanoparticle engineering and experimental medicine.* Trends Biotechnol, 2000. **18**(10): p. 412-20.

77. Juhasz, J., et al., *Diffusion of rat atrial natriuretic factor in thermoreversible poloxamer gels.* Biomaterials, 1989. **10**(4): p. 265-8.

78. Liu, T. and B. Chu, *Formation of homogeneous gel-like phases by mixed triblock copolymer micelles in aqueous solution: FCC to BCC phase transition.* J Appl Cryst, 2000. **33**: p. 727-730.

79. Dumortier, G., et al., *A review of poloxamer 407 pharmaceutical and pharmacological characteristics.* Pharm Res, 2006. **23**(12): p. 2709-28.

80. Xie, W., P. Xu, and Q. Liu, *Antioxidant activity of water-soluble chitosan derivatives.* Bioorg Med Chem Lett, 2001. **11**(13): p. 1699-701.

81. Muzzarelli, R.A.A. *Chitin, the human body.* in *Advances in Chitin Science*. 1995: Brest.

82. Demarger-Andre, S. and A. Domard, *Chitosan carboxylic acid salts in solution and in the solid state.* Carbohydr Polym, 1994. **23**: p. 211-219.

83. Demarger-Andre, S. and A. Domard, *Chitosan behaviors in a dispersion of undecylenic acid.* Carbohydr Polym, 1993. **22**: p. 117-126.

84. Taravel, M.N. and A. Domard, *Relation between the physicochemical characteristics of collagen and its interactions with chitosan: I.* Biomaterials, 1993. **14**(12): p. 930-8.

85. Denuziere, A., et al., *Chitosan-chondroitin sulfate and chitosan-hyaluronate polyelectrolyte complexes: biological properties.* Biomaterials, 1998. **19**(14): p. 1275-85.

86. Yan, X.L., E. Khor, and L.Y. Lim, *Chitosan-alginate films prepared with chitosans of different molecular weights.* J Biomed Mater Res, 2001. **58**(4): p. 358-65.

87. Berger, J., et al., *Structure and interactions in chitosan hydrogels formed by complexation or aggregation for biomedical applications.* Eur J Pharm Biopharm, 2004. **57**(1): p. 35-52.

88. Becheran-Maron, L., C. Peniche, and W. Arguelles-Monal, *Study of the interpolyelectrolyte reaction between chitosan and alginate: influence of alginate composition and chitosan molecular weight.* Int J Biol Macromol, 2004. **34**(1-2): p. 127-33.

89. Park, J.W. and B. Chakrabarti, *Optical characteristics of carboxyl group in relation to the circular dichroic properties and dissociation constants of glycosaminoglycans.* Biochim Biophys Acta, 1978. **544**(3): p. 667-75.

90. Chen, W.B., et al., *Characterization of polyelectrolyte complexes between chondroitin sulfate and chitosan in the solid state.* J Biomed Mater Res A, 2005. **75**(1): p. 128-37.

3 Effects of Chemical Penetration Enhancers on the Permeability of the Chinchilla Tympanic Membrane

3.1 Introduction

Localized drug delivery to the middle ear has been limited to invasive perforation of the tympanic membrane (TM) because of the TM's impermeability to most small molecules. The lateral surface of the TM is a stratified, squamous, keratinizing epithelium that is continuous with that of the external ear canal, and comprises the outermost of the TM's trilayer structure; its composition is identical to that of the epidermis and stratum corneum found elsewhere on the body's surface, except that it consists of 3-5 corneocyte layers rather than the 15-20 layers that cover the rest of the body. The medial, inner-most layer of the TM is also cellular, but consists of a single layer of low cuboidal epithelial cells. The middle layer between the epithelia comprises a complex arrangement of fibroelastic connective fibers, nerve endings, and vasculature [1]. Though fewer than 10 cell-layers and only 50-100 μm thick, the TM is virtually impermeable to all but the smallest, moderately hydrophobic molecules because of the lipid-corneocyte matrix of its outer layer.

Previous observation of the TM's impermeability, and its similarities in nature to that of the skin, has led to experimental adoption of transdermal iontophoresis for local anesthetic administration to the TM prior to myringotomy [2]. However, though chemical penetration enhancers (CPEs) predate iontophoresis in the transdermal literature, and would appear to be clinically more manageable and cost-effective than iontophoresis apparatus, there is no published evidence of attempts to increase small molecule flux across the TM with CPEs. This is likely

due to the lack of verified delivery vehicles approved for clinical use, and the absence of an established *in vitro* model for measuring TM permeability.

The work described herein addresses the latter of these barriers by demonstrating effective use of an in vitro model for small molecule trans-TM flux measurement, and provides the first evidence of increased TM permeability to antibiotics using surfactant, terpene, and amino amide CPEs. The relationship between TM permeability and resistivity is further investigated in order to facilitate continued use of this model for development of improved treatments of middle-ear disease.

3.2 Materials & Methods

3.2.1 Animal Care

All animals were cared for in accordance with protocols approved institutionally and nationally.

3.2.2 Chemical Enhancers & Formulation Preparation

All compounds were obtained from Sigma (St. Louis, MO), unless otherwise specified.

3.2.3 Skin Preparation

Fresh frozen, full-thickness, human abdominal skin (hairless) was obtained from the National Disease Research Interchange (NDRI, Philadelphia, PA), and kept at -80°C for up to 4 weeks before thaw and use. On experiment day 0, full-thickness skin samples were covered with aluminum foil and air-thawed at room temperature. Skin samples were then placed face (stratum corneum) down in a water bath maintained at 60°C for 2 minutes. Forceps and weighing spatula were then used to separate (i.e., "heat strip") the epidermis with stratum corneum from the underlying dermis. The dermis was discarded, and any remaining epidermis that was not immediately used for the present experiment was stored in a humidified chamber at 4°C for up to one week.

3.2.4 Tympanic Membrane Harvesting

Chinchillas were sacrificed by IP administration of a lethal dose of Nembutal, and decapitated to facilitate access to ventral and dorsal regions of the skull adjacent to the temporal bone. In some cases, disjointed heads were frozen, and later thawed in normal (0.9%) saline, before further dissection. Soft tissue of the external ear and surrounding temporal bone was removed by scissors and rongeurs to expose the temporal bone, external auditory meatus (EAM), and auditory bulla, bilaterally. The bullae were carefully opened with a scalpel blade, and the opening enlarged with small rongeurs until the interior-medial surface of the tympanic membrane (TM) and ossicles could be seen. A myringotomy knife was introduced into this opening to sever the malleus-incus ligament, thereby freeing the TM from the surrounding middle ear. The remaining bone surrounding the EAM, lateral to the tympanic ring, was carefully removed until the EAM, tympanic ring, and TM could be separated from the adjacent skull. The removed sample therefore consisted of an intact TM within the tympanic ring, exposed on both lateral and medial surfaces.

3.2.5 Skin Permeability Measurements

Heat-stripped epidermis with stratum corneum (HES) samples were secured between the adjoining orifices of both side-by-side (SxS) and vertical (Franz) diffusion cells (Permegear, Bethlehem, PA) with vacuum grease. The receiving chambers for all cells were filled with 3.5 or 5 mL PBS. The donor chamber volumes were 3.5 or 5 mL for the SxS cells and 100 or 200 μL for the Franz cells. At fixed time points (0.5, 2, 6, 24, 48, 120 hours), a 300 μL sample volume was removed from the receiving chamber and prepared for HPLC analysis of permeant concentration; an equivalent volume of PBS was returned to the receiving chamber.

3.2.6 TM Permeability Measurements

Each extracted TM (including the surrounding tympanic ring and adjacent EAM) was placed upright in a 12-well plate, with the TM surface perpendicular to the well base and the EAM longitudinal axis parallel to the well walls. A 3 mL volume of PBS was added to the well, so that the entire medial surface of the TM was submerged, and 100 μL of PBS, test solution, or gel formulation was pipetted into the EAM to cover the lateral TM surface. At pre-determined time points (0.5, 2, 6, 24, and 48 hours post treatment administration), a 100-μL sample from the 3-mL "receiving chamber" was removed, filtered, and transferred to an HPLC vial.

3.2.7 Skin and TM electrical resistance measurements.

The electrical impedance of the skin was measured as previously described [3]. Ag-Cl electrodes (In Vivo Metrics, Healdsburg, CA) were placed on either side of the biological membrane (human epidermis with stratum corneum or chinchilla TM), in the donor and receiving media, and a signal generator (Hewlett Packard, HP 33120A) provided a 100 mV (rms) AC voltage for 5 seconds at 10 Hz, 100 Hz, 1 kHz, and 10 kHz. The current passing through the membrane was measured with a Fluke Multimeter (Model 139, Fluke Corporation), and the electrical impedance was approximated using Ohm's Law from the current obtained a the 10 Hz signal. Background resistance measurements of PBS alone were made separately and subtracted from the initial resistance calculation to yield the membrane resistance; following the final time point in the extracted TM experiments, the TM surface was covered with a thin rubber disc and silicone adhesive, and the electrical resistance of the surrounding tympanic ring and EAM were measured and similarly subtracted from the initial TM+EAM resistance calculation. Any skin sample with an initial resistivity (electrical resistance * exposed area) of <35 kOhm*cm^2 was

considered damaged, was discarded, and was subsequently replaced with an intact sample (Kushner et al., 2004; Kasting & Bowman, 1990).

3.2.8 High Performance Liquid Chromotography (HPLC)

Samples from each time point were filtered with 0.2 μm syringe filters (Acrodisc, Sigma) and pipetted into 100 μL HPLC vial inserts. Assays were performed on a Hewlett-Packard HP 1100 HPLC system. Samples in 20-μL volumes were injected onto a 4.6 (ID) x 250 (L) mm Atlantis dC_{18} 5 μm column. The column was eluted with an aqueous solution of 80:20 acetonitrile:NaH_2PO_4/H_3PO_4 (0.01M, pH=2.8) at 1 mL/min. Ciprofloxacin was detected by UV absorbance at 275 nm wavelength. Separate dilution standards were prepared by diluting 1% Ciprofloxacin solution (Bayer HealthCare, West Haven, CT) in PBS, 0.01 % to 1.0 x 10^{-5} % (w/v), on the day of analysis.

3.2.9 *In Vitro* Toxicity Assessment

C2C12 myoblasts (ATCC CRL-1772) were cultured in DMEM with 10% fetal bovine serum and 1% penicillin streptomycin. Cells were plated in 24-well tissue culture plates with 50,000 cells/mL/well in DMEM with 2% horse serum and 1% penicillin streptomycin, and left to differentiate into myotubes for 9 days. Media was exchanged on days 3 and 6 of differentiation. CPE dilutions in DMEM with supplements were filtered with a 0.2 μm syringe filter and added to plated 3T3s and C2C12s aseptically. Cells were maintained at 37°C in 5% CO_2 balance air. At 24 hours, cell viability was assessed using a colorimetric assay (MTT kit, Promega G4100 Madison, WI), in which a yellow tetrazolium salt (MTT) is metabolized in live cells to form insoluble purple formazan crystals. The purple crystals are solubilized by the addition of a

detergent, and the color is then be quantified spectrophotometrically. At the 24-hour time point, 150 μL of MTT reagent was added to the cells, followed by a four-hour incubation at 37 °C and subsequent addition of 1 mL solubilization solution (detergent). The absorbance was read at 570 nm using the SpectraMax 384 Plus fluorometer (Molecular Devices, Sunnyvale, CA) after overnight incubation. Cells were also monitored visually to confirm the results of the MTT assay. Each plate contained media only wells whose absorbance was subtracted from the rest of the plate as noise. All groups were then normalized to blank media.

3.2.10 Statistical Analysis

All data populations were first assessed to determine which were normally distributed. Normally distributed data are presented as means with standard deviation, and compared by t-tests and analysis of variance (ANOVA), where specified; data not normally distributed are presented as medians with 25th and 75th percentiles and compared by Mann-Whitney U-test. MTT assay results are described parametrically with means with standard deviation, and compared by t-tests and analysis of variance (ANOVA). Statistical significance, for both parametric and nonparametric tests, is defined as $P < 0.05$.

3.3 Results

3.3.1 System description and validation

An initial aim of this work was to establish a reproducible *in vitro* method for studying tympanic membrane (TM) permeability and assessing the effects of chemical penetration enhancers (CPEs) on permeant flux. Immediately after middle ear dissection, TMs were inspected under 10X magnification for signs of perforation or unexpected discontinuities, but this alone is not sufficient to ensure membrane integrity of the TM *in vivo*. The first challenge was therefore to determine which TM samples were fit for diffusion studies. A similar challenge in transdermal drug delivery (TDD) research is met by measuring the electrical resistance of the skin and determining a threshold above which the samples' sodium ion permeability coefficient is similar to that of human skin *in vivo* [4, 5]. As a result of this and subsequent work, human epidermis with stratum corneum (HES) samples with a resistivity (resistance * exposure area) of < 35 kOhm*cm^2 are considered compromised and are not used for diffusion studies. However, as chinchilla TMs are not well characterized with respect to their ion permeability, determination of a resistivity threshold is relegated to inference based on comparative anatomy.

The current that passes through intact HES samples was found to increase linearly with signal frequency at a given voltage, due to the capacitive effects of lipid bilayers in the epidermis and stratum corneum. As biological membranes, including skin, are traditionally modeled electrically as *RC* parallel circuits (Figure 3.1), the observed current-frequency relationship suggests that the

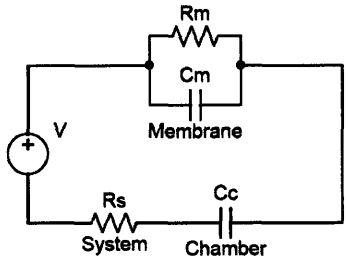

Figure 3.1. General RC circuit model for biological membrane and associated measuring apparatus.

membrane resistance calculated by Ohm's Law (R = V/I) at as low as 10 Hz is greater than the magnitude of the impedance of the capacitor:

$$R_m \geq \frac{1}{\omega C_m}$$

The lipid-corneocyte matrix of the human stratum corneum is known to consist of 70-100 lipid bilayers in sequence [6-8], comprising 15-20 corneocyte layers each separated by lipid domains of approximately 0.05 μm thickness [9-11]. The chinchilla TM is covered by 3 or 4 corneocyte layers of stratum corneum [12], and is approximately 20% the total thickness of the average human stratum corneum. The stacked corneocyte layers of the stratum corneum can be modeled as x serial RC current dividers (Figure 3.2), where x represents the number of corneocyte layers. According to this model, the resistance of a given corneocyte layer, R_n is

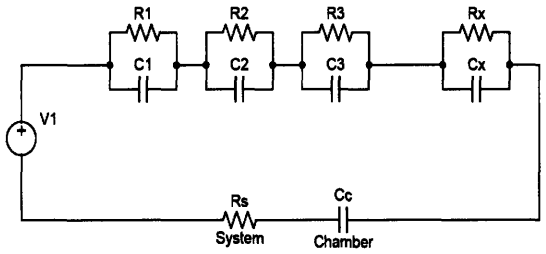

Figure 3.2. RC circuit model of multi-lamellar stratum corneum.

$$R_n = \frac{R_i}{1+(\omega C_i R_i)^2},$$

resulting in a total resistance, R_T, of

$$R_T = \sum_{i=1}^{x} \frac{R_i}{1+(\omega C_i R_i)^2},$$

assuming that $R_1 = R_2 = R_3 \ldots = R_x$ and $C_1 = C_2 = C_3 \ldots = C_x$, then $R_T = xR_n$. An intact skin resistance value of $R_{skin} \geq 178$ kOhm should therefore correspond to an intact TM resistance of $R_{TM} \geq 36$ kOhm, if the resistance of the stratum corneum scales linearly with corneocyte layer. Given a TM diameter of 8 mm, an acceptable TM resistivity should be approximately $RA_{TM} \geq 18$ kOhm*cm^2. The TMs harvested in these experiments had resistivity values that ranged from 0.8

to 30 kOhm*cm^2, including those with visible perforations. Three groups of TMs could then be classified based on their resistivity: (1) $RA \geq 18$ kOhm; (2) $1 < RA < 18$ kOhm*cm^2, grossly intact, with no visible perforation; and (3) $RA \leq 1$ kOhm*cm^2, or with visible perforation. When these three groups are plotted as current-frequency functions (Figure 3.3), one observes a rapid change in current-frequency relationship as RA decreases.

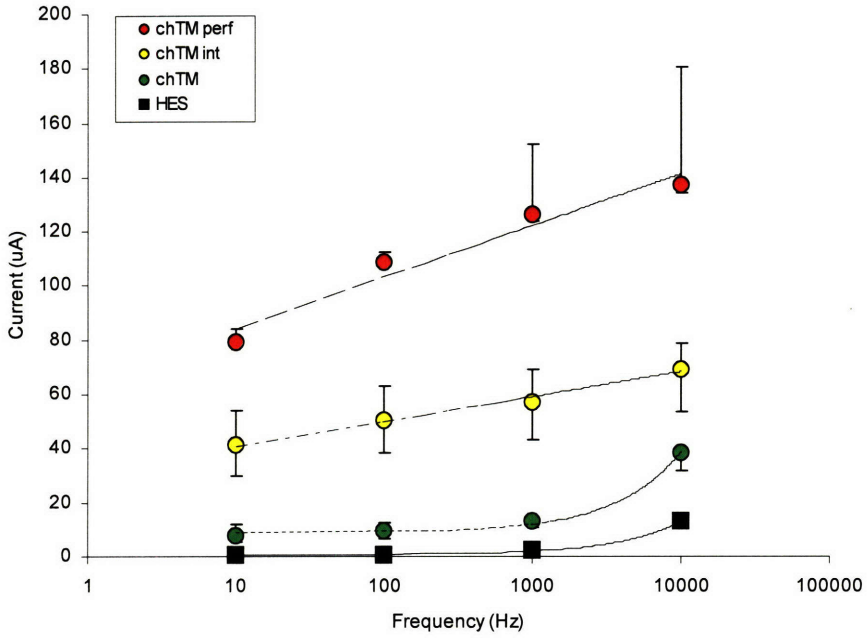

Figure 3.3. The relationship between trans-membrane current and signal frequency suggests a capacitive component of the membranes. TM populations were divided into three groups: (1) perforated (red); (2) acceptable (green), by the RA > 18 kOhm*cm^2 definition; and (3) all those in between (yellow). As the median resistance decreases among the groups, the current-frequency relationship changed. Data are presented as medians with 25th and 75th percentile error bars (those not seen are smaller than the data points).

If the bulk resistance, Rs, and capacitance, Cs, of the testing system are measured empirically, the model circuit of this system (Figure 3.2) can be used to generate the expected current-frequency relationship of membranes with different resistances. The applied sinusoidal voltage and measured currents can be described as phasors with magnitude and phase,

$$I = |I|e^{ej\theta_I} \quad V = |V|e^{ej\theta_V}$$

The current is therefore described by I = V/Y, where

$$Y = \frac{1}{R_T + \frac{1}{j\omega C_T} + R_S + \frac{1}{j\omega C_C}}, \text{ and } \frac{1}{j\omega C_T} = \sum_{i=1}^{x} \frac{-j\omega C_i R_i}{1 + (\omega C_i R_i)^2}.$$

The medians of the empirically determined current-frequency values for each of these three groups fit the output of this model (Figure 3.4).

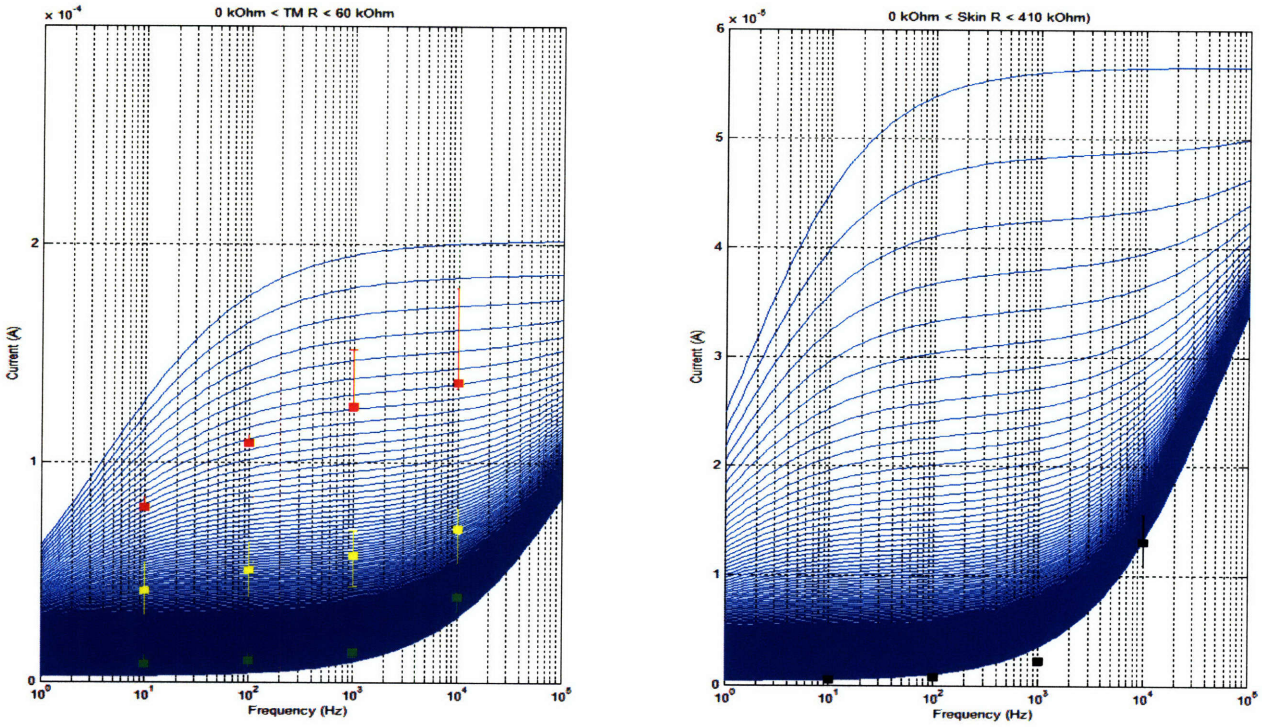

Figure 3.4. Experimental determination of trans-TM and trans-HES current on signal frequency (red squares) plotted with output current-frequency relationships generated from an RC circuit model (blue lines).

When the theoretical plots are generated using resistance ranges that match those of each empirical group (Figure 3.5), the results confirm the data-model agreement.

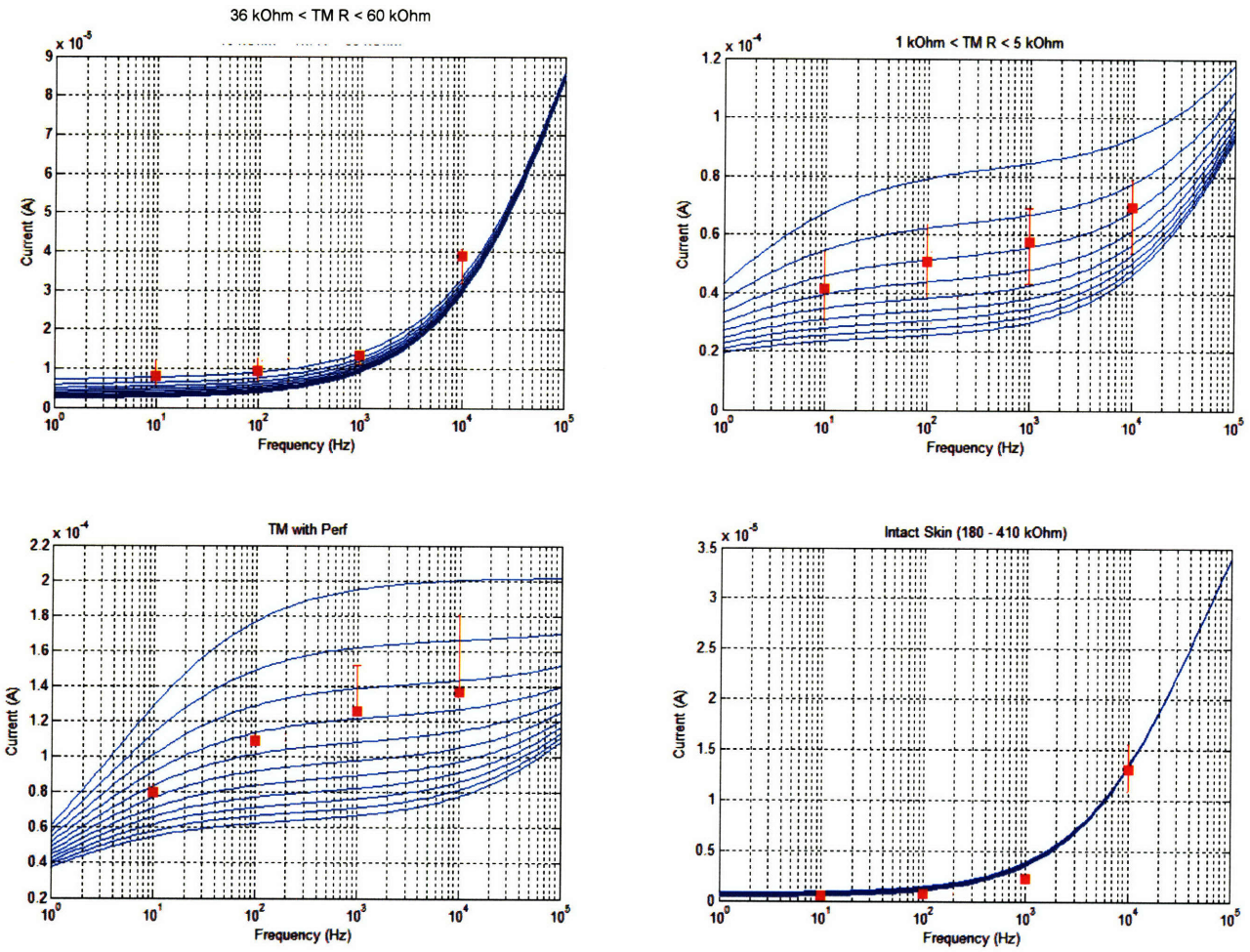

Figure 3.5. Experimental determination of trans-TM and trans-HES current on signal frequency (red squares) plotted with output current-frequency relationships generated from an RC circuit model (blue lines), using the same range of membrane resistance values. The top-left plot includes all TMs with R > 36 kOhm (RA > 18 kOhm*cm^2), the suggested cut-off for uncompromised membranes suitable for use in diffusion experiments. This current-frequency relationship is similar to that of intact skin (lower-right plot).

This model assumes a capacitance value previously measured in skin stratum corneum (10^{-8} F/cm^2 [13, 14]). Empirical resistance and capacitance values of the respective measuring apparatus (i.e., 12-well plate or glass diffusion (Franz) cell) were also employed. These parameters are as follows:

Parameter	Value	Unit
R_m	[0:410:410000]	Ω
V	0.1414	V
F	logspace(0,5,100)	Hz
w	2.*pi.*f	rad
C_m	5e-8	F
R_{sw}	700	Ω
R_{sfr}	2500	Ω
C_s	0	F
C_w	1e-4	F
C_{fr}	5e-5	F

where R_m is the membrane resistance; V is voltage; f is frequency; C_m is membrane capacitance; R_{sw} and R_{sfr} are the resistances of the measuring system including the 12-well plate and Franz cell, respectively; C_w is the capacitance of the 12-well plate system; and C_{fr} is the capacitance of the Franz cell system.

3.3.2 Ciprofloxacin flux v. condition

Only harvested TMs with $RA \geq 18$ kOhm*cm^2 were used for permeability experiments. Representatives from two CPE classes were selected for this study based on their history of use in transdermal drug delivery and their favorable enhancement/irritation ratio [15]: SLS (anionic surfactant) and limonene (monocyclic terpene). Bupivacaine, an animo amide local anesthetic, was incorporated in formulations for its potential clinical benefit on OM-associated otalgia, and because of prior evidence that amino amides (e.g., tetracaine [15]) have an enhancing effect on small molecule flux across skin [16]. CPE concentrations were selected based on those demonstrated to be effective and minimally toxic in previous transdermal studies [15]. Bupivacaine concentration was selected as the highest used clinically in injected IV solutions (0.5% (w/v)).

The cumulative ciprofloxacin to cross the TM was initially compared to that to cross HES after a 48-hour exposure to 1% ciprofloxacin solution alone and with SLS or limonene (Figure 3.6). In both cases, ciprofloxacin flux increased with the addition of CPEs: in TMs, flux increased from 0.15 (0-0.23) $\mu g/cm^2/hr$ with no CPE to 1.4 (1.2-1.4) $\mu g/cm^2/hr$ with 2% limonene and to 0.48 (0.45-0.50) $\mu g/cm^2/hr$ with 1% SLS; in HES, flux increased from 0 (0-0) $\mu g/cm^2/hr$ with no CPE to 0.53 (0.35-0.87) $\mu g/cm^2/hr$ with 2% limonene. Though the addition of 1% SLS did not significantly increase flux across HES within 48 hours, 120-hr flux values were significantly higher than with no CPE over the same time frame (0.25 (0.09-0.32) $\mu g/cm^2/hr$ versus 0 (0-0) $\mu g/cm^2/hr$).

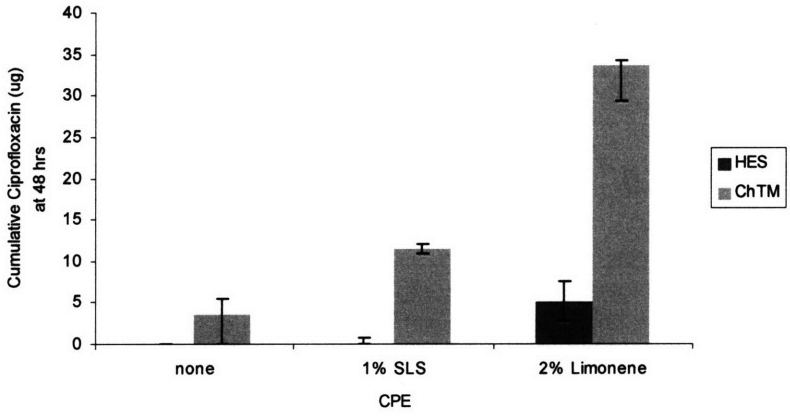

Figure 3.6. Comparison of ciprofloxacin delivery across human epidermis with stratum corneum (HES) and chinchilla tympanic membranes (chTMs). The two membranes showed similar relative sensitivity to 1% SLS and 2% limonene with respect to permeability to ciprofloxacin. Data are medians with 25th and 75th percentile error bars ($n \geq 4$).

Addition of 0.5% bupivacaine to 1% ciprofloxacin solutions alone and with 1% SLS or 2% limonene significantly increased ciprofloxacin flux across HES and TM (Figure 3.7). However, the magnitude of permeability was not consistent between HES and TM samples; though bupivacaine improved limonene-enhanced HES permeability only modestly (though still significantly), its addition to limonene in TM samples lead to effects that appear synergistic. By contrast, bupivacaine appeared to have a large effect on HES permeability regardless of combination with other CPEs, and its effects were not significantly increased with the addition of

SLS or limonene; bupivacaine enhancement in TMs was modest (yet significant), similarly unimproved by addition of SLS, but greatly increased when combined with limonene.

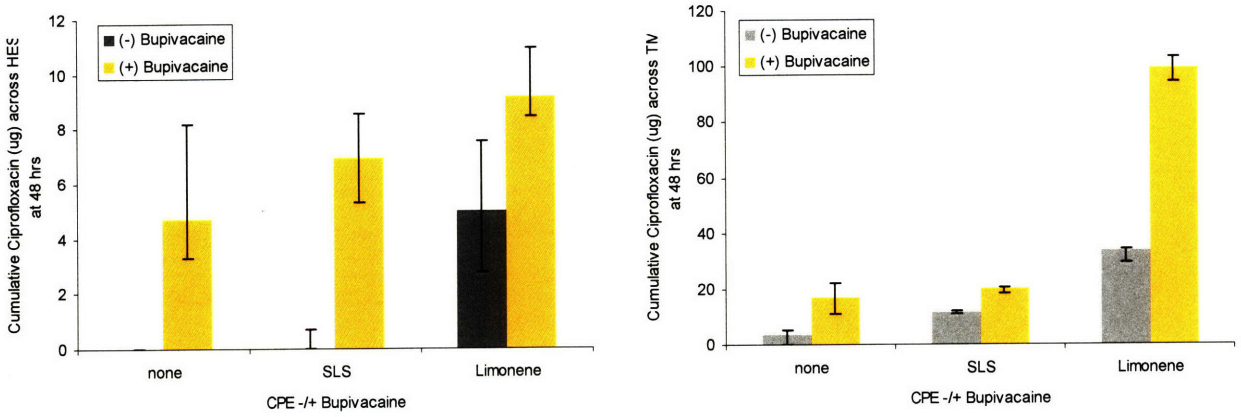

Figure 3.7. Addition of bupivacaine (0.5%) to ciprofloxacin/CPE mixtures resulted generally increased permeability to ciprofloxacin. Data are medians with 25th and 75th percentile error bars ($n \geq 4$).

Eradication of resistant *H. influenzae* or *S. pneumoniae* requires a minimum inhibitory concentration (MIC) of up to 4 μg/mL ciprofloxacin [17]. Given a median middle ear volume of 4-6 mL, effective localized treatment of OM requires delivery of at least 16 μg, preferably within 6-12 hours of application, with minimal irritation to TM tissue. Because limonene is known to have little toxicity in dermal keratinocytes and fibroblasts [15], crude mixtures of bupivacaine, SLS, and limonene were prepared in 1% ciprofloxacin solution in order to accelerate ciprofloxacin flux and investigate evidence of synergistic interactions among these CPEs. These mixtures' effects on TM permeability to ciprofloxacin resulted in decreased time needed to exceed the target MIC (Figure 3.8); with bupivacaine, SLS, and limonene combined, ciprofloxacin levels exceeded the MIC within 6 hours, and reached nearly 30X the MIC within 48 hours.

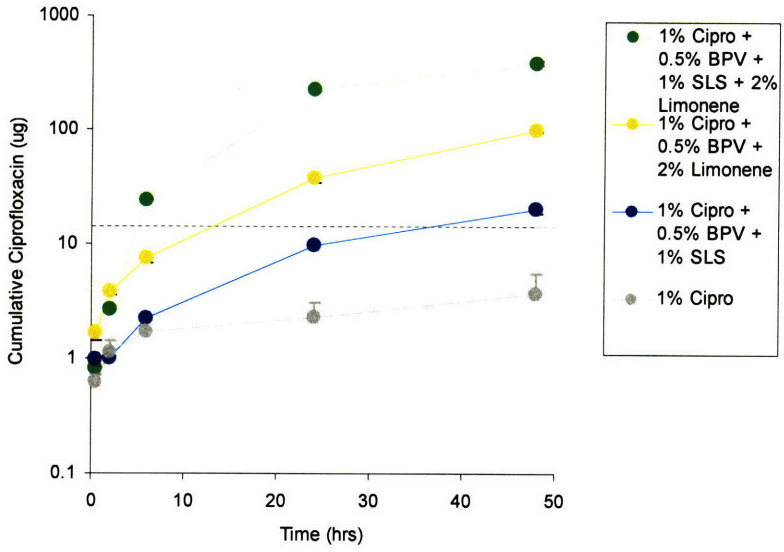

Figure 3.8. Trans-TM ciprofloxacin differed considerably with CPE environment. All CPE combinations involving bupivacaine exceeded the target ciprofloxacin MIC (shown as dashed line), but did so on different time courses. Trans-TM ciprofloxacin flux in the absence of CPEs was non-zero, but failed to reach MIC-levels within 48 hours. Data are presented as medians ($n \geq 4$) with 25th and 75th percentile error bars (smaller than data point radius if not seen).

3.3.3 *In vitro* toxicity

Increased permeability of the TM is not clinically useful if it cannot be achieved safely. Toxicity is especially relevant to two cell types: fibroblasts, which are important to the structural and functional integrity of the TM, and myoblasts, critical to normal middle ear muscle (MEM) function. Although the correlation between *in vitro* and *in vivo* toxicity is notoriously difficult to characterize [18, 19], *in vitro* toxicity assays can provide a first approximation of a drug or material's biocompatibility.

CPE toxicities have been previously assessed in keratinocyte-fibroblast co-cultures [15, 19] and indicate minimal toxicity due to limonene, but moderate toxicity due to SLS.

In vitro myotoxicity assays were conducted at CPE dilutions exceeding conservative expectations of middle ear concentrations (10% of initial formulation concentrations). Myoblast toxicity was minimal with bupivacaine, limonene, and bupivacaine plus limonene up to 18 hours (the longest time point tested), but SLS reduced cell viability by over 80% within 2 hours of exposure (Figure 3.9). This is consistent with previously published SLS toxicity in other cell types [20-22], though it is noteworthy that SLS is known to have only minimal *in vivo* irritation effects on skin, and is an FDA-approved food additive. It should also be mentioned that a middle ear concentration of 0.1% SLS assumes that 100% of the incorporated SLS in a 300 μL drop enters the middle ear.

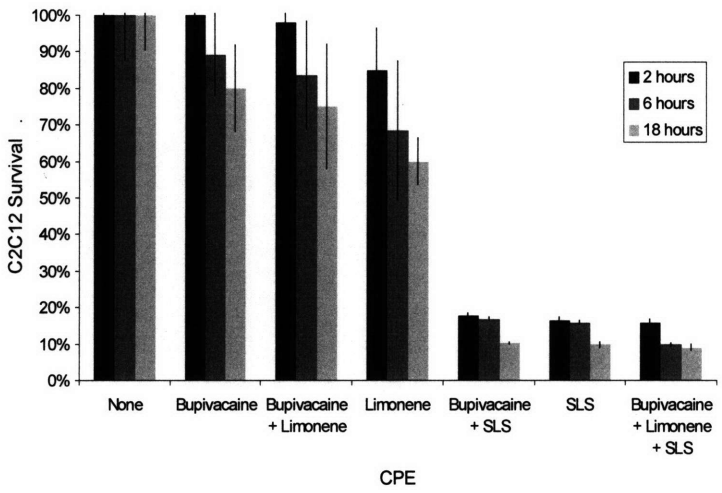

Figure 3.9. C2C12 myoblast toxicity was nonexistent or minimal for all conditions except those involving SLS, which reduced cell viability by 80%, regardless of its combination with other CPEs. Limonene toxicity was small but significant at 6 and 18 hours, but not at 2 hours. The concentrations used were: bupivacaine (0.05%), limonene (0.2%), SLS (0.1%), regardless of whether applied alone or in combination. Values are means ± standard deviations (n = 8).

3.4 Discussion

This work provides demonstration of analogous permeability changes in chinchilla TMs and HES in response to individual CPEs, but suggests differences in possible synergies of bupivacaine-limonene, bupivacaine-SLS, and bupivacaine-limonene-SLS combinations for increasing TM permeability to ciprofloxacin. Though data here are not sufficient to comment definitively on the comparative synergistic effects of the CPE combinations in HES v. TMs, we provide strong evidence that the difference in stratum corneum thickness between the two membranes influences the relative effects of bupivacaine on SLS and limonene (Figure 3.7). This raises questions regarding the transferability or interchangeability between from the transdermal literature to continued TM permeability studies.

Recent exploration of the correlation between skin electrical resistance and permeability to various hydrophilic and hydrophobic compounds has resulted in efforts to screen for effective CPEs in a high-throughput fashion, without need for extended, multi-day diffusion experiments. Within the transdermal literature there is demonstration of correlation between decreased skin resistivity and increased permeability to hydrophilic small molecules, and correlation between CPEs' effects on skin resistivity and on hydrophilic permeant flux [23]. However, changes in resistivity are less robust predictors of skin permeability to hydrophobic small molecules, presumably due to complex hydrophobic interactions with the lipid-rich matrix of the stratum corneum and the fact that hydrophobic molecules diffuse primarily through intercellular lamellar lipid bilayers [24]. Similar demonstration of *in vitro* correlation between TM electrical resistance and trans-TM permeant flux would help identify whether the relationships observed in skin hold true in the TM.

When trans-TM ciprofloxacin flux within CPE groups (none v. 1% SLS v. 2% limonene) is compared to the magnitude of their respective effects on TM resistance reduction, there is early evidence of a similar relationship to that reported in skin (Figure 3.10).

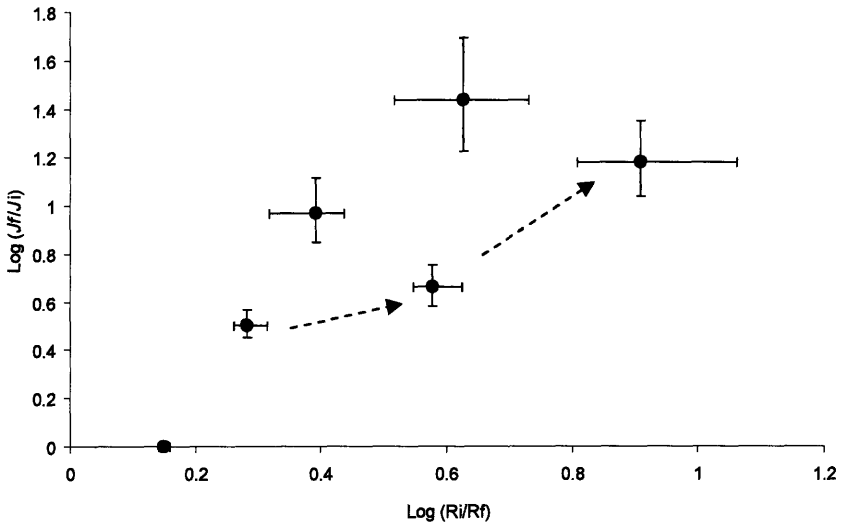

Figure 3.10. Increased ciprofloxacin flux and decreased TM resistance due to 48-hour exposure to single or combination CPEs. Each point represents median values obtained from TM populations ($n \geq 4$) treated with different CPE/ciprofloxacin mixtures. Dotted arrows point from a single CPE mixture (1% SLS) to one with 2 CPEs (1% SLS + 0.5% bupivacaine), to one with 3(1% SLS + 0.5% bupivacaine + 2% limonene).

Here, the log factor by which ciprofloxacin flux, J, is increased over the baseline ciprofloxacin flux (with no CPE), J_f/J_i, is plotted against the log factor of resistance decrease, R_i/R_f. Of interest here is that certain CPE combinations had a greater effect on membrane resistance than on ciprofloxacin flux. The addition of 0.5% bupivacaine to 1% SLS, for example, resulted in an insignificant increase in ciprofloxacin flux compared to 1% SLS alone, yet had a large impact on membrane resistance. This is perhaps due to CPE effects on ciprofloxacin solubility within the donor mixture, and is revisited in Chapter 5 for further discussion. When only single CPEs are

considered (i.e., 0.5% bupivacaine, 1% SLS, and 2% limonene), there is early evidence of correlation between CPE-induced flux increase and resistance decreased ($R^2 = 0.97$).

3.5 References

1. Secondi, U., *Structure and function of the lamina propria of the tympanic membrane in various mammals.* AMA Arch Otolaryngol, 1951. **53**(2): p. 170-81.
2. Hasegawa, M., Y. Saito, and I. Watanabe, *Iontophoretic anaesthesia of the tympanic membrane.* Clin Otolaryngol Allied Sci, 1978. **3**(1): p. 63-6.
3. Tang, H., et al., *Theoretical description of transdermal transport of hydrophilic permeants: application to low-frequency sonophoresis.* J Pharm Sci, 2001. **90**(5): p. 545-68.
4. Kasting, G.B. and L.A. Bowman, *Electrical analysis of fresh, excised human skin: a comparison with frozen skin.* Pharm Res, 1990. **7**(11): p. 1141-6.
5. Kasting, G.B. and L.A. Bowman, *DC electrical properties of frozen, excised human skin.* Pharm Res, 1990. **7**(2): p. 134-43.
6. Elias, P.M., et al., *X-ray diffraction analysis of stratum corneum membrane couplets.* J Invest Dermatol, 1983. **80**(3): p. 213-4.
7. Elias, P.M., J. Goerke, and D.S. Friend, *Mammalian epidermal barrier layer lipids: composition and influence on structure.* J Invest Dermatol, 1977. **69**(6): p. 535-46.
8. Madison, K.C., et al., *Presence of intact intercellular lipid lamellae in the upper layers of the stratum corneum.* J Invest Dermatol, 1987. **88**(6): p. 714-8.

9. Holbrook, K.A. and G.F. Odland, *Regional differences in the thickness (cell layers) of the human stratum corneum: an ultrastructural analysis.* J Invest Dermatol, 1974. **62**(4): p. 415-22.

10. Swartzendruber, D.C., et al., *Molecular models of the intercellular lipid lamellae in mammalian stratum corneum.* J Invest Dermatol, 1989. **92**(2): p. 251-7.

11. Swartzendruber, D.C., et al., *Evidence that the corneocyte has a chemically bound lipid envelope.* J Invest Dermatol, 1987. **88**(6): p. 709-13.

12. Vrettakos, P.A., S.P. Dear, and J.C. Saunders, *Middle ear structure in the chinchilla: a quantitative study.* Am J Otolaryngol, 1988. **9**(2): p. 58-67.

13. Elden, H.R., ed. *Biophysical Properties of the Skin.* 1971, John Wiley and Sons: New York. 513-550.

14. Chizmadzhev, Y.A., et al., *Electrical properties of skin at moderate voltages: contribution of appendageal macropores.* Biophys J, 1998. **74**(2 Pt 1): p. 843-56.

15. Karande, P., et al., *Design principles of chemical penetration enhancers for transdermal drug delivery.* Proc Natl Acad Sci U S A, 2005. **102**(13): p. 4688-93.

16. Walker, R.B. and E.W. Smith, *The role of percutaneous penetration enhancers.* Adv Drug Delivery Rev, 1996. **18**: p. 295-301.

17. Rodvold, K.A. and M. Neuhauser, *Pharmacokinetics and pharmacodynamics of fluoroquinolones.* Pharmacotherapy, 2001. **21**(10 Pt 2): p. 233S-252S.

18. Godin, B. and E. Touitou, *Transdermal skin delivery: predictions for humans from in vivo, ex vivo and animal models.* Adv Drug Deliv Rev, 2007. **59**(11): p. 1152-61.

19. Hawksworth, G.M., *Advantages and disadvantages of using human cells for pharmacological and toxicological studies.* Hum Exp Toxicol, 1994. **13**(8): p. 568-73.

20. Babich, H. and J.P. Babich, *Sodium lauryl sulfate and triclosan: in vitro cytotoxicity studies with gingival cells.* Toxicol Lett, 1997. **91**(3): p. 189-96.

21. Patil, S., et al., *Quantification of sodium lauryl sulfate penetration into the skin and underlying tissue after topical application--pharmacological and toxicological implications.* J Pharm Sci, 1995. **84**(10): p. 1240-4.

22. Jain, P.T., et al., *Studies of skin toxicity in vitro: dose-response studies on JB6 cells.* Toxicol Pathol, 1992. **20**(3 Pt 1): p. 394-404.

23. Karande, P., A. Jain, and S. Mitragotri, *Relationships between skin's electrical impedance and permeability in the presence of chemical enhancers.* J Control Release, 2006. **110**(2): p. 307-13.

24. Mitragotri, S., *Effect of bilayer distruption on transdermal transport of low-molecular weight hydrophobic solutes.* Pharm Res, 2001. **18**(7): p. 1018-23.

4 Effects of Chemical Penetration Enhancers on Local Anesthetics and Nerve Blockade

4.1 Introduction

Otologia (acute ear pain) is a defining, persistent symptom of acute otitis media (AOM). The inability of traditional local anesthetics to penetrate the stratum corneum of the tympanic membrane (TM) has led to reformulation and iontophoresis efforts aimed at overcoming the impermeable lipid-protein matrix [1, 2]. In addition to penetrating the stratum corneum of the TM, local anesthetics also must traverse the epineurium, perineurium and endoneurium of nerve fibers in order to reach their intended sight of action. Consequently, much higher concentrations of local anesthetics are required to be effective when used clinically than in isolated nerves [3-7]. Chemical penetration enhancers (CPEs), a diverse group of molecules that increase small molecule flux across biological barriers, may therefore increase the quality (density and/or duration) of nerve block.

CPEs have been used to increase the permeability of the lipid-protein barriers of the skin, and thereby increase drug flux, for over thirty years [8-11]. Surfactants, a heterogeneous group of amphiphilic organic molecules with hydrophilic heads and hydrophobic tails, are a well-known class of CPEs. Several sub-classes of surfactants (e.g., anionic, cationic, and nonionic) have been studied in the context of transdermal permeation, and are believed to reversibly modify lipids by adsorption at interfaces and removal of water-soluble agents that act as plasticizers [12, 13]. Cationic surfactants are known to produce greater increases in permeant flux than anionic surfactants, which, in turn, increase permeability more than nonionic surfactants [14-16]. Cationic surfactants, however, are generally more damaging to the skin [15]. A broad range of

non-surfactant chemical enhancers has also been investigated (e.g., alcohols, sulfoxides, polyols, fatty acids, esters, terpenes, and cyclodextrins), with mechanisms of action that typically include denaturation of proteins within and between keratinocytes, and/or modification or disruption of lipids that results in increased lipid bilayer fluidity [12-17].

The literature suggests that a small molecule's hydrophobicity has a U-shaped effect on its ability to penetrate biological barriers [18]: drugs with an intermediate degree of hydrophobicity penetrate more effectively than those that are very hydrophobic or very hydrophilic. There are some data to suggest that this relationship holds true for local anesthetics penetrating to or into peripheral nerve [19]. Consequently, one would expect that CPEs, if effective, would benefit hydrophilic compounds to a greater extent than those with intermediate degrees of hydrophobicity. To test this hypothesis, we have selected tetrodotoxin (TTX) as an example of the former category and bupivacaine (log P = 3.41 [20]) as an example of the latter [18].

TTX is a charged, very hydrophilic small molecule (318.28 g/mol) that blocks the sodium channel at site 1, on the outer surface of the neuron. It is a very potent local anesthetic, but does not cause the myo- and neurotoxicity associated with conventional local anesthetics. Bupivacaine is a partially neutral (pKa = 8.2), amphiphilic small molecule (288.43 g/mol) that binds the sodium channel on the cytosolic side of the axonal cell membrane.

Here, we test two principal hypotheses: that CPEs will improve the quality of nerve blockade from local anesthetics, and that the improvement will be proportionately better for hydrophilic (TTX) than for more hydrophobic (bupivacaine) compounds. The potential enhancement of the nerve blockade with TTX is of particular interest to us because the principal limiting factor to its clinical use is its systemic toxicity [21, 22]; it would be beneficial if CPEs reduced the TTX dose needed to provide a given duration of block. We also examine the effect of a range of CPEs

differing in charge (cationic, anionic, and nonionic) and hydrophobicities (differences in carbon chain length), and use cell culture and histology to assess the potential cytotoxicity and biocompatibility of the CPEs.

4.2 Materials & Methods

4.2.1 Animal Care

Young adult male Sprague-Dawley rats (350-420 g) were obtained from Charles River Laboratories (Wilmington, Massachusetts) and housed in groups of two per cage on a 6 a.m. to 6 p.m. light/dark cycle. All animals were cared for in accordance with protocols approved institutionally and nationally.

4.2.2 Chemical Enhancers & Solution Preparation

Representative enhancers from three different classes of surfactants were obtained from Sigma (St. Louis, MO): sodium lauryl sulfate (SLS) and sodium octyl sulfate (SOS), anionic surfactants; dodecyltriethylammonium bromide (DDAB) and octyltriethylammonium bromide (OTAB), cationic surfactants; and Tween 20 and Tween 80, nonionic surfactants (Table 4.1). Tetrodotoxin (TTX) and bupivacaine (Sigma) solutions were prepared in saline individually and in combination with each enhancer the night before scheduled injections. TTX and bupivacaine concentrations were chosen to be near the bottom of their respective dose-response curves [7, 23]; enhancer concentrations were initially chosen to be approximately 50% of those used successfully in transdermal applications, followed by lower and higher concentrations as needed to obtain a dose-response curve.

4.2.3 Sciatic Blockade Technique

Animals were cared for in compliance with protocols approved by the Massachusetts Institute of Technology (MIT) Committee on Animal Care, in conformity with the NIH guidelines for the care and use of laboratory animals (NIH publication #85-23, revised 1985). Rats were anesthetized using isoflurane in oxygen. A 23-gauge needle was introduced posteromedial to the greater trochanter, and 0.3 mL of the drug +/- enhancer solution was injected upon contacting bone in the left leg. To generate the dose-response curves for the CPEs, four animals were injected with each CPE at 5 different concentrations (each alone and with 30 μM TTX). Larger sample sizes were obtained at the following concentrations that were important for further experiments: 11 mM SOS, 2 mM SLS, 9 mM SLS, 17 mM SLS, 35 mM SLS, 46 mM Tween 80 (n = 8); 4 mM SLS (n = 16); and 23 mM Tween 80 (n = 22). For CPEs injected with 1.39 mM bupivacaine, n = 4 for each CPE-bupivacaine combination. A total of 12 animals were injected with 1.39 mM bupivacaine alone (no CPE).

4.2.4 Assessment of Nerve Blockade

In all experiments, the experimenter was blinded as to what treatment any given rat had received. Presence and extent of nerve blockade was investigated as previously described [7, 22-25]. Briefly, thermal nociception of each leg was assessed, with the right (uninjected) leg serving as an untreated control.

Thermal nociception was assessed by a modified hotplate test. Hind paws were exposed in sequence (left then right) to a 56°C hot plate (Model 39D Hot Plate Analgesia Meter, IITC Inc., Woodland Hills, CA). The time (latency) until paw withdrawal was measured with a stopwatch.

If the animal did not remove its paw from the hot plate within 12 seconds, it was removed by the experimenter to avoid injury to the animal or the development of hyperalgesia.

The duration of thermal nociceptive block was calculated as the time required for thermal latency to return to a value of 7 seconds from a higher value. Seven seconds is the midpoint between a baseline thermal latency of approximately 2 seconds in adult rats, and a maximal latency of 12 seconds. Latencies > 7 sec were considered to be effective blocks.

As previously reported [7, 25], the experimenter demonstrated >99% successful blocks with 0.1-0.3 mL of 0.25%-0.5% (8.7-17 mM) bupivacaine, therefore suggesting that differences in block duration reflected actual pharmacological differences rather than operator error.

4.2.5 Tissue Harvesting and Histology

Animals were euthanized with carbon dioxide, and the sciatic nerves and adjacent tissues were harvested for histology. Tissues were fixed in Accustain (formalin-free fixative) company, city, state, embedded in paraffin, sectioned, and stained with hematoxylin and eosin by the Department of Comparative Medicine at MIT (fee for service), using standard techniques.

4.2.6 Cell Culture

C2C12, a mouse myoblast cell line (American Type Culture Collection, ATCC, CRL-1772, Manassas, VA) was cultured to proliferate in Dulbecco's Modified Eagle's Medium (DMEM) supplemented with 20% Fetal Bovine Serum and 1% Penicillin Streptomycin (Pen Strep). All cell culture supplies were purchased from Invitrogen (Carlsbad, CA) unless otherwise noted.

Cells were plated in 24-well tissue culture plates with 50,000 cells/mL/well in DMEM supplemented with 2% Horse Serum and 1% Pen Strep, and left to differentiate into myotubules for 10-14 days. During differentiation, media was exchanged every 2 to 3 days. After one week of myotube differentiation, 100 μL of the 10x enhancer +/- TTX containing media was added to 900 μL of fresh media; 100 μL of PBS was added in control wells. The enhancer solution was prepared by dissolving the enhancer in PBS and stirring overnight. The solution was filtered aseptically using a 0.2 μm syringe filter. The TTX, or PBS for groups not containing drug, was added aseptically to the enhancer solution. At 2, 8, 24, or 96 hours the plates were assayed as described below. Cells were maintained at 37°C in 5% CO_2 balance air.

4.2.7 Assessing viability

Cell viability was assessed using a colormetric assay (MTT kit, Promega G4100 Madison, WI) in which a yellow tetrazolium salt (MTT) is metabolized in live cells to form insoluble purple formazan crystals. The purple crystals are solubilized by the addition of a detergent, and the absorbance is then be quantified spectrophotometrically. At each time point 150 μL of MTT reagent was added to the cells. Following a four hour incubation at 37 °C, 1 mL of solubilization solution (detergent) was added. The absorbance was read at 570 nm using the SpectraMax 384 Plus fluorometer (Molecular Devices, Sunnyvale, CA) after overnight incubation. Cells were also monitored visually to confirm the results of the MTT assay. Each plate contained media only wells whose absorbance was subtracted from the rest of the plate as noise. All groups were then normalized to blank media.

4.2.8 Statistical Analysis

In vivo neurobehavioral data were not normally distributed, and are therefore presented as medians with 25^{th} and 75^{th} percentiles and compared by Mann-Whitney U-test. MTT assay results are described parametrically with means +/- standard deviations and compared by t-tests and analysis of variance (ANOVA). Statistical significance, for both parametric and nonparametric tests, was defined as $P < 0.05$.

4.3 Results

Our hypothesis was that nerve block from a hydrophilic local anesthetic (TTX) would be more susceptible to prolongation by CPEs than that from a more hydrophobic one (bupivacaine). We therefore studied TTX first, to establish the effective concentration range for surfactants.

4.3.1 Effect of enhancers on nerve blockade with TTX

Injection of 0.3 mL of 30 μM TTX caused sensory blockade in 29% of animals tested (n = 24). The median duration of block was 0 minutes, with 25th and 75th percentiles of 0 minutes and 47 minutes, respectively. The selected concentration was based on previous observations [22] and chosen for further studies as improvement of nerve blockade could easily be detected. Dose-response curves were obtained for the duration of block from 30 μM TTX with varying concentrations of SLS and SOS (anionic surfactants), DDAB and OTAB (cationic surfactants), and Tween 20 and Tween 80 (nonionic surfactants) individually (Table 4.1; Figure 4.1). The group that received DDAB was also injected with 30 μM TTX in 32 mM of the enhancer, but those data are not included in Figure 4.1 because none of those rats' nerve blocks resolved (returned to normal function) within a 7-day observation period.

CPE	Structure	Class	MW	L
Sodium Octyl Sulfate (SOS)	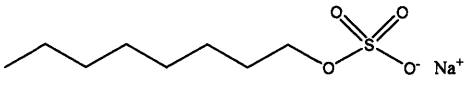	Anionic	232.28	8
Sodium Dodecyl Sulfate (SLS)	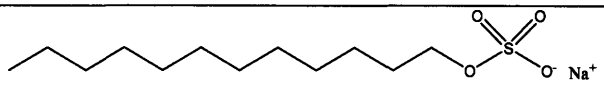	Anionic	288.38	12
Octyl-trimethyl-ammonium Bromide (OTAB)	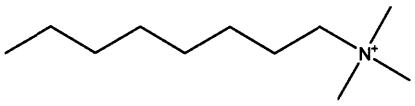	Cationic	252.23	8
Dodecyl-trimethyl-ammonium Bromide (DDAB)	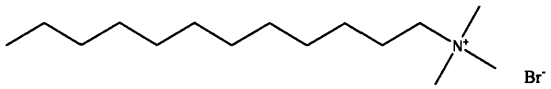	Cationic	308.34	12
Tween 20	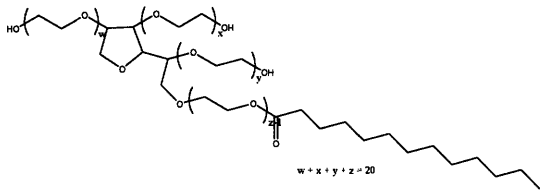	Nonionic	1228	12
Tween 80	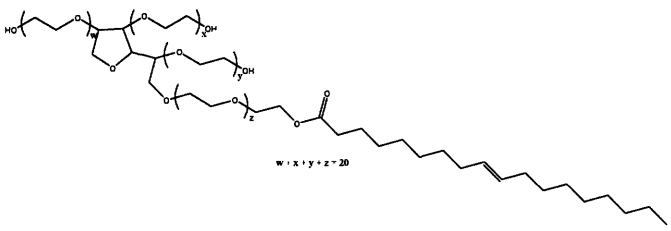	Nonionic	1310	17

Table 4.1. MW = molecular weight; L = length of carbon chain.

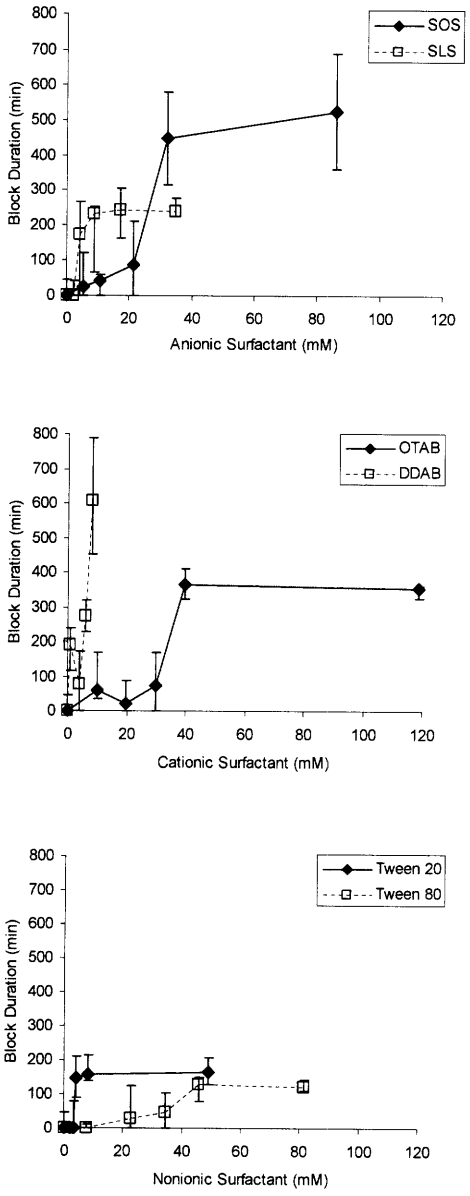

Figure 4.1. Effect of CPE concentration on the duration of sensory block from 30 μm TTX. Durations are expressed as medians with 25th and 75th percentiles ($n \geq 4$).

In most cases, the enhancers demonstrated a concentration-dependent increase in block duration before reaching a plateau. This maximal duration of block was used as a measure of efficacy for all CPEs except for DDAB, where we used the longest duration of block from which the animals recovered. There was a range of maximum durations of block due to the CPEs, the greatest being seen with DDAB (median maximum duration of block = 606 minutes; Figure 4.1, Table 4.2). All the CPEs increased the percentage of animals that developed effective nerve block from 29.2% with TTX alone to 88-100% (Table 4.3). At the concentrations needed to cause this maximum percentage of block, all CPEs significantly improved TTX block duration (for SOS, SLS, OTAB, DDAB, Tween 20, and Tween 80, $p < 0.001$ compared to the duration of block from TTX alone). In general, the maximum prolongation of TTX block by the cationic surfactants (OTAB, DDAB) was statistically significantly greater than prolongation by the other CPEs. The maximum prolongation of TTX block by the nonionic surfactants (Tween 20, Tween 80) was generally less than that by the others ($p < 0.05$ by Mann-Whitney U-test).

As a measure of the potency of the block-prolonging effect of the CPEs, we determined by interpolation the concentration of each enhancer required to achieve a duration of block of 100 minutes (the EC_{100min}, Table 4.2). Tween 20, SLS, and DDAB were more potent (lower EC_{100min}) than Tween 80, SOS, and OTAB (Figure 4.1; Table 4.2).

TTX 30 μM with:	**Maximum Block Duration (MBD, minutes)**	**EC_{MBD} (mM)**	**EC_{100min} (mM)**	**EC_{50eff} (mM)**
-	0 (0 – 47)	-	-	-
SOS	521 (361-669)	86	22	32
SLS	240 (255-277)	35	3	4
OTAB	353 (327-361)	119	31	30
DDAB	606 (452-788)	8	1	6
Tween 20	163 (129-206)	49	4	3
Tween 80	120 (111-143)	81	40	34

Table 4.2. CPEs markedly prolonged the maximum block duration (MBD) from 30 μm TTX. The EC_{MBD} is the CPE concentration that caused the maximum prolongation of block from 30 μm TTX. The EC_{100min} is the interpolated concentration of CPE that increased the block duration of 30 μm TTX to 100 min. The EC_{50eff} is the concentration of a given CPE that caused a half-maximal increase in duration of block (half-MBD) of 30 μm TTX. Block durations are medians with 25th and 75th percentiles in parentheses; n = 4 for all CPE concentrations, except those specified in *Materials and Methods* (where n = 8-22).

Within the classes of enhancers where the members differed only in the length of the carbon chain (SOS-SLS; OTAB-DDAB), those with the eight-carbon chain were less potent than those with the twelve-carbon chain. (In the case of the Tween compounds, that relationship was reversed, but there are other significant differences in the Tweens' structures.) Each enhancer was also injected alone, without TTX, to confirm that the increased duration of block was not due to analgesic or toxic effects of the enhancers themselves; with one exception (32 mM DDAB), the CPE alone did not cause nerve blockade.

TTX 30 μm with:	Highest % Animals with Effective Block	CPE Concentration (mM)
-	29	-
SOS	100	32
SLS	88	17
OTAB	100	40
DDAB	100	6
Tween 20	100	4
Tween 80	100	81

Table 4.3. CPEs increased the percentage of animals developing effective block from 30 μm TTX. Blocks were considered effective if latency was > 7 seconds at any point. The CPE concentration listed was the lowest needed to achieve the highest percentage of animals with block; n = 4 for all conditions except TTX alone (n = 24) and TTX + SLS (n = 8).

4.3.2 Effect of enhancers on nerve blockade with bupivacaine

We determined that 1.39 mM (0.04%) bupivacaine had performance characteristics comparable to 30 μm TTX with respect to percentage of animals blocked and median duration of block (Table 4.4) by producing a dose-response curve of sciatic nerve blocks with six bupivacaine concentrations spanning the range 0.69 mM – 6.9 mM, (n = 4-12 rats per concentration). We tested 1.39 mM bupivacaine with each of the CPEs at a concentration that created a half-maximal increase in the duration of block of TTX, the EC_{50eff} (Table 4.2). None of the 6 enhancers tested in these

Bupivacaine 1.4 mM with the EC_{50eff} of:	Duration of Sensory Block (minutes)	% Animals with Effective Block
-	0 (0-34)	42 (5/12)
SOS	0 (0-8)	25 (1/4)
SLS	22 (0-60)	50 (2/4)
OTAB	0 (0-0)	0 (0/4)
DDAB	0 (0-0)	0 (0/4)
Tween 20	0 (0-19)	25 (1/4)
Tween 80	0 (0-0)	0 (0/4)

Table 4.4. Duration and frequency of nerve block from bupivacaine with and without each of the CPEs at the EC_{50eff} from Table 2a. Durations of effective block (DEB) are expressed as medians with 25th and 75th percentiles in parentheses. For bupivacaine alone, n = 12; for bupivacaine + CPE, n = 4.

experiments resulted in a statistically significant change in the duration of bupivacaine nerve block (Table 4.4).

4.3.3 *In vitro* toxicity

C2C12 myotube cultures were exposed to each enhancer at its EC_{50eff} with and without TTX and assayed for viability after 2 hours (Figure 4.2). The most toxic enhancers were DDAB and SOS, followed by SLS, OTAB, Tween 80, and Tween 20, in order of decreasing toxicity. C2C12 viability decreased with increased duration of exposure to all CPEs except Tween 20, which remained at untreated-control levels after an 8-hour exposure (data not shown). Addition of TTX to the cell culture medium did not impact cell survival when given alone or in the presence of enhancers.

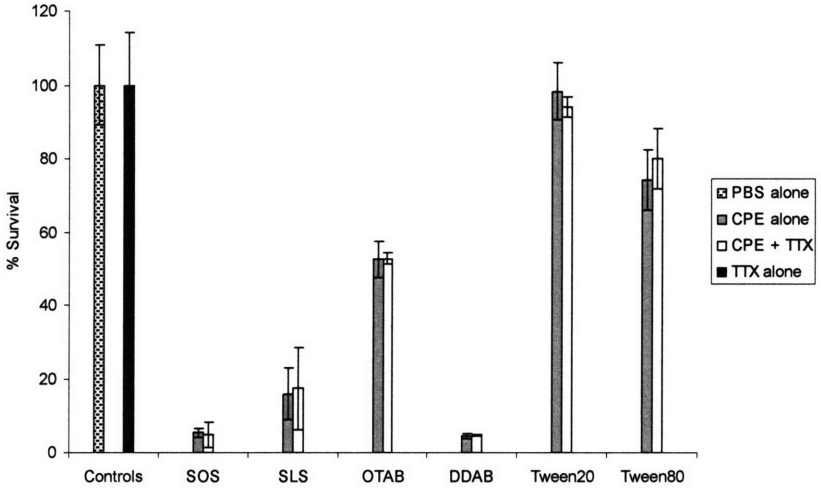

Figure 4.2. Survival of C2C12 myotubes after a 2-hour exposure to the EC_{50eff} of each CPE alone and with 30 μM TTX, *in vitro*. Controls include cells exposed to PBS or TTX alone. Data are shown as means ± standard deviations (n = 4).

4.3.4 *In vivo* toxicity

The sciatic nerves and surrounding muscle of rats injected with the EC_{50eff} of each enhancer (i.e., the same concentration used *in vitro*), with and without TTX, were examined for evidence of inflammation and tissue injury four days after injection (Figure 4.3, A-F). Four animals were injected in each group.

Animals injected with the EC_{50eff} of SOS, SLS, OTAB, Tween 20 and Tween 80 showed no significant muscle or nerve injury, although some samples in all groups showed mild inflammation with macrophages and lymphocytes around the muscle and nerve, without evidence of infiltration, fibrosis, or atrophy within the muscle or nerve (Figure 4.3, A). Because Tween 20 at its EC_{50eff} showed no evidence of toxicity *in vitro* or *in vivo*, additional concentrations were tested to determine the highest sub-toxic concentration. Tween 20 at 24.4 and 81.4 mM showed progressively worsening (mild to moderate) muscle atrophy and inflammation (Figure 4.3, B-C), similar in type but not severity to that seen with the DDAB EC_{50eff} (Figure 4.3, D). (Note that 81.4 mM is more than twenty times the EC_{50eff} of Tween 20.) Samples from animals injected with DDAB consistently showed moderate to severe infiltration of macrophages and lymphocytes, atrophy and degeneration of muscle fibers, and fibrosis of the tissue (Figure 4.3, D). An additional two animals were injected with 3% (97.3 mM) DDAB (the concentration at which animals developed irreversible nerve block). These showed deep and severe tissue damage, including ischemic necrosis, accompanied by severe and extensive inflammation.

Animals injected with the EC_{50eff} of the enhancers together with 30 μm TTX showed the same histological results as those without TTX (Figure 4.3, E-F). Again, some of the samples exposed to DDAB showed severe lymphocytic inflammatory infiltration of muscle with

degenerative changes, regenerative changes, and fibrosis (Figure 4.3, F). These samples also showed a mild lymphocytic infiltrate of nerve and focal fat necrosis.

Indicators of nerve fiber injury, including fibrosis and myelin ovoids, were not seen in any samples, but subtle degrees of damage to myelinated nerve fibers cannot be accurately assessed using paraffin-embedded, hematoxylin-eosin-stained sections.

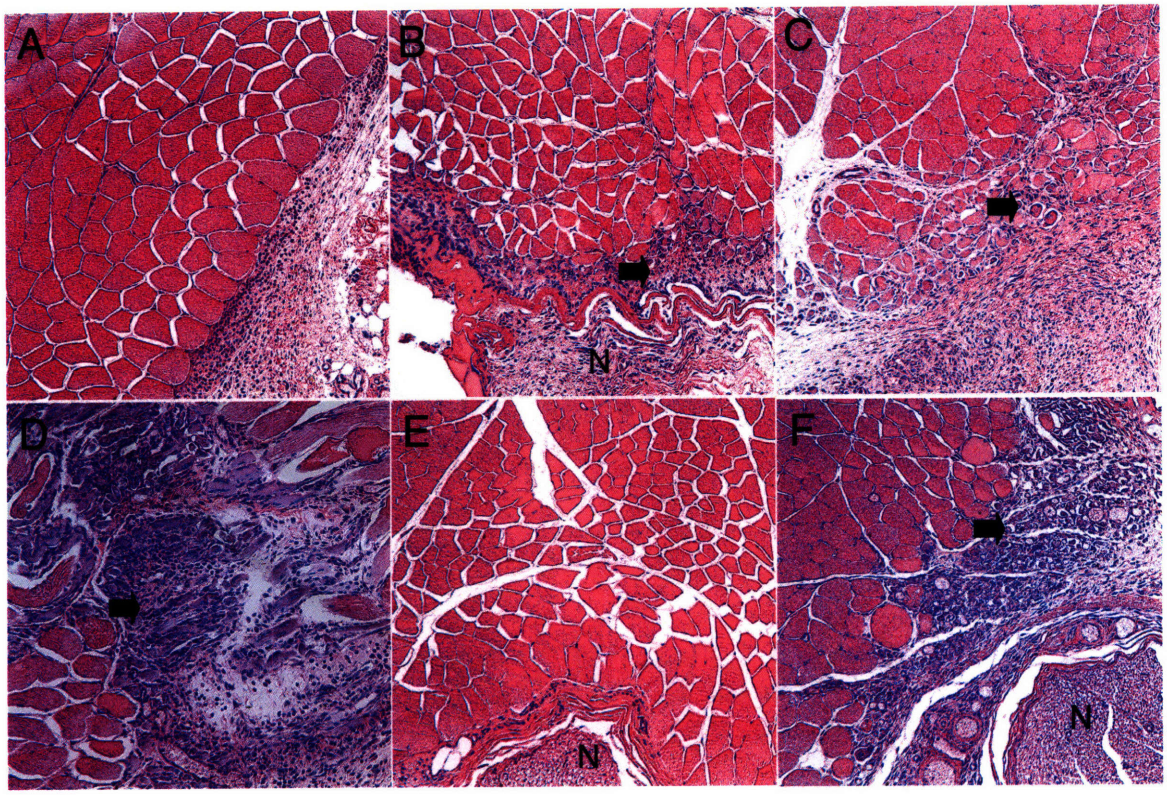

Figure 4.3. Histology of the site of injection CPEs at EC_{50eff} with or without TTX 4 days after injection. (A) Skeletal muscle and nerve from regions injected with Tween 20 (shown), SOS, SLS, OTAB or Tween 80 at their EC_{50eff} showed no evidence of injury to muscle or nerve. Tween 20 at higher concentrations, of 21.4 mM (B) and 81.4 mM (C), led to increased inflammation with muscle fiber atrophy (arrows). DDAB at its EC_{50eff} (D) showed surface inflammation similar to that seen with the higher Tween 20 concentrations. Injections of Tween 20 (shown, E), Tween 80, SOS, SLS, and OTAB with TTX showed no evidence of injury to muscle or nerve. Injection of DDAB with TTX (F) showed findings similar to those seen with DDAB in the absence of TTX. N = nerve. Magnification = 200X.

4.4 Discussion

Surfactant CPEs caused a concentration-dependent increase in TTX-induced nerve block, but, at the concentrations tested here, did not enhance block from bupivacaine. This difference is due to the fact that TTX is extremely hydrophilic, having an obligate charge, while bupivacaine – like all amino-ester and amino-amide local anesthetics – can be conditionally hydrophobic due to its aromatic moiety and tertiary amine. There is a pH-dependent equilibrium between the cationic protonated form of bupivacaine that is water soluble and the neutral form that is soluble in organic solvents (i.e. is hydrophobic), and therefore partitions relatively easily into cell membranes and other biological barriers. We postulate that the relatively pronounced improvement in block from TTX with CPEs relates to its lack of hydrophobicity, whereas bupivacaine does not benefit because its structure already permits easy crossing of biological barriers. We have previously described that high (millimolar) concentrations of adrenergic antagonists, far in excess of the range in which they are active on adrenergic receptors, greatly prolonged the duration of block by TTX [23]. The results presented here support the view that the prolongation of nerve block by those polycyclic compounds was due to flux enhancement (i.e. those compounds were acting as CPEs).

All the CPEs examined here resulted in prolongation of TTX block. Though there was a considerable range in the magnitude of enhancement, no individual CPE or class of CPE (anionic, cationic, or nonionic surfactant) clearly performed better than all the others. The nonionic agents' block prolongations, though significant, were shorter than those of the other CPEs. This is consistent with the effects of surfactants on permeant flux across the stratum corneum and epidermis of the skin [15].

The various CPEs resulted in a variety of patterns of block prolongation with respect to the magnitude of the increase in the maximum duration of block, or the improvement (reduction) in the EC_{100min}. It is important to be careful in using the EC_{100min} to make comparative statements regarding potency, since the shapes of the dose-response curves for each CPE are not always similar. In general, the magnitude of the maximal improvement in duration of block (the maximum block duration, MBD) did not correlate well with the potency (EC_{100min}, Figure 4.4).

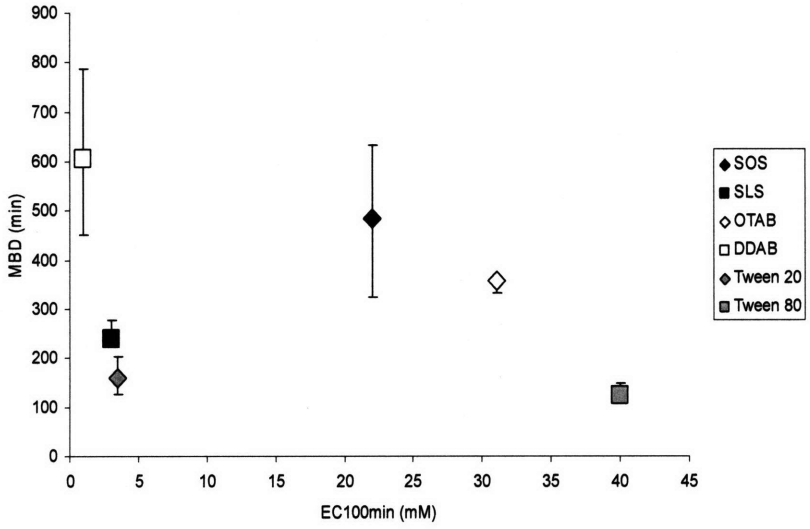

Figure 4.4. Maximum block duration (MBD) plotted against interpolated EC_{100min} values for each CPE indicate no correlation ($R^2 = 0.08$). Anionic, cationic, and nonionic surfactants are grouped by color (black, grey, and white, respectively). Block durations are expressed as medians with 25th and 75th percentiles ($n \geq 4$).

There also was no consistent pattern in the effect of hydrophobic chain length on duration of block. In the anionic surfactants, SLS and SOS differ only by 4 carbons and 8 associated hydrogens in their carbon chains, but are otherwise identical (Table 4.1). SLS, which has the longer carbon chain, had a lower EC_{100min}, while SOS produced longer maximal blocks. In the cationic surfactants, DDAB and OTAB similarly have 12 and 8 carbons in their carbon chains, respectively, but are otherwise identical. DDAB, which has the longer carbon chain, had both a lower EC_{100min} and produced longer maximal blocks than OTAB. Although Tween 20 and

Tween 80 have differing hydrocarbon chain lengths, the large difference in the remainder of their structures precludes statements on the effect of that variable on biological effects. The purpose of these experiments was to determine whether the prolongation of nerve blockade was feasible with various classes of enhancers. Further study is necessary to elucidate structure-activity relationships of these enhancers with respect to charge and hydrophobicity.

Efforts to understand the molecular structures responsible for transdermal potency and toxicity have focused on hydrophobicity (log P), polarity, dispersivity, and hydrogen bonding ability, and led to two CPE groupings, "fluidizers" and "extractors," that reflect two independent mechanisms of CPE action, based on independent molecular forces [26]. The potency of extractors is dependent on intramolecular forces (in particular, hydrogen bonding) that compete with the hydrogen bonding among lipid molecules responsible for lipid bilayer structural stability. However, because these same CPE hydrogen bonding forces compete with hydrogen bonds responsible for protein structure stability, extractor enhancement correlates with toxicity. With fluidizers, penetration enhancement and toxicity show less correlation because their ability to partition lipid membranes is less dependent on molecular forces that harm protein stability. As a result, potency tends to correlate with toxicity for anionic and cationic surfactants, but not for nonionic surfactants. Our data reveal severe shape differences in CPE-TTX dose-response curves (Figure 4.1) that make comparative statements of potency difficult, and suggest that structure-function generalizations based on a single concentration may be misleading.

CPEs varied widely in the cyotoxicity of their EC_{50eff}. In general, the agents that produced the longest maximal block durations were more toxic in cell culture (Figure 4.5, $R^2 = 0.66$). There was no correlation between the EC_{100min} and toxicity ($R^2 = 0.11$). With the cationic

surfactants, toxicity increased with molecular weight and carbon-chain length, while it decreased with the same parameters in anionic surfactants.

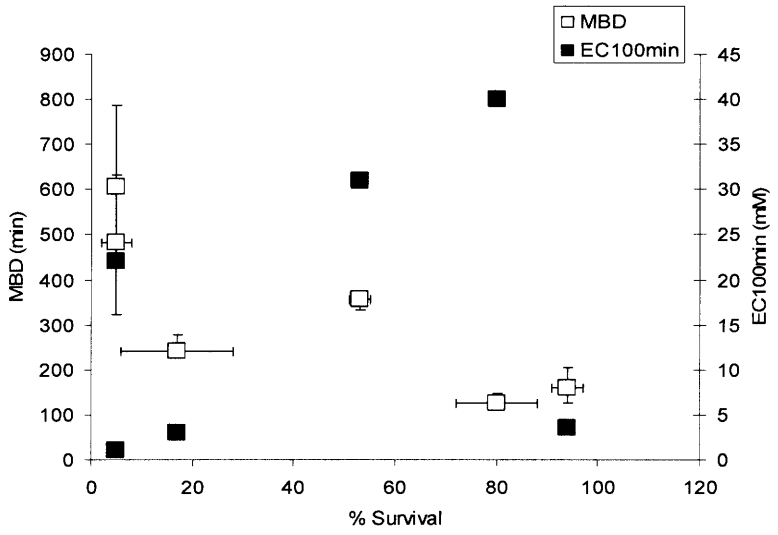

Figure 4.5. Maximum block duration (MBD) and EC_{100min} plotted against cell survival. The EC_{50eff} is the CPE concentration that caused a half-maximal increase in block duration. Cell survival data are means with standard deviations from C2C12 cells exposed to each CPE at its EC_{50eff} for 2 hours from Figure 2). Block durations are expressed as medians with 25th and 75th percentiles.

In assessing the trade-off between maximum block duration and cytotoxicity (Table 4.5), Tween 20 would appear to have the most favorable relevant ratios.

TTX 30 μm with:	**% Survival**	**MBD (100 - % Survival)**	**% Survival EC_{100min}**
SOS	5 ± 3	5.5	0.2
SLS	17 ± 11	2.9	5.7
OTAB	53 ± 2	7.5	1.7
DDAB	5 ± 0.2	6.4	5.0
Tween 20	94 ± 3	27	24
Tween 80	80 ± 8	6.0	2.0

Table 4.5. The maximum block duration (Table 2a), $EC_{100min\ (Tabl;)}$, and *in vitro* survival data (determined from C2C12 MTT assay). The values for maximal block duration and EC100 min are from Table 4.2; those for cell survival are derived from Figure 2. Cell survival data are mean percentages with standard deviations. For the two ratios in the columns on the right, a high value is favorable (good ratio of performance to toxicity).

However, this does not mean that Tween 20 would be the optimal enhancer for clinical use. The *in vivo* data showed that all compounds, with the notable exception of DDAB, caused little or no tissue injury when delivered at the same concentrations as used *in vitro* (the EC_{50eff}, which had caused approximately half-maximal increase in duration of block from TTX). This discrepancy between *in vitro* and *in vivo* results is not surprising. It may be explained by differences between cultured cell lines and *in vivo* tissue, but it is also possible that the local concentration of the CPEs dissipates rapidly after injection *in vivo*. We have seen a similar discrepancy with conventional local anesthetics [7]. Tetrodotoxin itself caused little or no toxicity, with or without enhancers, a finding consistent with prior experience [22]. The *in vivo* results suggest that enhancer toxicity can be minimal or non-existent within a concentration range that results in significant block duration, and that the most efficacious compounds could be used rather than those with the best toxicity profile from *in vitro* studies. There was little or no evidence of direct nerve injury in all the CPEs investigated, including concentrations of DDAB that resulted in long-term loss of nerve function. We note, however, that the use of paraffin-embedded tissue is relatively insensitive for the evaluation of damage to myelinated fibers. This study did not determine the ideal dose of TTX and enhancer to provide the longest safe nerve block.

Myotoxicity and neurotoxicity are well-known concomitants of conventional amino-ester and amino-amide local anesthetics, but not of tetrodotoxin [24, 27, 28]. However, TTX's principal disadvantage is systemic toxicity [24], which is dose-limiting. In these experiements, CPEs dramatically increased the median duration of block from a very low concentration of TTX (e.g. from 0 to 353 min by use of OTAB). These durations of block far exceed those that could be

achieved even by toxic, near-lethal concentrations of TTX in the absence of vasoconstrictors. For example, 50 μm TTX applied in the same manner without CPEs resulted in an average duration of block of approximately 150 minutes, but with a 20% mortality rate [24]. Although we have not demonstrated this formally, it would seem to follow from these facts that the use of CPEs would result in a marked improvement in the therapeutic index of TTX (the ratio of the effective to the lethal dose).

Flux enhancing agents caused a marked increase in nerve blockade duration from hydrophilic TTX, but did not improve block duration from amphiphilic bupivacaine. The prolongation of TTX block was provided by different types of surfactants. Although there was considerable cytotoxicity from some CPEs *in vitro*, histology from *in vivo* experiments showed little or no damage in muscle and nerve, except with DDAB. Further work is needed to better understand the relationship between enhancer molecular structure (e.g., charge and hydrocarbon chain length) and optimal efficacy-potency-toxicity profiles for potential use in a clinical setting.

4.5 References

1. Bingham, B., M. Hawke, and J. Halik, *The safety and efficacy of Emla cream topical anesthesia for myringotomy and ventilation tube insertion.* J Otolaryngol, 1991. **20**(3): p. 193-5.
2. Hoffman, R.A. and C.L. Li, *Tetracaine topical anesthesia for myringotomy.* Laryngoscope, 2001. **111**(9): p. 1636-8.
3. Schwartz, J.R., W. Ulbricht, and H.H. Wanger, *The rate of action of tetrodotoxin on myelinated nerve fibers of Xenopus laevis and Rana esculenta.* J Physiol (Lond), 1973. **233**: p. 167-194.
4. Hahin, R. and G. Strichartz, *Effects of deuterium oxide on the rate and dissociation constants for saxitoxin and tetrodotoxin action. Voltage-clamp studies on frog myelinated nerve.* J Gen Physiol, 1981. **78**(2): p. 113-39.
5. Chernoff, D.M. and G.R. Strichartz, *Kinetics of local anesthetic inhibition of neuronal sodium currents. pH and hydrophobicity dependence.* Biophys J, 1990. **58**(1): p. 69-81.
6. Lee-Son, S., et al., *Stereoselective inhibition of neuronal sodium channels by local anesthetics. Evidence for two sites of action?* Anesthesiology, 1992. **77**(2): p. 324-35.
7. Kohane, D.S., et al., *Sciatic nerve blockade in infant, adolescent, and adult rats: a comparison of ropivacaine with bupivacaine.* Anesthesiology, 1998. **89**(5): p. 1199-208; discussion 10A.
8. Bauerova, K., D. Matusova, and Z. Kassai, *Chemical enhancers for transdermal drug transport.* Eur J Drug Metab Pharmacokinet, 2001. **26**(1-2): p. 85-94.

9. Asbill, C.S., A.F. El-Kattan, and B. Michniak, *Enhancement of transdermal drug delivery: chemical and physical approaches.* Crit Rev Ther Drug Carrier Syst, 2000. **17**(6): p. 621-58.

10. Kanikkannan, N., et al., *Structure-activity relationship of chemical penetration enhancers in transdermal drug delivery.* Curr Med Chem, 2000. **7**(6): p. 593-608.

11. Karande, P., A. Jain, and S. Mitragotri, *Relationships between skin's electrical impedance and permeability in the presence of chemical enhancers.* J Control Release, 2006. **110**(2): p. 307-13.

12. Middleton, J.D., *Mechanism of action of surfactants on water binding properties of isolated stratum corneum.* J Soc Cosmet Chem, 1969. **20**: p. 399-403.

13. Ribaud, C., et al., *Organization of stratum corneum lipids in relation to permeability: influence of sodium lauryl sulfate and preheating.* Pharm Res, 1994. **11**(10): p. 1414-8.

14. Farber, E.M., ed. *Psoriasis*. 1982, Grune and Stratton: Orlando.

15. Kushla, G.P., et al., *Noninvasive assessment of anesthetic activity of topical lidocaine formulations.* J Pharm Sci, 1993. **82**(11): p. 1118-22.

16. Shen, W.W., A.G. Danti, and F.N. Bruscato, *Effect of nonionic surfactants on percutaneous absorption of salicylic acid and sodium salicylate in the presence of dimethyl sulfoxide.* J Pharm Sci, 1976. **65**(12): p. 1780-3.

17. Walker, R.B. and E.W. Smith, *The role of percutaneous penetration enhancers.* Adv Drug Delivery Rev, 1996. **18**: p. 295-301.

18. Bernards, C.M. and H.F. Hill, *Physical and chemical properties of drug molecules governing their diffusion through the spinal meninges.* Anesthesiology, 1992. **77**(4): p. 750-6.

19. Barnet, C.S., J.Y. Tse, and D.S. Kohane, *Site 1 sodium channel blockers prolong the duration of sciatic nerve blockade from tricyclic antidepressants.* Pain, 2004. **110**(1-2): p. 432-8.

20. Hansch, C., et al., *The expanding role of quantitative structure-activity relationships (QSAR) in toxicology.* Toxicol Lett, 1995. **79**(1-3): p. 45-53.

21. Kohane, D.S., et al., *The local anesthetic properties and toxicity of saxitonin homologues for rat sciatic nerve block in vivo.* Reg Anesth Pain Med, 2000. **25**(1): p. 52-9.

22. Kohane, D.S., et al., *A re-examination of tetrodotoxin for prolonged duration local anesthesia.* Anesthesiology, 1998. **89**(1): p. 119-31.

23. Kohane, D.S., et al., *Effects of adrenergic agonists and antagonists on tetrodotoxin-induced nerve block.* Reg Anesth Pain Med, 2001. **26**(3): p. 239-45.

24. Padera, R.F., et al., *Tetrodotoxin for prolonged local anesthesia with minimal myotoxicity.* Muscle Nerve, 2006. **34**(6): p. 747-53.

25. Masters, D.B., et al., *Prolonged regional nerve blockade by controlled release of local anesthetic from a biodegradable polymer matrix.* Anesthesiology, 1993. **79**(2): p. 340-6.

26. Karande, P., et al., *Design principles of chemical penetration enhancers for transdermal drug delivery.* Proc Natl Acad Sci U S A, 2005. **102**(13): p. 4688-93.

27. Benoit, P.W., A. Yagiela, and N.F. Fort, *Pharmacologic correlation between local anesthetic-induced myotoxicity and disturbances of intracellular calcium distribution.* Toxicol Appl Pharmacol, 1980. **52**(2): p. 187-98.

28. Sakura, S., et al., *Local anesthetic neurotoxicity does not result from blockade of voltage-gated sodium channels.* Anesth Analg, 1995. **81**(2): p. 338-46.

5 *In Situ* Hydrogel Formulations and Their Use in Trans-Tympanic Membrane Drug Delivery

5.1 Introduction

Localized, sustained drug delivery for treatment of otitis media (OM) can increase antibiotic efficacy and improve patient compliance, which together reduce the selective pressures responsible for antibiotic resistance generation. Increased permeability of the tympanic membrane (TM) to ciprofloxacin can be achieved using crude mixtures of various classes of chemical penetration enhancers (CPEs) individually, or in combination to minimize toxicity (Chapter 3). However, a sustained-release ear drop for trans-TM drug delivery must meet a number of criteria in order to be effective and clinically viable. In addition to delivering and sustaining sufficient drug concentrations to the sites of interest within hours of application, an appropriate delivery vehicle must be easily applied, should minimize auditory threshold shifts, and must be easily removed when necessary.

In situ gelation can be achieved by physical or chemical cross-linking using a number of mechanisms. Sensitivity to pH, light, temperature, and force can each provide the mechanism for controlled gelation, the choice of which depends on the site of application, the desired gelation kinetics, and the intended release kinetics of the incorporated therapies (see [1] for recent review of *in situ*-forming hydrogels). Therapy administered to the external auditory meatus (EAM) for treatment of OM benefits from a rapid liquid-gel transition, so that prolonged restraint or general anesthesia can be avoided in treating children. Two mechanisms are explored here based on their simple, rapid gelation, and their use of biocompatible polymers: (1)

reverse thermal gelation with poloxamer 407 (P407); and (2) polyelectrolyte complexing with chitosan and chondroitin sulfate.

P407 is a block copolymer (MW = 9,840-14,600) that consists of ethylene oxide (EO) and propylene oxide (PO) blocks arranged in a triblock structure EO_x-PO_y-EO_x, x = 95-105 and y = 54-60 [2]. It is a surfactant, with a hydrophilic-lipophilic balance (HLB) of 22 at 22°C, which improves solubility of and stratum corneum permeability to hydrophobic small molecules [3, 4]. However, its property most relevant to *in situ*-forming delivery systems is its thermoreversible gelation, which allows for easy application of a liquid drop into the external auditory meatus (EAM) and rapid gelation upon contact with the TM (35-37°C). Chitosan (Ch) and chondroitin sulfate (CS) are oppositely charged polyionic polysaccharides that can gel via polyelectrolyte complexing when properly mixed [5], thereby providing another means of *in situ* gelation with biocompatible, bioresorbable polymers. These *in situ* gelling mechanisms are selected because of their simplicity, low cost, and ease of use. The specific polymers are selected because of their previously demonstrated biocompatibility [6-8].

This work investigates the gelation kinetics and *in vivo* effects of P407 and Ch/CS hydrogels formulated for EAM application and trans-TM treatment of otitis media (OM).

5.2 Materials & Methods

5.2.1 Animal Care

All animals were cared for in accordance with protocols approved institutionally and nationally.

5.2.2 Chemical Enhancers and Formulation Preparation

All compounds were obtained from Sigma (St. Louis, MO), unless otherwise specified. Hydrogels were prepared as crude mixtures of gelling polymer (Poloxamer 407 (P407), chitosan (Ch), or chondroitin sulfate (CS)) and CPE (sodium lauryl sulfate (SLS), limonene, and/or bupivacaine) in antibiotic solution (1% ciprofloxacin). Antibiotic/CPE solutions were prepared separately and added to gelling polymers individually. P407 solutions at 18% (w/v) were prepared and allowed to mix overnight at 4°C; all other polymer solutions or suspensions were prepared at room temperature and set to mix on a stir plate overnight. All mixtures were applied *in vitro* and *in vivo* with 1-mL tuberculin syringes capped with a 20-gauge (1.1 x 48 mm) angiocatheter. Ch and CS polymers for the polyelectrolyte complexes were prepared individually and coinjected with a double-barreled syringe through a single 20-gauge angiocatheter-capped Y-piece.

5.2.3 Skin Preparation

Fresh frozen, full-thickness, human abdominal skin (hairless) was obtained from the National Disease Research Interchange (NDRI, Philadelphia, PA), and kept at -80°C for up to 4 weeks. On experiment day 0, full-thickness skin samples were covered with aluminum foil and air-thawed at room temperature. Skin samples were then placed face (stratum corneum) down in a water bath maintained at 60°C for 2 minutes. Forceps and weighing spatula were then used to separate the epidermis with stratum corneum from the underlying dermis. The dermis was discarded, and any remaining epidermis that was not immediately used for the present experiment was stored in a humidified chamber at 4°C for up to one week.

5.2.4 Tympanic Membrane Harvesting

Chinchillas were sacrificed by IP administration of Nembutal, and decapitated to facilitate access to ventral and dorsal regions of the skull adjacent to the temporal bone. In some cases, disjointed heads were frozen, and later thawed in normal (0.9%) saline, before further dissection. Soft tissue of the external ear and surrounding temporal bone was removed by scissors and rongeurs to expose the temporal bone, external auditory meatus (EAM), and auditory bulla, bilaterally. The bullae were carefully opened with a scalpel blade, and the opening enlarged with small rongeurs until the interior-medial surface of the tympanic membrane (TM) and ossicles could be seen. A myringotomy knife was introduced into this opening to sever the malleus-incus ligament, thereby freeing the TM from the surrounding middle ear. The remaining bone surrounding the EAM, lateral to the tympanic ring, was carefully removed until the EAM, tympanic ring, and TM could be separated from the temporal bone. The removed sample therefore consisted of an intact TM within the tympanic ring, exposed on both lateral and medial surfaces.

5.2.5 Skin Permeability Measurements

Heat-stripped epidermis with stratum corneum samples were secured between the adjoining orifices of both side-by-side (SxS) and vertical (Franz) diffusion cells (Permegear, Bethlehem, PA) with vacuum grease. The receiving chambers for all cells were filled with 3.5 or 5 mL PBS. The donor chamber volumes were 3.5 or 5 mL for the SxS cells and 100 or 200 μL for the Franz cells. At fixed time points (0.5, 2, 6, 24, 48, 120 hours), a 300 μL sample volume was removed from the receiving chamber and prepared for HPLC analysis of permeant concentration; an equivalent volume of PBS was returned to the receiving chamber.

5.2.6 TM Permeability Measurements

Each extracted TM (including the surrounding tympanic ring and adjacent EAM) was placed upright in a 12-well plate, with the TM surface perpendicular to the well base and the EAM longitudinal axis parallel to the well walls. A 3 mL volume of PBS was added to the well, so that the entire medial surface of the TM was submerged, and 100 μL of PBS, test solution, or gel formulation was pipetted into the EAM to cover the lateral TM surface. At pre-determined time points (0.5, 2, 6, 24, and 48 hours post treatment administration), a 100-μL sample from the 3-mL "receiving chamber" was removed, filtered, and transferred to an HPLC vial.

5.2.7 Skin and TM electrical impedance measurements

The electrical impedance of the skin was measured as previously described (Tang et al., 2001). Ag-Cl electrodes (In Vivo Metrics, Healdsburg, CA) were placed on either side of the

biological membrane (human epidermis with stratum corneum or chinchilla TM), in the donor and receiving media, and a signal generator (Hewlett Packard, HP 33120A) provided a 100 mV AC voltage for 5-10 seconds. The current passing through the membrane was measured with a Fluke Multimeter (Model 139, Fluke Corporation), and the electrical impedance was obtained using Ohm's Law. Background impedance measurements of PBS alone were made separately and subtracted from the initial impedance calculation to yield the membrane impedance; following the final time point in the extracted TM experiments, the TM surface was covered with a thin rubber disc and silicone adhesive, and the electrical impedance of the surrounding tympanic ring and EAM were measured and similarly subtracted from the initial TM+EAM impedance calculation. Any skin sample with an initial impedance x exposed area value of <50 kOhm*cm^2 was considered damaged, was discarded, and was subsequently replaced with an intact sample (Kushner et al., 2004; Kasting & Bowman, 1990).

5.2.8 High Performance Liquid Chromotography (HPLC)

Samples from each time point were filtered with 0.2 μm syringe filters (Acrodisc, Sigma) and pipetted into 100-μL HPLC vial inserts. Assays were performed on a Hewlett-Packard HP 1100 HPLC system. Samples in 20-μL volumes were injected onto a 4.6 (ID) x 250 (L) mm Atlantis dC_{18} 5 μm column. The column was eluted with an aqueous solution of 80:20 acetonitrile:NaH_2PO_4/H_3PO_4 (0.01M, pH=2.8) at 1 mL/min. Ciprofloxacin was detected by UV absorbance at 275 nm wavelength. Separate dilution standards were prepared by diluting 1% Ciprofloxacin solution (Bayer HealthCare, West Haven, CT) in PBS, 0.01 % to 1.0 x 10^{-5} % (w/v), on the day of analysis.

Chinchilla middle ear fluid (MEF) and plasma samples were prepared as previously described [9]. A 50-μL sample of MEF, plasma, or standard was added to 2 mL acetonitrile and 20 μL of 10 μg/mL levofloxacin (internal standard), vortexed, and centrifuged at 1500 *g* for 10 minutes. The 2 mL acetonitrile was then syringe-filtered into transferred to a 10 x 75 mm culture tube and evaporated at 50°C under nitrogen. The residue was constituted in 100 μL mobile phase and transferred to 100-μL HPLC vials inserts for analysis.

5.2.9 Hydrogel Mechanics & Formulation Assessment

Gelation times were measured in HPLC vials (10 x 25 mm) suspended in a 35°C water bath over a heated stir plate set to 200 rpm. After allowing for the vial temperature to equilibrate with that of the surrounding water, 0.1-1 mL of each gel was injected into a vial with an angiocatheter-capped 1-mL syringe. The gelation time was defined as the time required for the stir bar to stop rotating.

Release kinetics of ciprofloxacin from hydrogels was assessed in 12-well plates with transwell inserts. Transwell inserts (0.2 μm filter) were inserted into wells filled with 3 mL PBS. Equal volumes of gels were applied to the inserts, and 0.1 mL volumes of the PBS receiving medium were sampled at fixed time points (0.25, 0.5, 1, 2, 6, 24, 48 hrs) and replaced with an equal volume of PBS. Samples were chromatographically analyzed with HPLC for determination of ciprofloxacin concentrations.

Rheological data was collected with an ARG-2 controlled stress rheometer (TA Instruments). A 40 mm parallel plate was used with gap distances between 0.3 and 0.6 mm with 0.7 mL of hydrogel, depending on the formulation. Adhesive-backed 600-grit silicon carbide sandpaper was placed on the sample platform and oscillating plate in order to minimize slippage between

the hydrogel formulations and the shearing surface. Oscillatory stress sweep experiments were conducted with systematic ramping of stress amplitube from 0.5 to 200 Pa at 3 radians/sec oscillation frequency to identify the linear viscoelastic range. Frequency sweeps were conducted between 0.1 and 500 radians/sec at the stress value corresponding to the linear viscoelastic region of the oscillatory stress sweep output (typically between 10 and 40 Pa); these allowed for evaluation of elastic and loss moduli of the materials as a function of applied shear. Steady shear rate sweeps between 0.05 and 200 s^{-1} were applied to measure the shear thinning behavior of the polyelectrolyte gels.

5.2.10 Chinchilla Model of Otitis Media

Adult male chinchillas (400–600 g) were anesthetized with Ketamine (30 mg/kg) and Xylazine (4 mg/kg) and initially evaluated by tympanometry and otomicroscopy to confirm normal middle ear status. The fur covering the superior bullae was removed bilaterally, the bullae opened 3-5 mm with a scalpel, and 25 CFU non-typable *Haemophilus influenzae* (NTHi) in 100 μL Hanks balanced solution was inoculated directly into the middle ear, bilaterally, via the bullae openings. At 48 hours post-inoculation, tympanometry and otoscopy were again used to assess presence of TM inflammation, negative middle ear pressure, and/or middle ear effusion. Nasopharynx (NP) lavage was performed and cultured evidence of bacteria, and the bullae openings are re-opened for middle ear analysis. The contents of the middle ear were examined through an operating microscope, and mucosa samples collected for direct culture with a calcium alginate swab and streaked on chocolate agar plates. Middle ear fluid (MEF) was collected with an angiocatheter-capped 1-mL syringe; 500 μL Hanks balanced solution was used for lavage of

middle ear cavities if MEF was not present. Approximately 1.5 mL blood was obtained by superior sagital sinus puncture on day 2 post-inoculation, but before application of antibiotic treatment; samples were also drawn on day 7 post-inoculation (day 5 post-treatment).

Following tympanometric, otoscopic, and bacteriologic assessment of otitis media (OM) status on day 2, 500 μL hydrogel formulation was applied to the external autidory meatus (EAM) using a speculum and guided by a surgical microscope. Left ears were always treated with the test formulation, which consisted of antibiotic, gel polymers, and chemical penetration enhancers (CPEs). Right ears were used as controls; no-treatment controls, drug-gel controls (no CPEs), and gel-only controls (no CPEs, no drug) were all used. Middle ear and nasopharyngeal samples were collected on days 4 (post-treatment day 2), 7 (post-treatment day 5), and 11 (post-treatment day 9) and cultured to quantify CFUs.

5.2.11 Tissue Harvesting & Histology

Chinchillas were deeply anesthetized by IP administration of ketamine and Nembutal at twice the normal dosage. Middle ears were extracted as described above, quickly rinsed with PBS, and immediately soaked in Accustain (non-formalin fixative). Samples were kept in fixative at room temperature for one week, then transferred to 10% ethylene diamine tetraacetic acid (EDTA) to decalcify bone of the external auditory meatus (EAM), tympanic ring, and middle ear. After two weeks, the decalcified bone of the bulla was removed, leaving only the EAM, tympanic ring with intact TM, and the lateral wall of the middle ear cavity. Samples were then embedded in paraffin, sectioned (5 μm thick) to yield three cross-sections of the TM along the axis of the EAM, and stained with hematoxylin and eosin.

5.2.12 Auditory Brainstem Response (ABR) Measurements

ABR experiments were conducted with a custom-designed stimulus generation and measurement system built around National Instruments (Austin, TX) software (Lab View) and hardward. The hardware included a GPIB controller and an ADC board. The custom LabView program computed the stimuli, and downloaded the stimuli to a programmable stimulus generator (Hewlett Packard 33120A). The stimulus was then filtered by an antialiasing filter (KrohnHite 3901) and attenuated (Tucker-Davis Technologies). The filter and the attenuator were controlled by the LabView software. Simultaneous with stimulus output, the 2 ADC channels sampled the amplified ABR signal and the output of a microphone sealed in the ear canal of the animal.

The acoustic stimuli were pairs of 20-ms tone bursts of opposite polarity. The frequency of the bursts increased from 500 Hz to 16 kHz in octave steps. Each burst was sine windowed, with 40 ms between the two bursts. ABR responses to 250 pairs of stimuli were averaged at each stimulus level. The ABR response was computed from the sum of the averaged response to the two different polarities. Stimulus level was varied in 10 dB steps. A visual judgement of threshold at each stimulus frequency was determined post-measurement in a blinded fashion.

The attenuated stimulus was played through a hearing-aid earphone placed within the intact ear canal of adult female chinchillas (400-600 g) anesthetized by IP administration of Ketamine and Nembutal (50 mg/kg). The earphone coupler included a microphone that monitored the sound stimulus level. ABRs, obtained in a sound-attenuating booth, were measured with a differential amplifier with a gain of 10,000 and a measurement bandwidth of 100 Hz to 3 kHz. The measurements were obtained from the positive electrode in the muscle behind the measured

ear; the negative electrode was at the cranial vertex, and the ground electrode behind the contralateral ear.

5.2.13 Statistical Analysis

Data that were not normally distributed are presented as medians with 25^{th} and 75^{th} percentiles and compared by Mann-Whitney U-test. Normally distributed data, such as MTT assay results, are described parametrically with means +/- standard deviations and compared by t-tests and analysis of variance (ANOVA). Statistical significance, for both parametric and nonparametric tests, was defined as $P < 0.05$.

5.3 Results

5.3.1 P407 formulations and release kinetics

P407 in 1% ciprofloxacin solution has a shifted gelation temperature (T_{gel})-concentration curve compared with that of P407 prepared in water (Figure 5.1). This is consistent with P407's behavior in other solvents [10-12], suggesting that the dependence of micelle formation on temperature is altered, but not fundamentally inhibited by the ciprofloxacin or its low pH of 3-4. The P407 concentration identified as that which gels at 35°C is 18% (w/v) in 1% ciprofloxacin solution, with or without 0.5% bupivacaine + 1% SLS or 0.5% bupivacaine + 2% limonene. The time required for these P407 mixtures to gel at 35°C, from 22°C, was less than 10 seconds, and increased slightly with increased volume, from 0.1 to 1 mL, when applied to a geometry similar to that of the EAM (Figure 5.2).

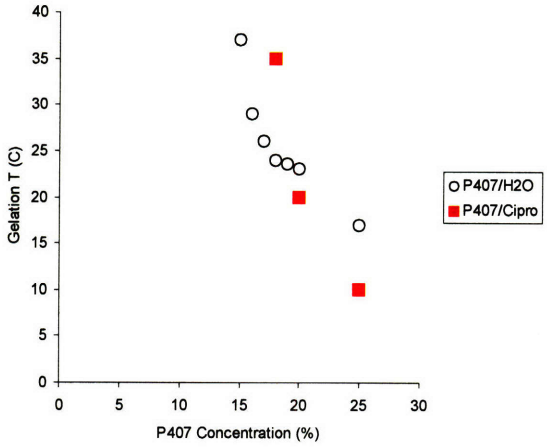

Figure 5.1. Sol-gel transition temperature for increasing P407 concentrations prepared in dH_2O and 1% ciprofloxacin solution. Average values shown with standard deviations (n = 3, standard deviation error bars smaller than data points).

Though ciprofloxacin (MW = 331.346) is small enough that it should be minimally effected by the micelle or cross-linked networks of polymer gels, the formulation environment

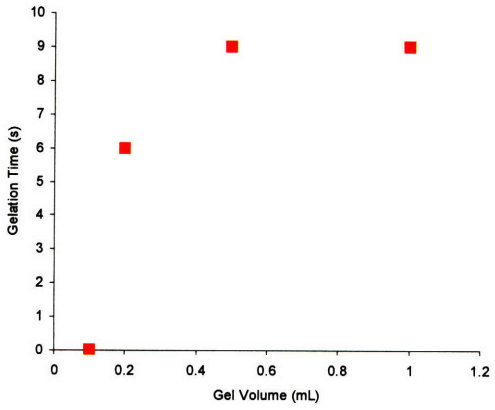

Figure 5.2. Time required for 18% P407 in 1% ciprofloxacin solution to gel after transfer from 22 to 35°C. N = 3 (standard deviation error bars smaller than data points).

can change the solubility of ciprofloxacin, and thereby alter its release kinetics. To investigate the effects of adding gelling polymers and CPEs to the ciprofloxacin solution, release of ciprofloxacin from P407 into PBS was compared between gels with and without CPEs (Figure 5.3).

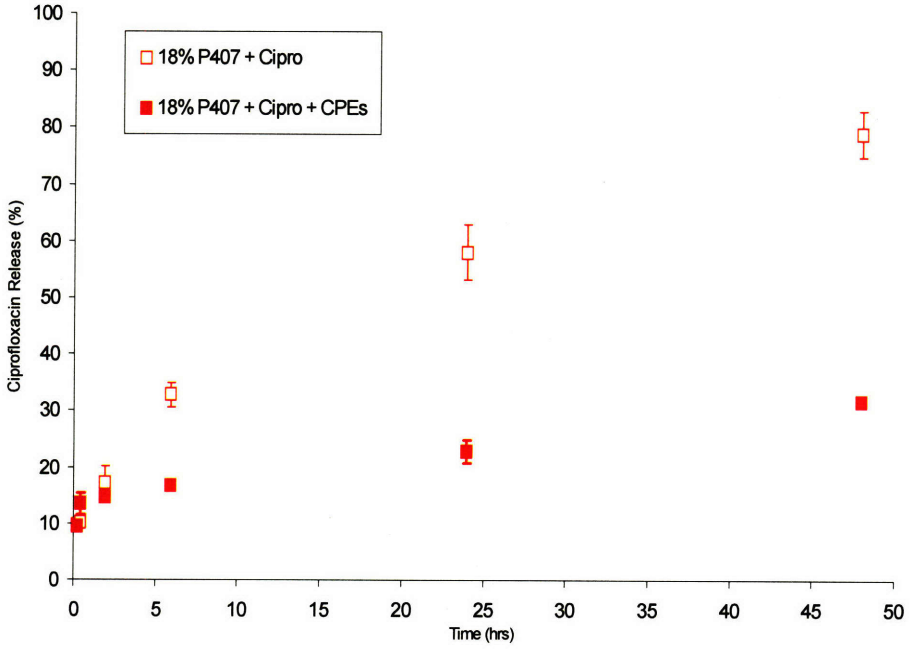

Figure 5.3. Ciprofloxacin release from P407 hydrogels with and without chemical penetration enhancers (0.5% BPV + 1% SLS). Percentages are calculated as the cumulative ciprofloxacin mass in the receiving chamber divided by the total original mass in the delivered mixture. Data are presented as means ± standard deviations (n = 8).

Release kinetics from 18% P407 both with and without CPEs demonstrate sustained release into an aqueous receiving medium. Though these release percentages do not necessarily correlate with release into or across the stratum corneum of the TM, they suggest a decrease in free ciprofloxacin with the addition of 0.5% BPV and 1% SLS.

5.3.2 Chitosan-chondroitin sulfate formulations and release kinetics

A 1:1 mixture of 12% chitosan (Ch) and 12% chondroitin sulfate (CS) in 1% ciprofloxacin solution was found to gel through polyelectrolyte complexing when extruded through a 20-gauge angiocatheter-capped double-barreled syringe (Figure 5.4). Gelation was dependent on initial separation of the polycationic chitosan and polyanionic chondroitin sulfate, as well as on the diameter of the extruding vessel; pre-mixture of the two polymers appeared to inhibit complex formation, as did lower-gauge needles or angiocatheters. The gelation time of the Ch/CS polyelectrolyte complex was more difficult to quantify; though complex formation increased viscosity enough to keep between 0.1 and 1 mL of gel at the bottom of an inverted vial indefinitely, the gel consistency was such that stir bar rotation was never impeded. Still, Ch/CS complexes sufficiently gelled in less than 30 seconds and were not sensitive to temperature (22-35°C), nor to the presence of CPEs.

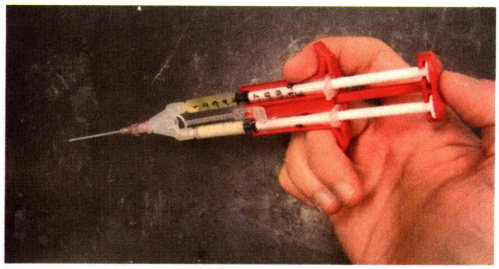

Figure 5.4. Double-barreled syringe apparatus used for *in vitro* and *in vivo* application of Ch/CS polyelectrolyte complexes. Equal volumes of the component Ch and CS were loaded separately into a syringe and co-injected via a Y-piece through a flexible, soft-tipped 20-gauge angiocatheter.

Ciprofloxacin release from Ch/CS gels into an aqueous receiving medium did not significantly differ between formulations with and without CPEs (Figure 5.5), but the release rate of both was intermediate between those of P407 ± CPEs.

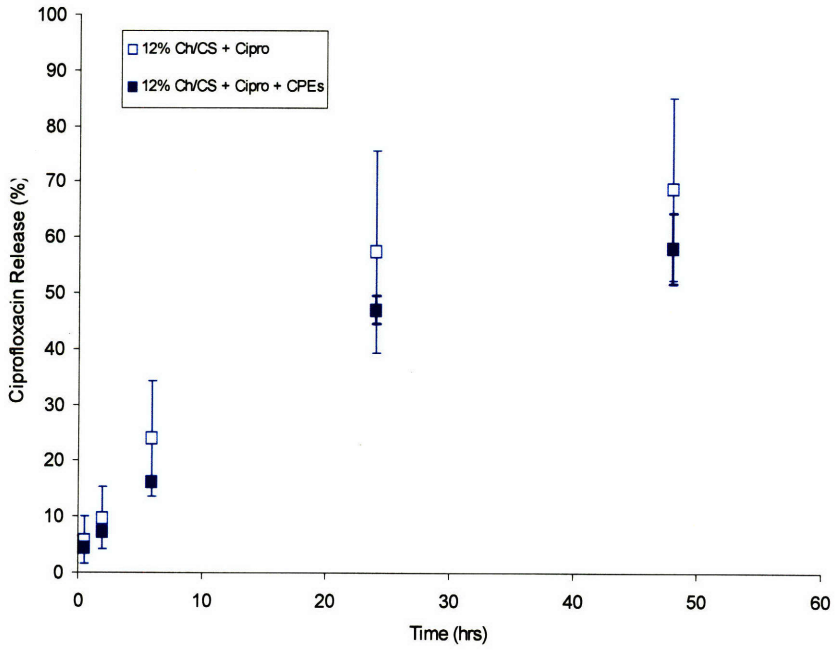

Figure 5.5. Ciprofloxacin released from Ch/CS polyelectrolyte complexes into an aqueous receiving medium. Percentages are calculated as the cumulative ciprofloxacin mass in the receiving chamber divided by the total original mass in the delivery complex. Means ± standard deviations are shown (n = 8).

5.3.3 Ciprofloxacin flux across the tympanic membrane v. condition in gel

Ciprofloxacin release from P407 and Ch/CS hydrogels across the TM is expected to be different from those measured from gels into an aqueous solution. Release into an aqueous medium is dominated by concentration differences between the gel and the receiving medium, the porosity and tortuosity of the gel, and the relative size of the molecule(s) being released. Trans-TM penetration of the same molecule(s), however, is additionally influenced by the gel-TM partition coefficient, the diffusivity of the TM, and the TM-receiving medium partition coefficient. *In vitro* trans-TM flux of ciprofloxacin from P407 and Ch/CS hydrogel carriers is also different from that observed from otherwise identical CPE-ciprofloxacin mixtures in solution, in the absence of gelling polymers (Figure 5.6). The effect of hydrogel polymers on

ciprofloxacin release across the TM is similar to that seen on release into an aqueous medium: the reservoir environment results in decreased ciprofloxacin solubility, and therefore a decrease in steady-state flux.

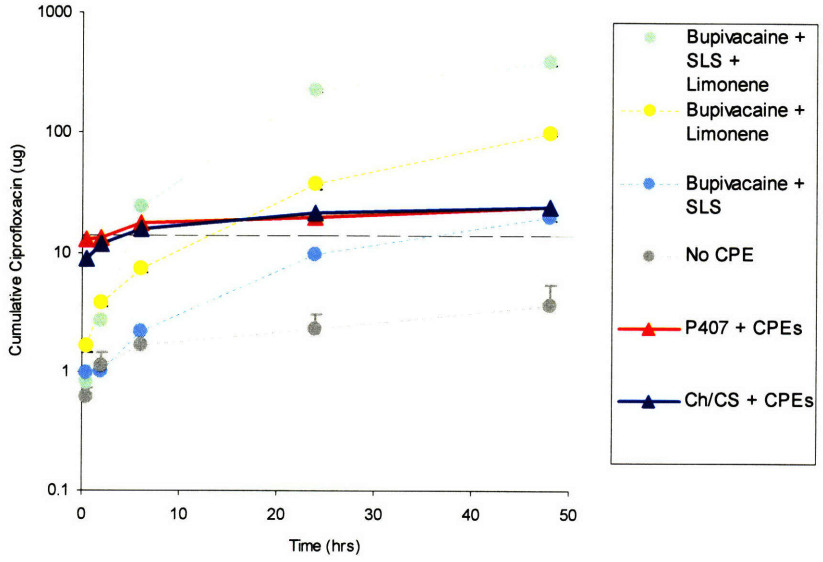

Figure 5.6. Trans-TM ciprofloxacin delivery from P407 (red) and Ch/CS (blue) gels compared to that from polymer-free mixtures. Both gels provide delivery of super-MIC ciprofloxacin levels (dashed line) within 12 hours of application, but steady-state rate of release is decreased compared to drug/CPE mixtures lacking a sustained-release delivery medium. For each point, medians are presented with 25th and 75th percentile error bars ($n \geq 4$); error bars not seen are smaller than the radius of plot point.

However, the time lag to reach this steady-state is decreased with the addition of the gels, resulting in decreased time required to exceed the minimum inhibitory concentration (MIC) for eradication of resistant *H. influenzae* and *S. pneumoniae*.

5.3.4 Auditory Brainstem Response (ABR)

ABR measurements provide noninvasive assessment of hearing sensitivity by collecting multiple averages of compound action potentials in response to acoustic stimuli. Baseline

measurements, before application of gels, reveal increasing sensitivity (decreased thresholds) from 500-Hz to 4-kHz tones, and a subsequent increase in thresholds from 4 to 16 kHz. The applied P407 solution was able to form a thin, near-uniform layer, covering all or most of the TM surface before gelling; the Ch/CS gel, however, took the form of an adherent, viscous bolus, typically in the middle of the TM inferior to the umbo. Ch/CS resulted in small threshold increases immediately after application, but P407 had no significant effect on hearing sensitivity (Figure 5.7). The Ch/CS-induced threshold increases were observed across all frequencies, but were significant only at 1 kHz based on the distribution of the pre-application measurements across all animals. At 1 kHz, Ch/CS increased thresholds by 20 dB ($p < 0.05$).

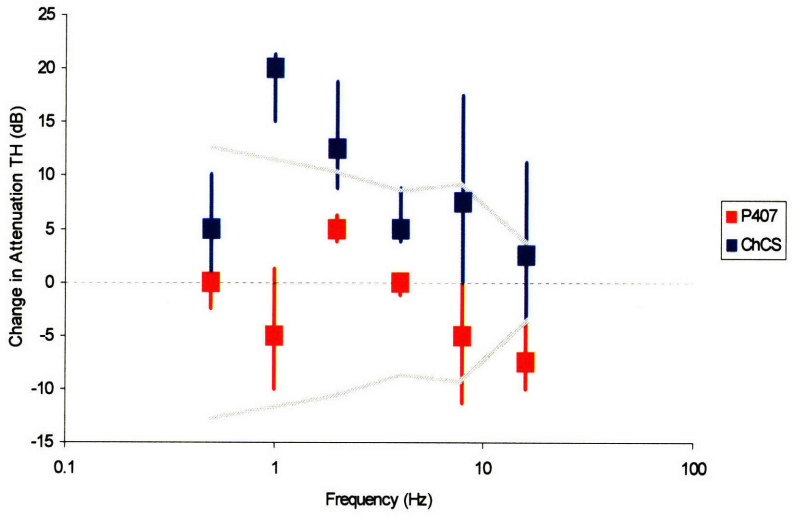

Figure 5.7. Changes in sensitivity thresholds as a function of frequency immediately following application of P407 (red) and Ch/CS preparations. Points on the dotted line indicate no change in ABR attenuation thresholds compared to pre-application measurements. The gray line indicates the observed standard deviation of pre-application measurements (n = 9). Other values are medians with 25th and 75th percentiles (n = 4).

Subsequent ABR measurements were made 2 and 10 days after gel application for evidence of harmful effects to the TM that might result from prolonged exposure to the CPEs. The median change in thresholds among individual animals at days 0, 2, and 10 revealed no systematic trend

or significant differences in threshold shift as a function of time. Though some individual thresholds changed from the immediate (day 0) post-application measurement to the day 10 measurement, there were no significant changes found within the two populations (i.e., P407 and Ch/CS) between day 0 and day 10.

5.3.5 OM eradication

Though sufficient ciprofloxacin flux across the TM is achieved *in vitro* by simple mixtures of P407 or Ch/CS with CPEs, structural and physiological changes in the TM during active disease [13] may alter the kinetics of ciprofloxacin permeating the TM and entering the middle ear fluid (MEF) and middle ear mucosa. The efficacy of P407 and Ch/CS mixtures was therefore investigated in an *in vivo* model of OM. Compared to no-treatment controls, gel-drug controls (no CPEs), and gel-only controls (no ciprofloxacin or CPEs), both P407 and Ch/CS mixtures were effective at eradicating *H. influenzae* infection (Figure 5.8). Though the majority of animals in each treated group experienced complete eradication of bacteria within 48 hours of treatment, a minority of animals in each group remained with non-0 CFU counts (1 of 4 in the P407 group; 3 of 8 in the Ch/CS group).

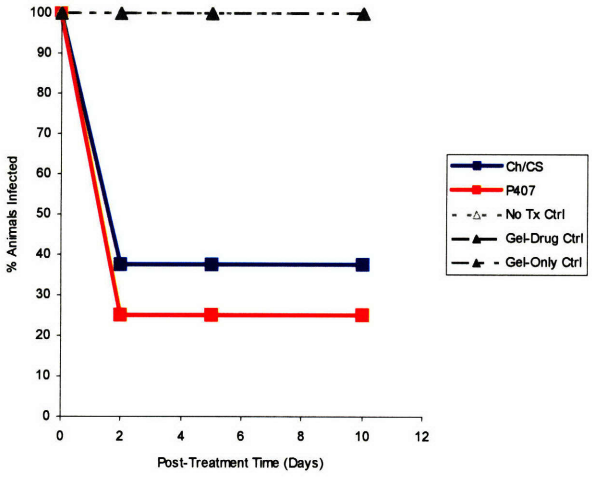

Figure 5.8. Treatment with both P407 (red) and Ch/CS (blue) preparations resulted in a decreased infection rate within 48 hours of drop application. All untreated ears remained infected throughout the 10-day observation period, and all ears cleared of infection within 48 hours remained clear after 10 days.

To investigate the possibility that incomplete eradication of disease in all animals was due to insufficient ciprofloxacin levels reaching the middle ear, MEF samples were analyzed to determine levels of ciprofloxacin at 48 hours post-treatment (Figure 5.9). Animals in which infection was eradicated (0 CFU at 48 hours) consistently had MEF ciprofloxacin concentrations greater than 1 μg/mL and as high as 19 μg/mL; those animals with remaining infection were found to have less than 0.5 μg/mL MEF ciprofloxacin concentrations.

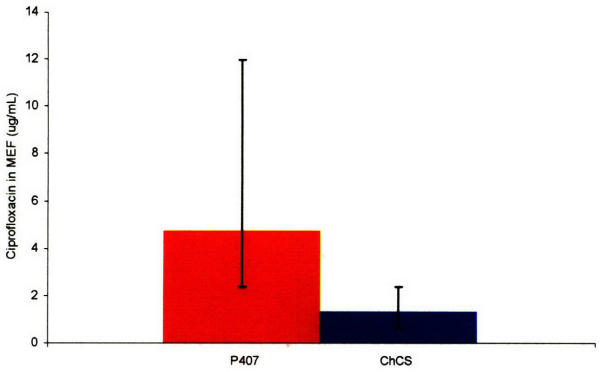

Figure 5.9. Ciprofloxacin concentrations in middle ear fluid (MEF) 48 hours after single treatment application. Data are shown as medians with 25th and 75th percentiles (n = 4).

Plasma samples were also analyzed for evidence of systemic ciprofloxacin delivery via TM vasculature. Though significant sink effect was not anticipated based on estimates of the metabolic activity of the TM and skin of the EAM [14], it is possible that OM-induced inflammation and associated increases in blood flow might result in significant systemic absorption. Plasma samples collected from the superior sagital sinus at 2 and 5 days post-treatment contained no detectable ciprofloxacin (detection limit approximately 100 ng/mL; 97±2% recovery from spiked control plasma samples).

5.3.6 Toxicity

Continued investigation of acceptable topical formulations for trans-TM drug delivery in general or OM treatment in particular is dependent on *in vivo* demonstration of safety. Though the individual components of the mixtures used here are minimally toxic in keratinocyte and

fibroblast *in vitro* assays [15], the *in vivo* effects of prolonged exposure to the TM have not been studied. P407 and Ch/CS mixtures, including ciprofloxacin and CPEs, were exposed to TMs *in vivo* in normal and *H. influenzae*-infected chinchillas for 7-10 days. Histopathology of TMs was compared at stereotyped cross-sections (Figure 5.10) for evidence of changes in inflammatory indicators, such as polymorphonucleocyte (PMN) and granulocyte infiltration, blood vessel dilation, or edema.

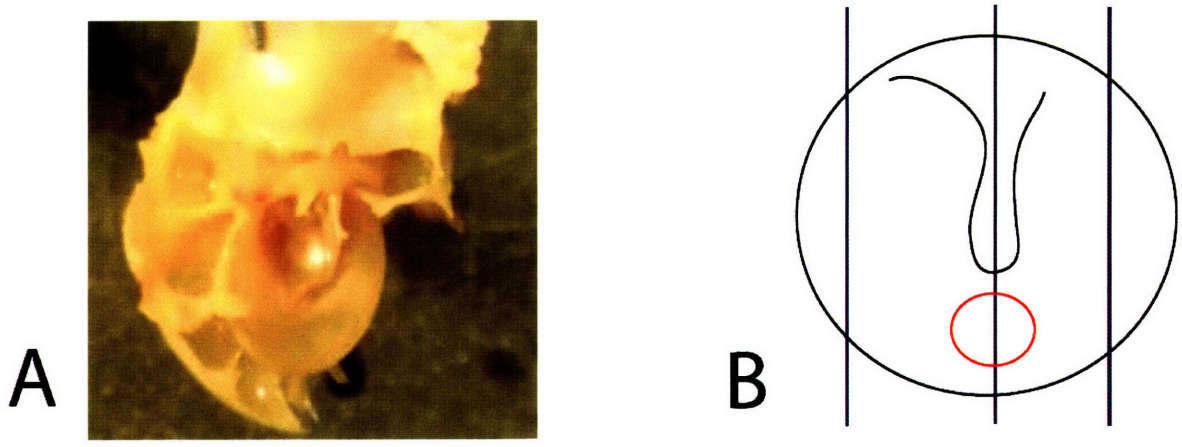

Figure 5.10. Intact TMs with tympanic ring and EAM (A) were sectioned along three vertical cross-sectional planes (B). Comparisons among samples were made at the mid-inferior portion of the central cross-section (red circle), as this was the location which most likely maintained sustained contact with the hydrogel mixtures.

Sections of normal TM (Figure 5.11, A) were consistently 15-20 μm thin, with a clearly visible stratum corneum and a dominant fibrous middle layer. Normal TMs treated with Ch/CS or P407 mixtures (Figure 5.11, B and C, respectively) showed signs of minor toxicity, primarily in a slight thickening of the TM due to an apparent reactive hyperplasia in the stratified, squamous epithelium; though generally very similar, TMs treated with the P407 mixture were consistently slightly thicker than those exposed to the Ch/CS treatment. TMs extracted after 11 days of untreated *H. influenzae* middle ear infection (Figure 5.11, D) were 5-10 times thicker than normal TMs due to edema and hyperplasia in both lateral and medial layers on either side of

the fibrous middle layer. However, when the same infections were treated with a single application of either P407 or Ch/CS mixture, TMs were found to return to near-normal thickness by day 7-post treatment (Figure 5.11, E)

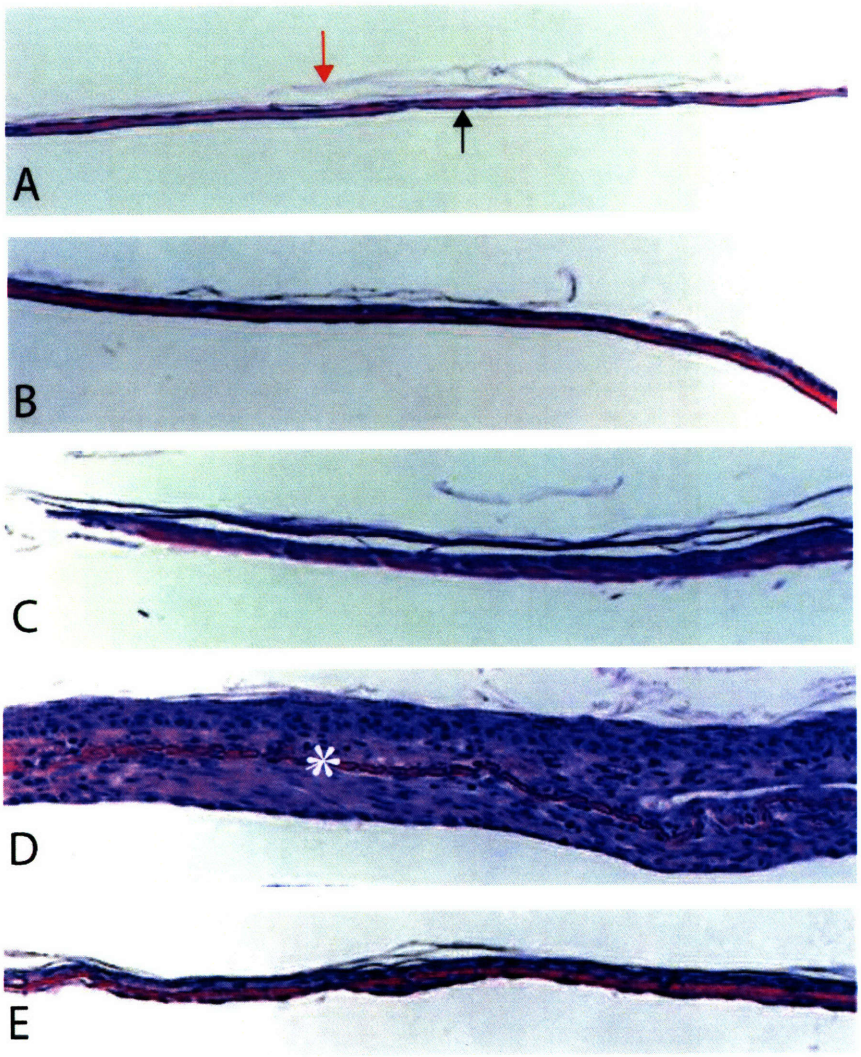

Figure 5.11. Mid-inferior central cross-sections of (A) normal, untreated TM; (B) normal TM exposed to Ch/CS treatment for 10 days; (C) normal TM exposed to P407 treatment for 10 days; (D) TM from animal with untreated OM; (E) TM from animal with OM, 7 days after single treatment with Ch/CS mixture. The stratum corneum (red arrow) of each sample indicates the lateral TM surface that faces the EAM; the middle ear mucosa (black arrow) is the medial surface facing the middle ear cavity. The fibroelastic layer between the stratum corneum and mucosal epithelium is the pink layer in each sample, marked with an asterisk (*) in (D). All images are captured at 200X magnification.

5.4 Discussion

Despite a decrease in ciprofloxacin release from the P407 gel system with the introduction of CPEs (Figure 5.3), the P407/CPE treatment was at least as effective as the Ch/CS/CPE system at eradicating *H. influenzae* in an animal model of OM (Figure 5.8). To maximize the efficacy of either treatment, however, it is important to understand the reservoir environment so that the concentration of free ciprofloxacin is maximized within the given carrier. P407/ciprofloxacin solutions with and without 0.5% bupivacaine + 1% SLS remain at similar pH (between 3.2 and 3.5), suggesting the altered release rate is not due to a change in ciprofloxacin solubility resulting from pH increase. More likely, the presence of an additional 10 mg/mL of solute leads to saturation and ciprofloxacin precipitation.

Trans-TM delivery of ciprofloxacin from P407 prepared with 0.5% bupivacaine and 2% limonene, without 1% SLS, was investigated because aqueous ciprofloxacin release was not altered by limonene in the Ch/CS/bupivacaine/limonene mixture. However, poor trans-TM delivery of ciprofloxacin *in vitro* (data not shown) was found, likely as a result of limonene binding within the hydrophobic domains of the P407 during micelle formation. Future work will investigate the effects of increased limonene concentration on P407/ciprofloxacin formulations and trans-TM ciprofloxacin delivery from these formulations. However, it should be emphasized that the *in vitro* trans-TM ciprofloxacin flux was statistically equivalent for the P407/bupivacaine/SLS and Ch/CS/bupivacaine/limonene mixtures. It is possible that the decrease in free ciprofloxacin in the P407 preparation is functionally counteracted by a permeabilizing effect of P407 as a surfactant.

The CPEs used in each preparation were selected on the basis of previous demonstration of their ability to increase *in vitro* trans-TM ciprofloxacin flux, when prepared as crude mixtures in

1% ciprofloxacin solution (Chapter 3). The exclusion of limonene from the final P407 mixture and of SLS from the final Ch/CS mixture was due to practical considerations regarding the gels' mechanical properties. Addition of 2% limonene to P407 + bupivacaine + SLS resulted in grossly heterogeneous mixtures with widely variant mechanical/gelation properties. Incorporation of 1% SLS to Ch/CS mixtures, with or without inclusion of bupivacaine and/or limonene, inhibited Ch/CS complex formation, likely because of SLS's anionic interference with the normal polyelectrolyte interactions. The trans-TM ciprofloxacin delivery profiles (Figure 5.6) suggest the incorporated CPEs in both P407 and Ch/CS mixtures are sufficiently effective at rapidly increasing stratum corneum permeability, based on the short time required to reach MIC levels. Continued work to increase the free ciprofloxacin concentration in the formulations should result in an increased steady-state flux, and therefore in higher ciprofloxacin concentrations within a therapeutically relevant time window.

OM commonly increases auditory thresholds because of inflammation, negative middle ear pressure, and/or middle ear fluid (MEF), which alone or in combination change TM admittance, and therefore its conductive properties [16-20]. As hydrogel density is close to 1 g/mL and TM diameter about 8 mm, a 100 μL drop is approximately 100 mg distributed across a 2 mm-thick layer. Given that P407 and Ch/CS mixtures have similar densities, the observed differences in induced auditory threshold shifts (Figure 5.7). Preliminary rheological data (Figure 5.12) provide storage (G') and loss (G") moduli of P407 and Ch/CS gels that imply a high degree of elasticity in both gels (G' > 5,000-10,000 Pa), but different viscosity effects. While Ch/CS demonstrates classic elasticity in the consistent phase angle ($\delta = 0.191 \pm 0.00970$) across frequencies, P407 shows more viscoelastisity ($\delta = 0.434$ to 0.067 with increasing frequency).

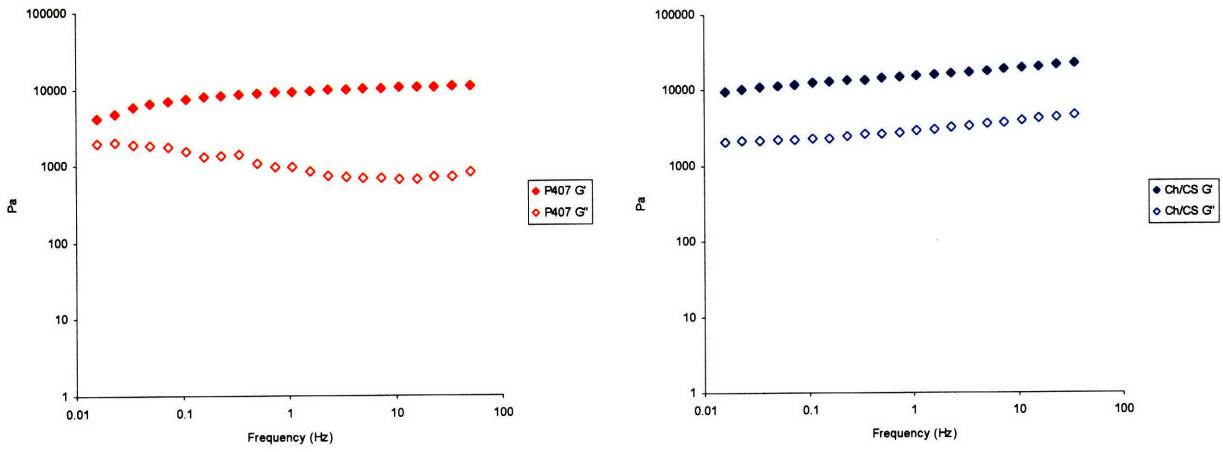

Figure 5.12. Storage modulus (G') and loss modulus (G") of P407 (red) and Ch/CS (blue) as function of shear frequency.

Future analyses such as these may be used to identify other *in situ*-forming polymer carriers with optimal mechanical properties that minimize changes in TM compliance and attenuation of incident acoustic signals.

Gel application to animals with OM led to median MEF ciprofloxacin levels that appeared to be higher in the P407 group than in the Ch/CS group. However, it should be considered that this is perhaps biased due to the higher number of culture-positive animals remaining in the Ch/CS group after treatment. Though it is likely true that the Ch/CS group had a lower cure rate because a lower concentration of cipro permeated the TM on average, it is likely that the Ch/CS group had a MEF cipro levels and lower cure rate because the gel did not stay in the ear canal as consistently as in the P407 popultion. This possibility is confirmed by *in vitro* demonstration that Ch/CS gelation takes longer than P407 gelation. Though Ch/CS mixtures gel quickly (less than 30 s), the animals with remaining infection were noted to be lightly anesthetized during application, and shook their heads immediately upon or shortly after administration.

The minimal toxicity observed *in vivo* in normal TMs, and the demonstrated reversal of the inflammatory effects of OM on the TM are encouraging as efforts continue to develop an optimally formulated delivery carrier. Though *in vitro* trans-TM delivery experiments suggest the present CPE mixtures sufficiently increase TM permeability, the low *in vivo* toxicity of these formulations leaves room for increased CPE concentrations, if necessary.

5.5 References

1. Van Tomme, S.R., G. Storm, and W.E. Hennink, *In situ gelling hydrogels for pharmaceutical and biomedical applications.* Int J Pharm, 2008. **355**(1-2): p. 1-18.
2. Takats, Z., K. Vekey, and L. Hegedus, *Qualitative and quantitative determination of poloxamer surfactants by mass spectrometry.* Rapid Commun Mass Spectrom, 2001. **15**(10): p. 805-10.
3. Ruel-Gariepy, E. and J.C. Leroux, *In situ-forming hydrogels--review of temperature-sensitive systems.* Eur J Pharm Biopharm, 2004. **58**(2): p. 409-26.
4. Ruel-Gariepy, E., et al., *A thermosensitive chitosan-based hydrogel for the local delivery of paclitaxel.* Eur J Pharm Biopharm, 2004. **57**(1): p. 53-63.
5. Chen, W.B., et al., *Characterization of polyelectrolyte complexes between chondroitin sulfate and chitosan in the solid state.* J Biomed Mater Res A, 2005. **75**(1): p. 128-37.
6. Salyers, A.A. and M. O'Brien, *Cellular location of enzymes involved in chondroitin sulfate breakdown by Bacteroides thetaiotaomicron.* J Bacteriol, 1980. **143**(2): p. 772-80.
7. Morreale, P., et al., *Comparison of the antiinflammatory efficacy of chondroitin sulfate and diclofenac sodium in patients with knee osteoarthritis.* J Rheumatol, 1996. **23**(8): p. 1385-91.
8. Ronca, F., et al., *Anti-inflammatory activity of chondroitin sulfate.* Osteoarthritis Cartilage, 1998. **6 Suppl A**: p. 14-21.
9. Lovdahl, M., et al., *Determination of ciprofloxacin levels in chinchilla middle ear effusion and plasma by high-performance liquid chromatography with fluorescence detection.* J Chromatogr, 1993. **617**(2): p. 329-33.

10. Yong, C.S., et al., *Effect of sodium chloride on the gelation temperature, gel strength and bioadhesive force of poloxamer gels containing diclofenac sodium.* Int J Pharm, 2001. **226**(1-2): p. 195-205.

11. Ryu, J.M., et al., *Increased bioavailability of propranolol in rats by retaining thermally gelling liquid suppositories in the rectum.* J Control Release, 1999. **59**(2): p. 163-72.

12. Choi, H., et al., *Effect of additives on the physicochemical properties of liquid suppository bases.* Int J Pharm, 1999. **190**(1): p. 13-9.

13. Magnuson, K. and S. Hellstrom, *Early structural changes in the rat tympanic membrane during pneumococcal otitis media.* Eur Arch Otorhinolaryngol, 1994. **251**(7): p. 393-8.

14. Krueger, G.G., et al., *The development of a rat/human skin flap served by a defined and accessible vasculature on a congenitally athymic (nude) rat.* Fundam Appl Toxicol, 1985. **5**(6 Pt 2): p. S112-21.

15. Karande, P., et al., *Design principles of chemical penetration enhancers for transdermal drug delivery.* Proc Natl Acad Sci U S A, 2005. **102**(13): p. 4688-93.

16. Merchant, S.N., et al., *Analysis of middle ear mechanics and application to diseased and reconstructed ears.* Am J Otol, 1997. **18**(2): p. 139-54.

17. Merchant, S.N., J.J. Rosowski, and M.E. Ravicz, *Middle ear mechanics of type IV and type V tympanoplasty: II. Clinical analysis and surgical implications.* Am J Otol, 1995. **16**(5): p. 565-75.

18. Rosowski, J.J., et al., *Cadaver middle ears as models for living ears: comparisons of middle ear input immittance.* Ann Otol Rhinol Laryngol, 1990. **99**(5 Pt 1): p. 403-12.

19. Rosowski, J.J., S.N. Merchant, and M.E. Ravicz, *Middle ear mechanics of type IV and type V tympanoplasty: I. Model analysis and predictions.* Am J Otol, 1995. **16**(5): p. 555-64.

20. Voss, S.E., et al., *Acoustic responses of the human middle ear.* Hear Res, 2000. **150**(1-2): p. 43-69.

6 Summary, Continued Work, and Future Directions

This work comprises a proof of concept for a safe and efficacious eardrop for treatment of OM, and points to specific challenges that should be met in order for the technology to be optimized for effective clinical use. Simple mixing of model CPEs with ciprofloxacin solution resulted in increased TM permeability to the drug; SLS and limonene each significantly increased ciprofloxacin flux. Bupivacaine, an amphiphilic amino amide local anesthetic, also increased ciprofloxacin flux across the TM. Binary combinations of bupivacaine and limonene suggested possible synergistic interactions, as did ternary combinations of bupivacaine, limonene, and SLS. These and other potentially synergistic CPE combinations can be used in future work to maximize TM permeability while minimizing associated toxicity.

CPE-local anesthetic interactions are an important finding in this thesis. In addition to bupivacaine's role in improving the permeability enhancement of CPEs, CPEs, in turn, can be combined with hydrophilic local anesthetics to increase both potency and maximum duration of block. Considering the important role of ear pain in the pathology, diagnosis, and treatment of OM, the data presented in Chapter 4 are important for the selection of CPEs and local anesthetics used in ear drop formulations.

Finally, the *in situ*-forming hydrogel reservoirs employed in Chapter 5 demonstrate that a sustained-release delivery system applied to the surface of the TM can be used to eradicate *H. influenzae* in the middle ear, without increasing auditory thresholds acutely. Though it is not presently understood why a minority subset of animals was not cleared of infection, there are three important next steps that will elucidate the underlying explanation: (1) monitoring of the extent and duration of gel contact with the TM; (2) increasing the concentration of ciprofloxacin

in solution; and (3) increasing CPE effects by identifying synergistic combinations that maximize enhancement-to-toxicity ratios.

Localized delivery is important to the future effectiveness of antimicrobial therapy in general, and to optimal treatment of OM specifically. Safe increases in TM permeability can be achieved with individual and combination CPEs, including some that have additional clinical benefit (e.g., bupivacaine). *In situ*-forming hydrogels can be formulated for easy application to the TM, sustained release of super-MIC levels of antibiotic across the TM and into the middle ear, and with minimal effects on auditory thresholds. However, there are additional benefits of localized delivery that have not been addressed in this work, and which require additional work before they can be explored.

6.1 Formulation Refinement

The crude mixtures used in this work do not optimize concentrations of drug (ciprofloxacin) or CPE (bupivacaine, limonene, SLS) for best possible performance. An increase in free ciprofloxacin substantially increases its diffusion potential and resultant flux across the TM, as the concentration gradient is the driving force for one-dimensional diffusion according to Fick's first law, $J = -D\frac{\partial \phi}{\partial x}$, where J is the diffusion flux, D is the diffusivity, and $-\frac{\partial \phi}{\partial x}$ is the concentration gradient for an ideal mixture. The CPE concentrations used in this study were selected to be equal to or less than those previously demonstrated to be safe and minimally irritating to the skin [1-3], but the highest non-toxic CPE concentrations have not yet been investigated in the context of the sustained-release reservoirs used here. Furthermore, though the CPEs used here have been previously demonstrated as having a high ratio of transdermal enhancing effect to toxicity [3], there are likely CPE combinations not investigated here with

greater synergistic activity that result in improved efficacy without an associated increase in toxicity.

The delivery reservoirs described in this work can also be refined on the basis of their interactions with drug and CPE pH and hydrophobicity for optimized release profiles. Furthermore, incorporation of drug-CPE liposomal or polymeric microspheres into topical formulations might provide prolonged delivery beyond the typical 10-15-day treatment in order to accelerate regression of residual or persistent effusions, treat ET patency problems, or weaken biofilms on the middle ear mucosa.

Systematic optimization of formulations will also facilitate incorporation of various antibiotics with efficacy profiles targeted toward the microbe of interest. Other quinolones that are structurally similar to ciprofloxacin, such as levofloxacin, have higher efficacy against *S. pneumoniae*, and are therefore preferred for use in situations where pneumococcal infection is likely. As the gelation kinetics of the reservoirs used in these experiments are sensitive to solution pH and total molar content, an improved understanding of the phenomenological relationships of these parameters would allow for the broadest use of the delivery system, regardless of the active compounds of interest.

6.2 Pharmacokinetics of Formulation Components

Future work will more rigorously assess the distribution of locally-delivered antibiotics within the middle ear mucosa by sampling of stereotyped regions within the middle ear cavity and quantifying ciprofloxacin concentrations via chromatographic analysis [4-6]. The trans-TM flux of the formulation CPEs will also be investigated, and concentration-dependent effects of CPEs on biofilm formation and clearance will be studied *in vitro*.

Topical ciprofloxacin drops approved for acute otorrhea in children with tympanostomy tubes include dexamethasone. As dexamethasone (MW = 392.46) is of similar size to ciprofloxacin (MW = 331.34) but more hydrophobic (log P = 1.83 [7] v. 0.28 [8]) and highly potent, its flux across the TM is expected to be at least that of ciprofloxacin. However, considering its high protein binding (70%), dexamethasone distribution within the middle ear cavity is of interest, especially regarding the extent to which it permeates the mucosa of the ET; the anti-inflammatory effects of sufficient dexamethasone concentrations could reduce ET obstruction, restore the ET's pressure-regulating function, and thereby accelerate resolution of ME effusion.

Additional *in vivo* work comparing the levels of antibiotic reaching the middle ear versus those distributed systemically will be investigated as a function of reservoir volume and concentration of drug and CPE within a given formulation. As the idea formulation provides maximum antibiotic to the middle ear and minimal to the systemic circulation, a small-volume drop that maximizes the ratio of TM:EAM contact area must contain enough drug and CPE to exceed the target MIC with 12 hours and sustain maximum levels for 5-10 days.

6.3 Applications of Other TDD for Middle Ear Drug Delivery and Diagnosis

Iontophoresis has been used to increase TM permeability to local anesthetics [9], but other methods of transdermal drug delivery have not yet been investigated for their ability to improve treatment or diagnosis of middle ear disease. Low-frequency ultrasound (LFU) has been used to safely deliver therapeutically relevant amount of macromolecules and hydrophilic small molecules across the skin by reversible formation of localized transport regions within the stratum corneum [10-17]. Though concern over LFU's effects on hearing may likely have discouraged investigation of middle ear applications to date, recent demonstration of strong

synergisms with CPEs [18, 19] suggest that sufficient ultrasonic energy transmitted through the proper CPE-loaded coupling medium could be low enough to be safe for use at the ear.

The advantages of LFU are potentially beneficial to both treatment and diagnosis of OM. LFU-induced localized transport regions within the stratum corneum of the TM could allow for embedded degradable micro- or nanoparticles within the TM that provide sustained release into the middle ear without the continued need for a reservoir in the EAM. More importantly, LFU could provide the first noninvasive molecular diagnosis of OM by trans-TM detection of bacterial markers, such as specific bacterial sugar fragments or exotoxins similar to LFU-mediated glucose monitoring [20-23].

References

1. Jibry, N. and S. Murdan, *In vivo investigation, in mice and in man, into the irritation potential of novel amphiphilogels being studied as transdermal drug carriers.* Eur J Pharm Biopharm, 2004. **58**(1): p. 107-19.
2. Sugibayashi, K., et al., *Kinetic analysis on the in vitro cytotoxicity using Living Skin Equivalent for ranking the toxic potential of dermal irritants.* Toxicol In Vitro, 2002. **16**(6): p. 759-63.
3. Karande, P., et al., *Design principles of chemical penetration enhancers for transdermal drug delivery.* Proc Natl Acad Sci U S A, 2005. **102**(13): p. 4688-93.
4. Barron, D., et al., *Determination of residues of enrofloxacin and its metabolite ciprofloxacin in biological materials by capillary electrophoresis.* J Chromatogr B Biomed Sci Appl, 2001. **759**(1): p. 73-9.
5. Ba, B.B., et al., *Determination of moxifloxacin in growth media by high-performance liquid chromatography.* J Chromatogr B Biomed Sci Appl, 2001. **754**(1): p. 107-12.
6. Samanidou, V.F., E.A. Christodoulou, and I.N. Papadoyannis, *Recent Advances in Analytical Techniques used for the Determination of Fluoroquinolones in Pharmaceuticals and Samples of Biological Origin - A Review Article.* Current Pharmaceutical Analysis, 2005. **1**: p. 155-193.
7. Hansch, C., et al., *The expanding role of quantitative structure-activity relationships (QSAR) in toxicology.* Toxicol Lett, 1995. **79**(1-3): p. 45-53.

8. Takacs-Novak, K., et al., *Relationship between partitioning properties and (calculated) molecular surface. SPR investigation of imidazoquinazolone derivatives.* Acta Pharm Hung, 1992. **62**(1-2): p. 55-64.

9. Hoffman, R.A. and C.L. Li, *Tetracaine topical anesthesia for myringotomy.* Laryngoscope, 2001. **111**(9): p. 1636-8.

10. Alvarez-Roman, R., et al., *Skin permeability enhancement by low frequency sonophoresis: lipid extraction and transport pathways.* J Pharm Sci, 2003. **92**(6): p. 1138-46.

11. Kushner, J.t., D. Blankschtein, and R. Langer, *Heterogeneity in skin treated with low-frequency ultrasound.* J Pharm Sci, 2008.

12. Kushner, J.t., D. Blankschtein, and R. Langer, *Evaluation of the porosity, the tortuosity, and the hindrance factor for the transdermal delivery of hydrophilic permeants in the context of the aqueous pore pathway hypothesis using dual-radiolabeled permeability experiments.* J Pharm Sci, 2007. **96**(12): p. 3263-82.

13. Kushner, J.t., D. Blankschtein, and R. Langer, *Evaluation of hydrophilic permeant transport parameters in the localized and non-localized transport regions of skin treated simultaneously with low-frequency ultrasound and sodium lauryl sulfate.* J Pharm Sci, 2008. **97**(2): p. 894-906.

14. Kushner, J.t., D. Blankschtein, and R. Langer, *Experimental demonstration of the existence of highly permeable localized transport regions in low-frequency sonophoresis.* J Pharm Sci, 2004. **93**(11): p. 2733-45.

15. Kushner, J.t., et al., *First-principles, structure-based transdermal transport model to evaluate lipid partition and diffusion coefficients of hydrophobic permeants solely from stratum corneum permeation experiments.* J Pharm Sci, 2007. **96**(12): p. 3236-51.

16. Kushner, J.t., et al., *Dual-channel two-photon microscopy study of transdermal transport in skin treated with low-frequency ultrasound and a chemical enhancer.* J Invest Dermatol, 2007. **127**(12): p. 2832-46.

17. Paliwal, S., G.K. Menon, and S. Mitragotri, *Low-frequency sonophoresis: ultrastructural basis for stratum corneum permeability assessed using quantum dots.* J Invest Dermatol, 2006. **126**(5): p. 1095-101.

18. Johnson, M.E., et al., *Synergistic effects of chemical enhancers and therapeutic ultrasound on transdermal drug delivery.* J Pharm Sci, 1996. **85**(7): p. 670-9.

19. Lavon, I., N. Grossman, and J. Kost, *The nature of ultrasound-SLS synergism during enhanced transdermal transport.* J Control Release, 2005. **107**(3): p. 484-94.

20. Kost, J., *Ultrasound-assisted insulin delivery and noninvasive glucose sensing.* Diabetes Technol Ther, 2002. **4**(4): p. 489-97.

21. Kost, J., et al., *Transdermal monitoring of glucose and other analytes using ultrasound.* Nat Med, 2000. **6**(3): p. 347-50.

22. Mitragotri, S., et al., *Transdermal extraction of analytes using low-frequency ultrasound.* Pharm Res, 2000. **17**(4): p. 466-70.

23. Mitragotri, S., et al., *Analysis of ultrasonically extracted interstitial fluid as a predictor of blood glucose levels.* J Appl Physiol, 2000. **89**(3): p. 961-6.